PART FIVE

Scientific Research

Nature and Distribution of Cohesion Forces in Earthen Building Materials

Henri Van Damme, Mokhtar Zabat, Jean-Paul Laurent, Patrick Dudoignon, Anne Pantet, David Gélard, and Hugo Houben

Abstract: *Is there a certain type of interparticle force to which earth-based materials owe their cohesion and which has to be absolutely preserved in order to avoid deterioration? Considering the complex fabric of most earthen materials and the variety of conditions to which they are exposed, it is unlikely that there is one single type of dominant interaction for all types of earthen materials. It is much more likely that there are a number of forces, each of them dominant in given composition and hydration conditions. The collaborative study (GCI, CRATerre-EAG, ICCROM) discussed in this paper aims to provide a basic understanding of this, through a combination of experimental and modeling techniques. First, a review is presented of the main cohesive forces that have been identified in sand, clays, and Portland cement, pointing to the properties of the most universal among them: capillary forces and van der Waals forces. Second, an experimental study is presented of the cohesion of a model material made of a sand-kaolinite mixture, in which the cohesion is precisely expected to stem from capillary and van der Waals forces. This composition is representative of a wide range of earthen materials. The fabric of the samples was characterized by scanning electron microscopy and synchrotron radiation microtomography. Both techniques revealed sand grains surrounded and bridged by clay particles. Cohesion was measured by using classical soil mechanics techniques. Third, a model for the cohesion is proposed and compared with the experimental results, taking into account both the capillary forces and the van der Waals forces. The main conclusion is that water is an essential component of earth cohesion, even in clay-rich materials, and that finding the optimum water content is essential for successful conservation.*

The deterioration of earthen cultural heritage, including wall paintings on earthen supports, is most often due to a loss of cohesion of the base material. This makes the understanding of the source of this cohesion an integral part of a rational conservation approach. What are the interparticle forces responsible for the cohesion of earthen walls, substrates, or plasters? Considering the extreme compositional variability of the raw materials used in earthen construction and artwork, ranging from sandy soils to lateritic crusts or almost pure clay deposits, it is unlikely that a single type of interaction dominates.

Earth is a highly heterogeneous material, with many different components interacting with each other and with interstitial fluids. Unlike that of metals or ceramics, the cohesion of earth is the result of a complex equilibrium between attractive, repulsive, and frictional interparticle forces that depend in a subtle way on the raw mineral composition, preparation method, water content, and atmospheric conditions. Yet knowledge of these forces and their dependency on environmental parameters is essential for successful conservation.

In this paper we report some results from a collaborative study that aims to provide a basic understanding of these forces, through a combination of experimental and modeling approaches applied to a simple model material representative of a wide range of earthen materials. This research was conducted within the framework of Project TERRA,[1] in coordination with research at the Getty Conservation Institute on

the interaction of water with earthen building materials and at ICCROM on the compositional and textural characterization of original materials from archaeological and historical earthen structures.

Cohesion and Interparticle Bonds

Before examining the different forces that may be operating in earthen materials, it is worth looking at the concept of cohesion itself. What is the difference between a 1-meter-high sand castle on a beach and a seven-story earthen building in Yemen? In terms of the mechanics of elementary granular materials going back to Coulomb in 1773, the difference is cohesion, *C*. Cohesion is the internal stress that, together with intergranular friction, prevents a granular material subject to a force (its own weight) from dividing in two, that is, sliding along a failure plane.

In its simplest form, the failure criterion (Nedderman 1992) for a dry, cohesionless sand heap is

$$\Delta P_{cap} = 2\gamma_{LV} / \rho \tag{1}$$

where τ and σ are the shear and normal stresses on the sliding plane, respectively, and μ is the friction coefficient. This equation states that the top layer of a sand heap cannot withstand a stress along the slope larger than a fraction μ of the stress perpendicular to the slope (fig. 1a). A simple geometric argument shows that μ can also be expressed as $\tan\theta$, where θ is the maximum angle of stability. If attractive interparticle forces provide some cohesion to the material, a larger stability angle can be achieved (fig. 1b), and equation 1 becomes

$$\tau = \mu\sigma + C \tag{2}$$

The cohesion *C* has units of energy per unit of material volume. At the microscopic level, cohesion is the energy necessary to break all the interparticle bonds.

There are several ways to classify bonds between atoms, molecules, or mineral particles. One of them is to consider chemical forces, on the one hand, and physical forces, on the other. Chemical forces are quantum mechanical in nature. The very strong attractive force called the covalent bond, which stems from electrons being shared between atoms, is one such chemical force, operating at very short interatomic separations on the order of 0.1 or 0.2 nanometer. Molecules, like the water molecule, or solids, like quartz, graphite, or glass, owe their cohesion to covalent bonds.

Physical forces are much more diverse. They originate either from purely electrostatic interactions between electric charges of ions, or dipoles, or from polarization effects. They can be almost as strong as covalent forces, but most of them are weaker. They also operate over a much longer range, up to several nanometers. Physical forces are responsible for the cohesion of all living matter. Since they act between macroscopic bodies close to each other, physical forces are also called surface forces.

In the case of earthen materials, an extensive network of chemical (covalent) bonds between mineral particles is highly unlikely. Unlike for other porous materials, such as sandstone, brick, or porous glass, the interatomic chemical bonding continuity of earthen materials is very limited, if there is any. When earthen material is scrutinized on the microscopic level, it is interrupted almost everywhere by air voids or liquid water films in the *inter*particle space. The best demonstration of this is the swelling and loss of cohesion that is observed when earth is dispersed in water. Yet earthen materials are often able to withstand stresses of the same order of magnitude as a soft rock or a low-cement mortar.

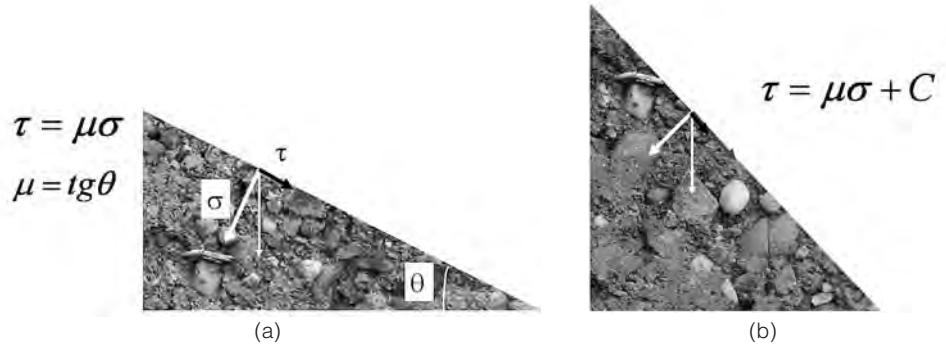

FIGURE 1 In a noncohesive material (a) tilted at an angle θ, the top layer remains stable as long as the shear stress parallel to the slope, τ, does not exceed a fraction, $\mu = \tan\theta$, of the normal stress perpendicular to the slope, σ. If this limit is exceeded, an avalanche starts. The parameter is the intergranular friction coefficient. In a cohesive material (b), larger slopes are allowed, thanks to attractive intergranular forces. The extra shear stress is, by definition, the cohesion *C* of the material.

Capillary Cohesion: The Art of Building Sand Castles

In dry sand, cohesion is vanishingly small, and building even the smallest vertical wall with this material is virtually impossible. An avalanche starts and flows until the slope reaches the equilibrium angle determined by the friction coefficient. As soon as the air contains water vapor, some cohesion may be detected, due to microscopic liquid bridges between the grains. These bridges form by condensation of the vapor, well before the dew point temperature is reached, due to the attractive forces between the water molecules and the surface atoms of the sand grains. This is so-called capillary condensation (Adamson and Gast 1997). Then, building a vertical wall is still risky but feasible, up to moderate heights. The cohesion stems from the pressure difference between the pressure in the liquid in the bridge and that of the humid air outside (fig. 2). This pressure difference is called the Laplace pressure or capillary pressure, the negative curvature of the meniscus (the center of curvature is outside the liquid). This is a result of the pressure being less in the liquid than in the air, giving rise to a net attractive force.

The capillary pressure across the air/water meniscus is written as

$$\Delta P_{cap} = 2\gamma_{LV} / \rho \tag{3}$$

where γ_{LV} is the air/water surface tension and ρ the meniscus radius. Under equilibrium conditions, the meniscus radius is determined by the relative humidity (RH), via the Kelvin equation,

$$\ln RH = -\frac{\gamma_{LV}\overline{V}}{RT\,\rho} \tag{4}$$

where $\overline{V}$ is the molar volume of water (18 cm³ per mole). So, if the relative humidity is known, the capillary or Laplace pressure is automatically determined. The larger the RH, the larger the meniscus radius in equilibrium with that RH; at 100 percent RH the meniscus radius is infinite, which means that the liquid surface is flat. Conversely, the lower the relative humidity, the smaller the meniscus radius and the larger the attractive pressure will be. For small meniscus radii, say, in the submicrometer range, the capillary pressure becomes considerable. For instance, in dry conditions at 30 percent RH, which corresponds to equilibrium meniscus radii on the order of 1 nanometer, the capillary pressure would reach the extreme value of 1,000 atmospheres. What is yet unclear is what happens in very narrow pore conditions, when the meniscus radius is approaching the size of a water molecule. It is likely that the macroscopic theories leading to Kelvin equation break down under these molecular-level conditions.

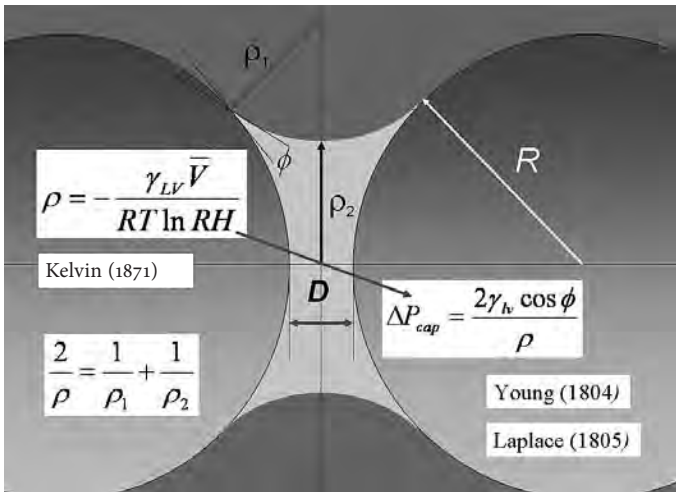

FIGURE 2 A liquid bridge between two particles is characterized by an average curvature radius ρ, which is directly related to the two principal curvature radii of the meniscus, and ρ_1 and ρ_2. Kelvin established the conditions of capillary condensation, that is, the relationship between this average curvature radius and the relative humidity *RH,* whereas Young and Laplace established the relationship between the average curvature radius and the attractive pressure ΔP_{cap} inside the liquid bridge.

On the basis of equations 3 and 4, assuming that macroscopic theories remain valid, one might think that extreme dry conditions are the best conditions for cohesion resulting from capillary pressure. This is not true for one simple reason: *what is important is not the pressure in the liquid bridge but the* force *that pulls the particles to each other.* Since [*Force*] = [*Pressure*] × [*Bridge cross-sectional area*], the shrinkage of the liquid bridge has to be considered also. As the atmosphere becomes dryer, the attractive pressure increases but, simultaneously, the area decreases. The mathematical analysis shows that for two *smooth* spherical particles, the liquid bridge shrinkage when the RH decreases is exactly compensated by the increase of the attractive capillary pressure. This leads to the following result for the

capillary force between two spherical particles in contact (Fisher and Israelachvili 1981):

$$F_{cap} \cong 2\pi R\,\gamma_{LV}\,\cos\theta_e \tag{5}$$

where R is the particle radius and θ_e the equilibrium contact angle between the liquid and the solid particles (see fig. 2). Surprisingly, this expression does not contain any parameter related to the meniscus size. In other words, it predicts that the force should be independent of the volume of liquid in the bridge, even in very dry conditions. This is in contrast to the experience of any child who knows that the cohesion of sand totally saturated by water is as small as that of sand that is totally dry and that the optimum cohesion is obtained at some intermediate water content. The decrease in cohesion when the amount of water is so large that it starts filling all the space between the sand grains is easy to understand, because in those conditions approaching liquid saturation the menisci progressively coalesce, and the water/air interface is repelled toward the outer surface of the sand heap and water flows around the particles. The decrease in cohesion when the amount of water becomes very small is much less obvious and has been explained only recently (Albert et al. 1997; Halsey and Levine 1998; Hornbaker et al. 1997). The explanation lies in the roughness of the particles. All surfaces are rough at some length scale, and sand grains are no exception. At very small RH, say, of the order of 5 percent, capillary condensation occurs only between the two asperities (or spikes) in contact. This is the "asperity regime." "Asperity" refers to single spikes. "Roughness" refers to a whole profile with many spikes in which the force increases nonlinearly with RH. A second regime appears when the menisci between neighboring asperities merge but the cross section of the liquid bridge is still small compared to the radius of curvature of the particles. Here the force increases linearly with the liquid volume. A third regime, the classical saturation regime, in which the force is independent of liquid volume, is recovered when the size of the bridge becomes comparable to the roughness. Finally, the cohesion vanishes when all liquid bridges coalesce, and water percolates through the medium. All four regimes are summarized in figure 3. The important point—trivial for all experienced sand castle builders—is that there is an optimum water content for cohesion that provides the strength, bounded by humidity conditions, both high and low, both of which lead to collapse.

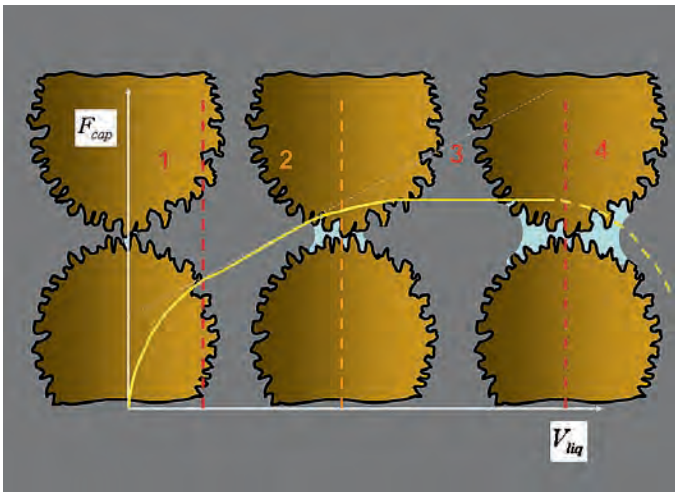

FIGURE 3 The attractive force due to a capillary condensation bridge between two spherical particles with a rough surface exhibits four different regimes. In regime 1 (asperity regime), condensation takes place between the asperities in contact, and the cohesive force increases nonlinearly with the amount of water. In regime 2 (roughness regime), the force increases linearly with the amount of water due to the lateral spreading of the liquid bridge over several asperities. However, in this regime, the meniscus is not yet sensitive to the average spherical curvature of the particles. In regime 3 (classical regime), the meniscus is no longer sensitive to the roughness, and the cohesive force is independent of the amount of water, as between two smooth spheres. Finally, in regime 4 (saturation regime), when so much water has been added that neighboring liquid bridges coalesce, the cohesion vanishes.

Can the cohesion of clays be explained only in terms of capillary forces, like that of sand? No universally valid answer can be given to this question, due to the extreme variability of clay surface properties, but capillary forces always contribute at least to some part of cohesion. However, the calculation of the cohesion is not simple because the form and nature of the clay particles is not simple either. We will come back to this subject later.

Electronic and Ionic Polarization Forces: The Strength of Cement

Besides capillary forces, the most universal attractive forces are undoubtedly dispersion or van der Waals forces, which are due to electronic polarization phenomena. As electrons orbit the nuclei of a molecule, they induce a temporary deformation of the electron cloud of the neighboring molecule.

This in-phase deformation of the two electron clouds generates an attractive force that is strong when the molecules are in contact but that decays rapidly as the separation distance increases. Doubling the separation distance leads to a sixty-four-fold decrease in the force. Between larger bodies, for instance, mineral particles, containing a large number of atoms, the situation is different because one has to sum the interaction of every atom of the first particle with all the atoms of the second particle. This leads to a force that is still very strong at contact but that decays much more slowly with distance. The theory of van der Waals forces has been extensively developed, and the forces can be computed very accurately, provided the shape of the particles and their separation are known. For instance, the expression for the attractive van der Waals pressure between two plates that are alike and of finite thickness, *t,* parallel to each other at distance *D* in a third medium, is shown in equation 6 (Israelachvili 1992). It has been confirmed experimentally by direct force measurements between two mica surfaces.

$$P_A = -\frac{A}{6\pi}\left[\frac{1}{D^3} + \frac{1}{(D+2t)^3} - \frac{2}{(D+t)^3}\right] \tag{6}$$

where *A* is the Hamaker constant, which represents the physics of the dipolar interactions between atoms giving rise to the attractive force. A known feature of van der Waals forces is that the Hamaker constant *A* is not very sensitive to the precise composition of the material, within a given family of minerals. The Hamaker constant for the surface of muscovite mica in water, determined experimentally, is 2.2×10^{-20} J (Bergström 1997). The Hamaker constant for different clays such as illite, kaolinite, montmorillonite, and chlorite is not much different. Thus the van der Waals pressure between two 1-nanometer-thick montmorillonite platelets at a separation of 1 nanometer is approximately 10 atmospheres, which is smaller than the capillary pressure. At a separation of 0.5 nanometer, it is close to 100 atmospheres. For kaolinite or illite platelets, which are thicker, the pressure would be approximately 20 percent more, which is not a significant difference.

Akin to van der Waals forces are the so-called ion-ion correlation forces. Instead of being due to the polarization of electron clouds, they are due to the polarization of ion clouds. Many mineral particles bear an electric charge. Whatever the origin of the surface charge, it has to be compensated by a charge of equal magnitude and opposite sign. This compensating charge is brought about by a cloud of ions of opposite sign, the counterions. The cloud of counterions constitutes the ionic double layer. When two double layers face each other, they undergo strong fluctuations. An excess of ions on one side with respect to the midplane generates a fluctuating deficit of charge on the other side. This generates an attractive force that may become highly significant when the charge density on the particles is high and when the counterions are multivalent ions, like Ca^{2+} ions. This is the case in ordinary Portland cement and also in calcium-exchanged smectite clays (Van Damme 2002). On the other hand, ion correlation forces are totally inactive in neutral or weakly charged clays such as kaolinite.

Can Water Be the Glue? A Sample Case

In light of the previous discussion, an experimental study was performed on a model earthen material, with the aim of comparing measured cohesion values with calculated ones (Gélard 2005). The samples were prepared by mixing fine sand with a kaolinite clay slurry in water at neutral pH. Enough water was added to produce a soft paste consistency. The mixture was placed into cylindrical molds (height: 76 mm; diameter: 38 mm) and allowed to dry at room temperature at about 60 percent RH. Samples with three different clay/sand ratios were prepared: 5, 10, and 15 percent, weight by weight.

Scanning electron microscopy (SEM) (fig. 4) and synchrotron radiation microtomography (fig. 5) of this experimental earthen material show that the sand particles are covered by a layer of clay platelets and are linked by clay bridges with a shape that is clearly reminiscent of liquid capillary bridges. This shape may be interpreted as the signature of the kaolinite bridges that formed during impregnation of the sand with the clay in water slurry. Similar configurations are found in natural sedimentary rock samples (lower right inset of fig. 4).

Cohesion in the experimental earthen material was measured by classical soil mechanics testing methods in a triaxial apparatus allowing for application of a confining pressure to the sample (Muir Wood 1990). Cohesion was found to be highest in the sample containing 15 percent clay, at a value of 120 KPa, or 1.2 atmospheres (Gélard 2005). A cohesion value of a few atmospheres is low, and, indeed, our samples are very brittle, but this is expected for this type of illite- and smectite-free sandy material.

This cohesion value (120 KPa) can be compared to the cohesion calculated for a simple model fabric inspired by the micrographs of the experimental material, that is, two

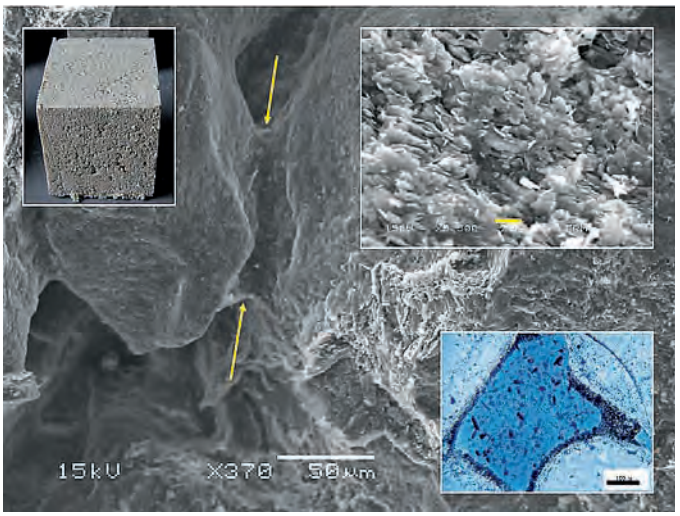

FIGURE 4 SEM image of the model experimental earthen material used in this study. A clay bridge between two sand particles is clearly visible in the background image. Upper left inset: A picture of the molded earthen block (size ~ 10 cm). Upper right inset: High-magnification SEM image of the clay coating on the sand particles. Lower right: For comparison with the experimental earthen material, an SEM image of a naturally occurring, clay-rich sandstone, showing the clay bridge (dark blue area) between the sand grains.

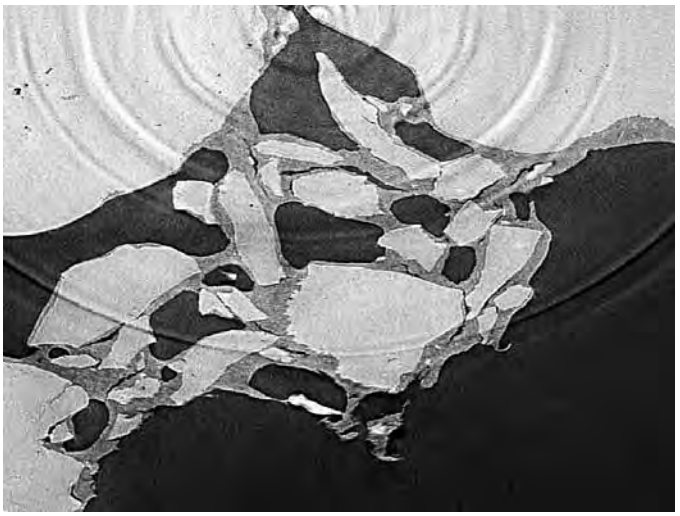

FIGURE 5 2D slice of a 3D image of our experimental earthen material obtained by X-ray synchrotron radiation microtomography. Notice the clay coatings and the clay bridges around and between the sand particles.

spherical sand particles separated by a porous bridge of kaolinite particles (fig. 6). As pointed out earlier, it is difficult to take fully into account the complex fabric of the clay platelets in the experimental material. However, the essential features of this fabric can be incorporated into the model. Those features are (a) the platelets are rigid particles with a high width/thickness ratio, which brings them on average in *almost* parallel orientation when they are densely packed; and (b) due to this small but significant disorientation, the true edge-to-face contact area between platelets is also small, on average. These two features were incorporated into the model by keeping a small contact area but replacing the orientational disorder with a stacking disorder. The platelets were assumed to be parallel to each other but with a strong lateral disorder such that only a small fraction of the surface of each platelet is facing its nearest neighbors. In addition, the disorder is self-similar, meaning that the overall geometry of the system is the same at all length scales (fig. 7). This model has already been used to calculate the contribution of van der Waals forces to the cohesion of pure clay deposits (Van Damme et al. 1985; Fripiat and Setton 1987).

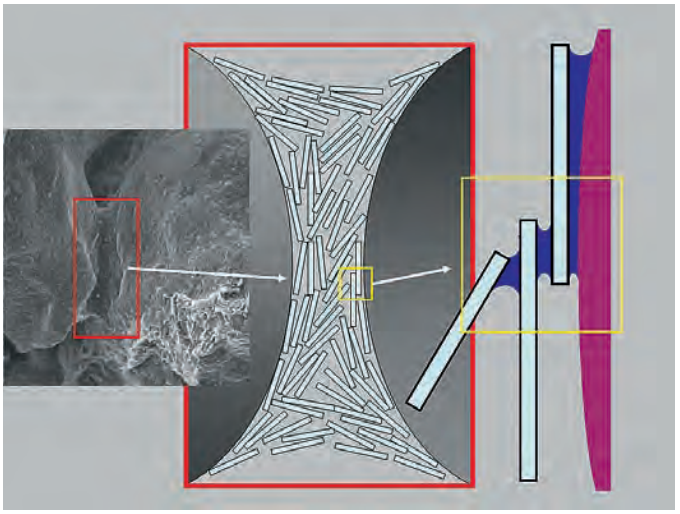

FIGURE 6 Center: Simplified model of the sand/clay fabric based on the SEM image (left) and the X-ray synchrotron radiation microtomography (see fig. 5) of the experimental earthen material. Two sand particles are bridged by clay. The clay bridge is made of rigid kaolinite platelets, mostly in low angle, edge-to-face contact (center). Capillary condensation occurs between clay platelets and also between sand grains and clay platelets (right).

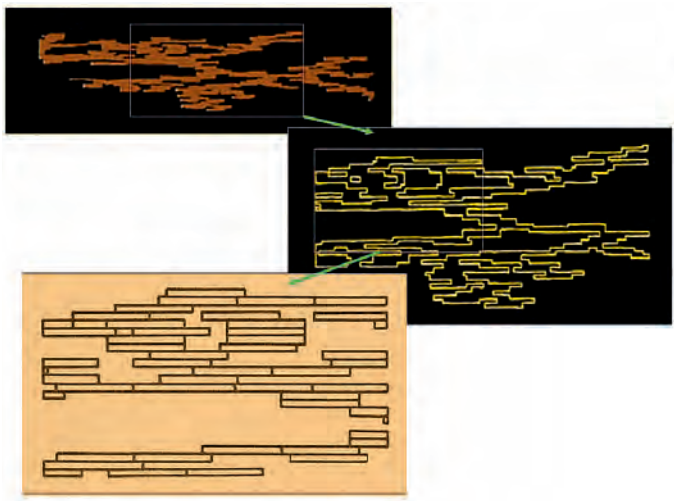

FIGURE 7 Sketch of the simplified model used to calculate the cohesion in the clay bridge between sand grains (see fig. 6, center): the orientational disorder of figure 6 has been replaced by a translational disorder. The average overlap area between neighboring platelets is small, as in the edge-to-face contacts.

We used the same model here, allowing the platelets to be separated by liquid water coming from condensation of the vapor. Capillary condensation starts between neighboring particles and extends progressively toward larger separations. A capillary gap is either totally filled by water, if the relative humidity is higher than the value given by Kelvin equation (eq. 4), or totally empty, if the relative humidity is lower. We assumed that the distance of closest approach of the platelets was the equilibrium meniscus curvature radius at the relative humidity of the experiments (60%), that is, ≅2 nm. Thus only capillary forces between nearest neighboring platelets contribute to the cohesion. The capillary pressure for a radius of 2 nm amounts to $\sim 7 \times 10^7$ Pa, that is, 700 atmospheres. At the same distance, with a Hamaker constant of 3×10^{-20} J, the van der Waals pressure is only 2×10^5 Pa (2 atmospheres), which is 350 times smaller than the capillary pressure. Without any further calculation, this means that the van der Waals contribution to the cohesion of our sample is negligible.

Two ingredients are still missing before a quantitative estimate of the macroscopic cohesion can be made. One is the fraction of platelet surfaces in nearest-neighbor configuration. We assumed, as previously (Fripiat and Setton 1987), that this is on the order of 1 percent. This is low, but it is well in line with edge-to-face contacts between platelets in kaolinite. The last data needed is the cross section of the clay bridge, *s*, relative to the sand grain cross section. From the SEM and synchrotron data, this was estimated to be between 0.1 and 0.4. The cohesion values obtained for these two boundaries are summarized in table 1. The calculated capillary cohesion is of the right order of magnitude. It is very close to the experimentally measured value for $s \cong 0.3$. This value is in qualitative agreement with the SEM and microtomography data.

What can we learn from this discussion of cohesion forces and from the comparison between experiments and simplified models? The first lesson is certainly that cohesion of earthen materials is a property controlled by several different factors. Depending on the types of minerals in the earthen materials and their morphology, particle size, and texture, the important forces may be quite different.

Another lesson is that water is not itself necessarily the enemy of cohesion. Water films control capillary forces, but they also mediate the action of ion correlation forces, and they lubricate contacts between grains, allowing for particle position adjustment toward stable positions. In some cases, such as the model experimental material used in this study, capillary water is virtually the only source of cohesion. In other earthen materials containing highly charged mineral particles and ions, such as some calcium-smectites, the water-controlled contribution of the ion correlation forces to cohesion may be much higher (this is not the case for sodium-smectites, due to the low charge of the sodium ions). Thus, in general, the best conditions for high cohesion are not the driest conditions. For any earthen material, there should be an optimal water content for optimal cohesion and preservation. In dry and hot climates, this optimal water content may be greater than the existing water content in equilibrium with the surrounding atmosphere. Appropriate

Table 1 Calculated Cohesion (*C*) of the Sand/Kaolinite Experimental Material as a Function of the Fraction of Kaolinite Platelet Surfaces in a Nearest-Neighbor Situation (*s*)

s	*C* (kPa)
0.1	15
0.2	60
0.3	135
0.4	240

rehumidification may prove necessary, up to the optimum. Finally, it should be pointed out that finding and maintaining this optimum water content may also be important for the cohesion of any decorative coating made of fine-grained pigments.

Acknowledgments

The authors gratefully acknowledge the Conseil Régional Rhône-Alpes for providing a grant to David Gélard. We are also indebted to Stephane Sammartino for providing access to the ESRF synchrotron facility in Grenoble, France.

Notes

1 Established in 1997, Project TERRA is a partnership between the Getty Conservation Institute, the International Centre for Earth Construction–School of Architecture of Grenoble (CRATerre-EAG), and the International Centre for the Study of the Preservation and the Restoration of Cultural Property (ICCROM), Rome. Among other goals, Project TERRA fosters cooperative scientific research on binding and deterioration mechanisms of earthen materials.

References

Adamson, A. W., and A. P. Gast. 1997. *Physical Chemistry of Surfaces.* 6th ed. New York: Wiley.

Albert, R., I. Albert, D. Hornbaker, P. Schiffer, and A.-L. Barabási. 1997. Maximum angle of stability in wet and dry spherical granular media. *Physical Review E—Statistical Physics, Plasmas, Fluids, and Related Interdisciplinary Topics* 56 (6): R6271–74.

Bergström, L. 1997. Hamaker constants of inorganic materials. *Advances in Colloid and Interface Science* 70 (1–3): 125–69.

Fisher, L. R., and J. N. Israelachvili. 1981. Direct measurement of the effect of meniscus forces on adhesion: A study of the applicability of macroscopic thermodynamics to microscopic liquid interfaces. *Colloids and Surfaces* 3 (4): 303–19.

Fripiat, J. J., and R. Setton. 1987. Cohesion energy in anisotropic particles aqueous slurries. *Journal of Applied Physics* 61 (5): 1811–15.

Gélard, D. 2005. Identification et caractérisation de la cohésion interne du matériau terre dans ses conditions naturelles de conservation. Ph.D. diss, Université de Grenoble.

Halsey, T. C., and A. J. Levine. 1998. How sandcastles fall. *Physical Review Letters* 80 (14): 3141–44.

Hornbaker, D. J., R. Albert, I. Albert, A.-L. Barabasi, and P. Schiffer. 1997. What keeps sandcastles standing? *Nature* 387 (6635): 765.

Israelachvili, Jacob N. 1992. *Intermolecular and Surface Forces.* 2nd ed. Ed. Jacob N. Israelachvili. London: Academic Press.

Muir Wood, David. 1990. *Soil Behaviour and Critical State Soil Mechanics.* Cambridge: Cambridge University Press.

Nedderman, R. M. 1992. *Statics and Kinematics of Granular Materials.* New York: Cambridge University Press.

Van Damme, H. 2002. Colloidal chemo-mechanics of cement hydrates and smectite clays: Cohesion vs. swelling. In *Encyclopedia of Surface and Colloid Science,* ed. A. T. Hubbard, 1087–1103. New York: Marcel Dekker.

Van Damme, H., P. Levitz, J. J. Fripiat, J. F. Alcover, L. Gatineau, and F. Bergaya. 1985. Clay minerals: A molecular approach to their fractal microstructure. In *Physics of Finely Divided Matter: Proceedings of the Winter School, Les Houches, France, March 25–April 5, 1985,* ed. N. Boccara and M. Daoud, 24–30. Springer Proceedings in Physics, no. 5. Berlin: Springer-Verlag.

Geology and Hydrogeology at the Mogao Grottoes, Dunhuang

Chikaosa Tanimoto, Chunze Piao, Keigo Koizumi, Shuichi Iwata, Tadashi Masuya, Li Zuixiong, Wang Xudong, and Guo Qinglin

Abstract: *The Mogao Grottoes are located at the eastern edge of the Mingsha Dunes and face toward the Sanwei Mountains, a range within the Qilian Mountains. The caves were excavated into a cliff along the west bank of the Daquan River. The rock stratum in which the caves were excavated is the alluvial and pluvial Jiuquan conglomerate, containing argillaceous and calcareous cementation. The wall paintings in the caves are subject to severe deterioration caused by recrystallization of salt, related to the movement of liquid water and water vapor in the rock formation. This deterioration has resulted in the partial separation of plaster from the cave roofs and walls. Our measurements of relative humidity in drill holes made into the walls of caves 72 and 108 suggest that even if the cave surface registers low humidity (30–50%), the humidity at a depth of 30 centimeters is almost 95 to 100 percent. This suggests that moisture moves from inside the rock formation to the cave surface. We consider four possible sources for the water and moisture affecting the Mogao caves: river water from the Daquan, rainwater from the top of the cliff, moisture moving through pores in the permeable rock formation and through fissures, and excessive irrigation of the vegetation in front of the caves. This paper describes the regional movement of groundwater that reaches the Mogao caves and the possibility that this groundwater is the source of moisture moving through the rock in which the caves were excavated.*

Knowledge of geology and rock mechanics can play an important role in the preservation and conservation of natural stone monuments. Not only does this knowledge directly contribute to repairs and reinforcement of these monuments; it also deepens our understanding of the geologic environment, construction method, long-term durability, weathering and deterioration processes, the effect of rock joints, movement of groundwater and moisture, and global climate change. We have focused our research on the relationship between the movement of moisture within relatively young porous rocks and the resulting deterioration of these rocks.

Contrary to what may be the common wisdom, groundwater must exist even in an arid area such as the widespread desert of Egypt (Tanimoto, Tonouchi, and Yoshimura 1992; Tanimoto, Yoshimura, and Kondo 1993). Groundwater can move incredibly long distances, sometimes over several thousand kilometers, through faults, fissures, and pores in solid rock. As groundwater, even water vapor, moves along the same path repeatedly over a long time, it transports salt substances from one place to another, and evaporation accelerates the accumulation of salts inside the rock and on the rock surface. The Mogao caves are no exception to this process. It occurs in the rock behind many of the caves' wall paintings and causes the paintings to separate from the walls.

Considering the rivers and oases, vegetation, and subsurface structure in the Dunhuang area, we suggest through our geologic survey and satellite image analysis that a certain network of groundwater exists in the area.

Geographic and Geologic Environments of the Mogao Area

The Mogao Grottoes are located on the southeastern margin of the Dunhuang oasis 25 kilometers from the city of Dunhuang, as shown in figure 1. The figure is a composite obtained by superposing possible surface water flows onto a LANDSAT5/TM satellite image. The Sanwei Mountains are to the east of the Mogao Grottoes, and the Mingsha sand

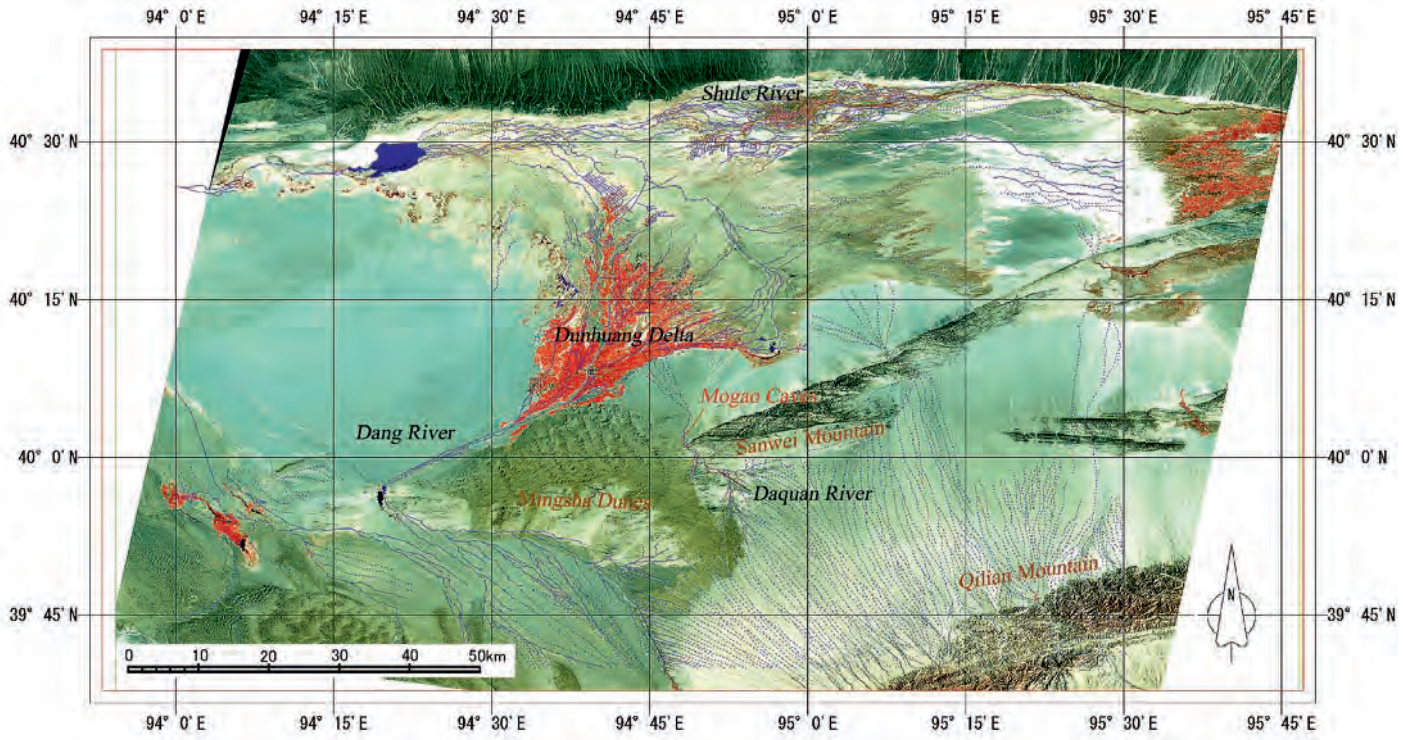

FIGURE 1 Composite topography and LANDSAT5/TM satellite image of the Dunhuang area. Red areas show vegetation.

dunes are to the west, with the Daquan River valley in between. The vast Gobi Desert is to the north. The Mogao area lies at the western end of the Hexi corridor, a long and narrow basin in northwestern China, and is constantly under the influence of the Mongolian high pressure system. The climate is characterized by extreme aridity, low precipitation, great seasonal temperature variation, and frequent windblown sand activity. The average annual precipitation is 23.2 millimeters; annual evaporation is 3,479 millimeters, which is 150 times the precipitation level; and the average relative humidity is 32 percent (Ling Yuquan et al. 1997).

From the topography of the Dunhuang area, it can be seen that the basin surrounded by the Sanwei and Aerjin (Qilian) Mountains is the catchment area for the Dang, Yulin, and Daquan Rivers (fig. 2). The Aerjin fault belt, which consists of shear-compression faults, stretches over 1,000 kilometers in western China. The Daquan River, which runs in front of the Mogao Grottoes, was formed by a conjugate fault system and frequent floods since the beginning of the Quaternary period around 1.8 million years ago.

The rock of the Mogao area consists of two different strata, the Precambrian gneiss and the Pleistocene conglomerate. During the Quaternary period, about one million years ago, aggressive tectonic movements took place, causing granite to be intruded into the gneiss in the Dunhuang area. It can be seen that the major direction of high mountain ridges, which were subjected to extraordinarily high thrust forces, is generated from the south. The magnitude of the tectonic stress in this area is believed to be the highest in the world (Kaizuka 1997; Ma Lifang, Qiao Xiufu, and Liu Nailong 2002). Many textbook reverse faults can be seen along the Daquan River. During the Quaternary period, the Precambrian gneiss was strongly thrust over the Pleistocene conglomerate (fig. 3).

The Aerjin Mountains, whose highest peak is 5,788 meters, are the **western extension of the Qilian mountain** range and form a tremendous wall 3,600 to 4,400 meters high in the east-west direction. There is a huge highland basin 4,000 to 5,000 meters above sea level to the south and another at 1,400 to 2,000 meters between the Aerjin and Sanwei Mountains. These plateaus, highlands, and basins contribute to a large underground reservoir (aquifer) that provides steady groundwater year-round. It is important to note that many highland lakes exist at the several-thousand-

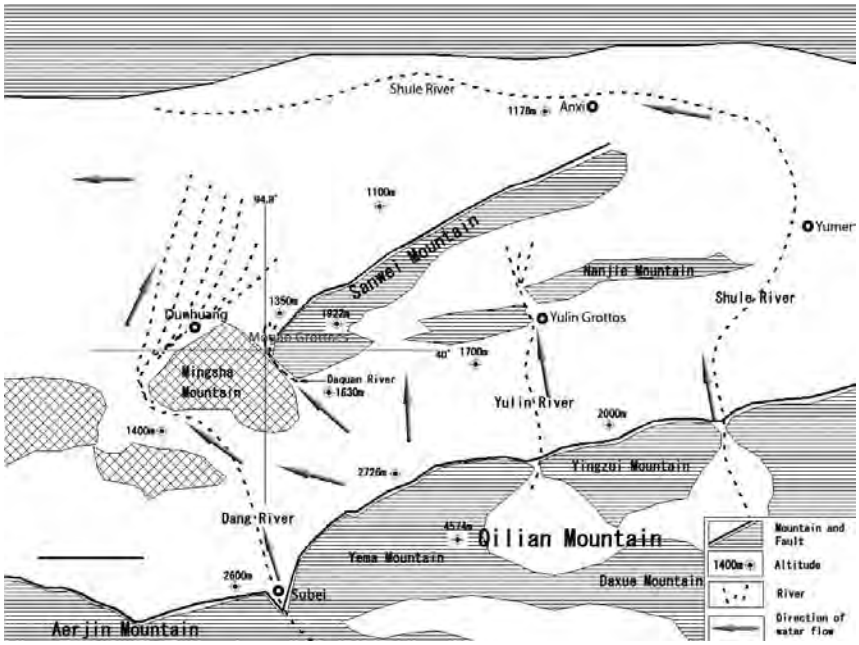

FIGURE 2 Topographical location of the Dunhuang area.

meter level. That is, the existence of many large highland lakes in Qinghai province (not visible in fig. 1) strongly suggests that the area is rich in groundwater.

The underground reservoir sandwiched between the Aerjin (Qilian) and Sanwei Mountains provides water from south to north and from east to west as the main stream. A large amount of water is received by the Dang River, running from south to north, which resulted from faulting in the north-south direction. Since the magnitude and scale of the faulting at the Daquan River are much less than that at the Dang River, the water volume of the Daquan is much less than that of the Dang south of the Mogao Grottoes. However, the movement of water along the Daquan River could be a possible source of water and moisture affecting the Mogao Grottoes.

FIGURE 3 Reverse fault seen along the upper Daquan River where the Precambrian gneiss has been thrust over the Pleistocene conglomerate.

Geologic Profile of Mogao Conglomerate

The geologic profile of the Mogao area is described by Kuchitsu and Duan Xiuye (1997). The 215- to 230-meter-thick local conglomerate was formed with sediments/deposits from frequent floods in the early, middle, and late Pleistocene. The different strata in this conglomerate are classified into three groups, Q1, Q2, and Q3, which date respectively to 1.8–0.78, 0.78–0.13, and 0.13–0.01 million years ago (Ma). The youngest formation formed in the Holocene (0.01 Ma–present); this group is called Q4. In the literature, the Q1 and Q2 groups are designated old alluvial fan deposits, and the Q3 and Q4 groups are designated new alluvial fan deposits (Kuchitsu and Duan Xiuye 1997). In cross section, the approximate thicknesses of the four groups on the south side of the Nine-Storey Pagoda at Mogao are 35–40 meters, 160–70 meters,

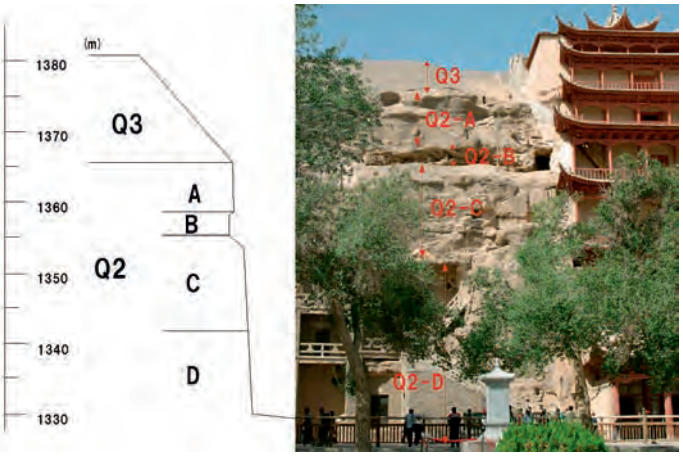

FIGURE 4 Geologic profile of the Q2 conglomerate layer in which the Mogao Grottoes were excavated.

and less than 20 meters for Q1, Q2, Q3, and Q4 in total thickness from the bottom to the top.

Many different kinds of gravels are observed in the conglomerate, showing that floods and glaciers in the past had transported these gravels from the Qilian mountain range over both near and far distances. Most of the Mogao Grottoes were excavated between the fourth and fourteenth centuries in the Q2 group, which is about 30 meters thick. The Q2 group is further subdivided into four layers—A, B, C, and D—based on the particle size distribution (fig. 4). In front of the Nine-Storey Pagoda, ground level is at an elevation of 1,330 meters. The Precambrian basement rock is believed to be below 1,100 meters elevation.

Satellite Remote Sensing

Because the Dunhuang basin between the Sanwei and Aerjin Mountains is situated in an arid region with little vegetation, it is easy for us to understand its geologic structure through satellite remote sensing. For our work, we examined satellite images of the Mogao area taken by LANDSAT5 and JERS-1 in 1996 and 1997. The LANDSAT5 image clearly shows a zigzag-like flow of the Daquan River (fig. 5a) and alluvial fan deposits (fig. 5b).

For our analyses, several combinations of spectral bands were chosen that emphasize differences in the reflec-

FIGURE 5 LANDSAT5 false-color image of the Mogao Grottoes.

(a)

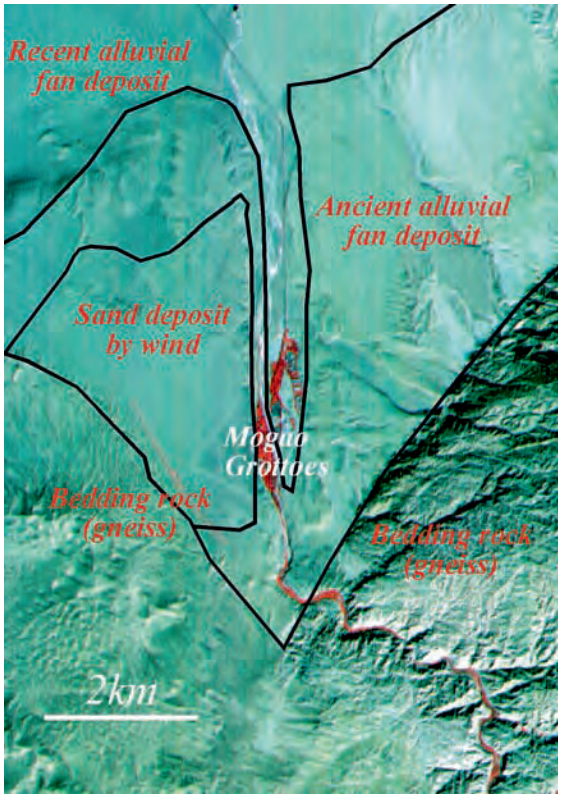

(b)

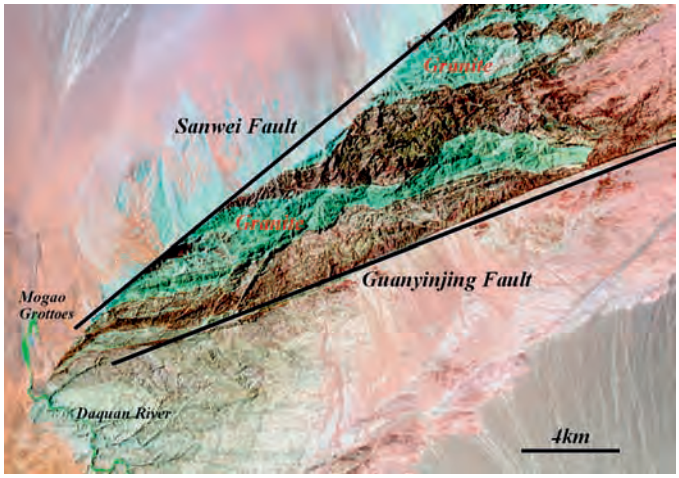

FIGURE 6 False-color satellite image showing faulting and granite intrusion (blue) in the Mogao area.

tance patterns of rocks. First a false color image (e.g., B:G:R = 2:3:4, where B:G:R shows the band that assigns blue, green, and red, respectively) was created from the satellite image. Then a *ratioing* image was obtained; that is, digital image processing was used to enhance the contrast between features in the image. Figures 5a and 5b are examples of false color images through B:G:R = 2:3:4. Figure 6 is another example of a false-color image of the Sanwei Mountains through B:G:R = 2:4:7. Two straight lines clearly appear in this image. They correspond to the Sanwei Mountain and the Guanyinjing faults, and they meet at the base of the Mingsha dunes, which are at the westernmost end of the Sanwei Mountains. Figure 6 shows that granite (blue in this image) intruded into the Sanwei Mountain formation (gneiss). On the north side of the Sanwei Mountains, the granite is cut off by the Sanwei Mountain fault, suggesting that tectonic movement took place after the intrusion of the granite.

Based on our satellite image analyses, we conclude that the present geologic situation of the Mogao area was produced in the following order:

1. formation of Precambrian metamorphic rock (gneiss) as the basement rock;
2. intrusion of granite;
3. fault movement and resulting crushing action;
4. uplifting of the earth's crust;
5. fault movement and resulting crushing action; and
6. formation of conglomerate strata in the Quaternary.

As figure 5a shows, the Daquan River changes its flow direction at many points along the faults. The Precambrian gneiss (fig. 5b) has been crushed heavily and turned counterclockwise. A large dislocation is clearly visible in the strike direction.

Possible Water Sources Affecting the Mogao Area

It is suggested that young geologic formations with high porosity, such as the Eocene limestone in Giza, Egypt, and the Pleistocene conglomerate in Dunhuang, hold groundwater. Furthermore, depending on the hydraulic gradient (slope of the aquifer), not only groundwater but also water vapor slowly but constantly moves down through the chains of pores and fissures under high hydraulic pressure. Therefore, possible water sources affecting the Mogao Grottoes are the following:

1. capillary rise of water from the Daquan River through the conglomerate;
2. rainwater seeping down from the top of the Mogao cliff;
3. moisture moving through pores in the permeable strata and through fissures; and
4. irrigation water applied to vegetation close to the Mogao Grottoes.

Daquan River

Table 1 shows data obtained by the Dang River Control Office in Subei for the catchment areas and annual flow rates of the Daquan, Yulin, and Dang Rivers. The observed annual flow rate of the Daquan River was approximately 1.5 percent that of the Dang River from the observed water volume in 1980.

Table 1 Water Supply from the Qilian Mountains to the Daquan, Yulin, and Dang/Shule Rivers (Data from 1980)

	Catchment Area (km^2)	Annual Flow Rate ($\times 10^6$ m^3/yr)
Daquan	~250 (1%)	5
Yulin	>3,500 (12%)	48
Dang	>25,000 (87%)	366

Source: Dang River Control Office, Subei (Gansu province), China.

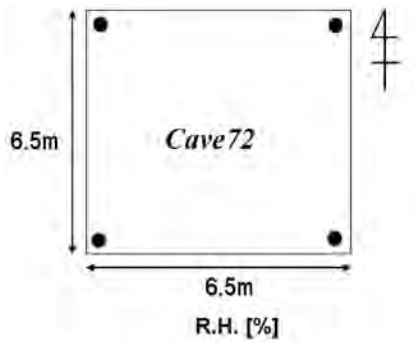

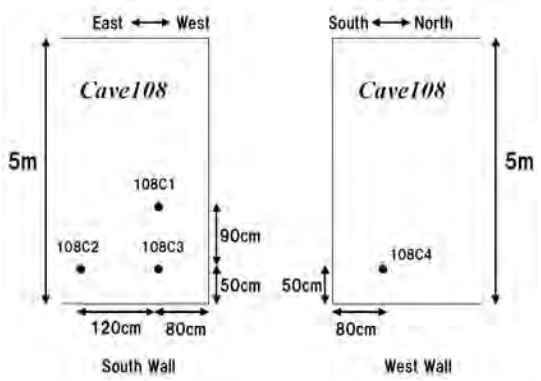

FIGURE 7 Depth profiles of relative humidity measured in drill holes made in (a) the floor of cave 72 and (b) the south and west walls of cave 108. Black dots show location of drill holes.

		NW	SW	SE	NE
Depth [cm]	0	34.3	30.7	30.7	30.4
	10	64.9	70.4	83.1	67.1
	20	73.7	73.6	83.3	75.9
	30	94.5	89.6	99.5	94.2

(a)

		South			West
		108 C1	108 C2	108 C3	108 C4
Depth [cm]	0	35.6	32.1	34.1	35.7
	10	47.6	55.7	76.0	68.5
	20	55.3	66.8	88.4	77.4
	30	59.0	73.0	96.7	85.4

(b)

Water and Moisture Movement

Figures 7a and 7b show the depth profiles of relative humidity measured in drill holes, 30 centimeters deep and 4 centimeters in diameter, made in caves 72 and 108 at Mogao. The caves are located at the bottom of the cliff on the south and north sides of the Nine-Storey Pagoda. Figure 7a shows the aggressive change in humidity in cave 72 along holes drilled vertically downward into the floor at the four corners of the cave. The relative humidity at depths of 0 meter (floor surface), 10 centimeters, 20 centimeters, and 30 centimeters rapidly changes from 30–34 percent (floor surface) to 65–83 percent (10 cm) to 74–83 percent (20 cm) to 90–100 percent (30 cm). The same tendency is seen in cave 108. Figure 7b shows the depth profile of relative humidity along holes drilled horizontally into the wall at the southwest corner of cave 108. These results strongly suggest that moisture moves upward through the rock.

The movement of moisture or water through the rock formation beneath the floor of cave 72 has been verified through electric resistivity measurements carried out between the irrigation field in front of the cave and the cave. The irrigation field is filled with enough water to create a 20- to 30-centimeter-deep pond. The irrigation water moves from east to west, showing a low value of electric resistivity in the range of 60 to 80 Ωm (fig. 8). These results suggest that the irrigation water should be minimized to the extent possible.

Summary

Based on our work at Mogao, we make the following observations:

1. Rivers run along faults with few exceptions, and these faults tend to be a cause of the deterioration of buildings and monuments over time. Therefore, in general, we should pay more attention to the existence of potential fissures relating to not only instability but also water conductivity, for better preservation of stone monuments.
2. Deterioration processes should be studied more intensively from the mechanical aspect (i.e., slaking, or the deterioration of rock due to the repetition of dry-wet conditions, salinization, loss of cementation, etc.).
3. Hydrogeologic features of the Mogao area should be examined from the macroscopic to the microscopic level.

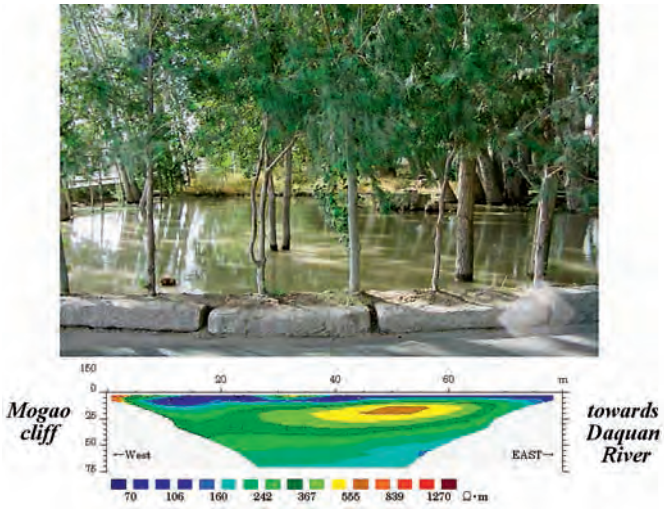

FIGURE 8 Irrigation pond in front of cave 72 (top) and electric resistivity measurements (bottom) in the rock beneath the cave.

It is important to obtain results from a variety of analytic methods in order to significantly contribute to a better understanding of the Mogao area's complicated geologic and hydrological issues. Only such an integrated approach will open up possibilities for preserving World Heritage Sites.

Acknowledgments

This joint work has been carried out with the help of many colleagues in China. The authors would like to express their sincere thanks to them, especially Xue Ping, Li Weitang, and Ding Shujun of the Dunhuang Academy.

References

Kaizuka, S. 1997. *Landforms of the World.* Tokyo: University of Tokyo Press.

Kuchitsu, N., and Duan Xiuye. 1997. Geological environment of the Mogao Grottoes at Dunhuang. In *Conservation of Ancient Sites on the Silk Road: Proceedings of an International Conference on the Conservation of Grotto Sites,* ed. N. Agnew, 244–48. Los Angeles: Getty Conservation Institute.

Ling Yuquan, Qu Jianjun, Fan Jinshi, and Li Yunhe. 1997. Research into the control of damage by windblown sand at the Mogao Grottoes. In *Conservation of Ancient Sites on the Silk Road: Proceedings of an International Conference on the Conservation of Grotto Sites,* ed. N. Agnew, 213–26. Los Angeles: Getty Conservation Institute.

Ma Lifang, Qiao Xiufu, and Liu Nailong, eds. 2002. *Geological Atlas of China.* Beijing: Geological Publishing House.

Tanimoto, C., S. Tonouchi, and S. Yoshimura. 1992. Rock mechanical observation and high-tech use of latest prospecting techniques in archaeological findings in Egypt. In *Rock Characterization: ISRM Symposium, Eurock 92, Chester, UK, 14–17 September 1992 = Caractérisation des roches = Gesteinsansprache,* ed. J. A. Hudson, 456–61. London: British Geotechnical Society.

Tanimoto, C., S. Yoshimura, and J. Kondo. 1993. Long-term stability of the underground cavern for the Pharaoh and the deterioration of the Great Sphinx. *International Journal of Rock Mechanics and Mining Sciences & Geomechanics Abstracts* 30 (7): 1545–51.

The Influence of Water on the Stone Carvings of the Yungang Grottoes

Huang Jizhong

Abstract: *The Yungang Grottoes World Heritage Site in Shanxi province was created in the late fifth and sixth century during the Northern Wei dynasty. The stone sculpture has suffered severely from capillary rise of groundwater, condensation, dissolution of mineral components, transformation of feldspar into clays, and freeze-thaw cycles. In recent decades coal industry–related pollution has worsened deterioration. This paper describes the types of stone weathering and the role of water and discusses current and future plans to mitigate deterioration through the exclusion or control of access of water to the cave temples.*

The Yungang Grottoes, excavated during the Northern Wei dynasty (460–524 C.E.), are located in the western suburb of Datong City, Shanxi province. Carved into the cliff of the Wuzhou Mountains and extending 1 kilometer from east to west, the site, with 45 major caves and 51,000 Buddha statues including reliefs, is one of the largest ancient grotto groups in China. The Yungang Grottoes were ratified as a key cultural heritage protected site in China by the State Council in 1961 and inscribed in the list of World Heritage Sites in 2001.

Over the centuries, the Yungang Grottoes have experienced weathering due to natural forces, primarily water (fig. 1), as well as man-made problems such as pollution from coal mining. Studies have shown that water at the site has four sources: capillary groundwater, condensation, seepage from the rock, and direct impact of rain.

Since 1960 channels have been dug on top of the escarpment above the grottoes to drain water to the east and west ravines and away from the site. In 1992 the Yungang Grottoes Research Institute for Historical and Cultural Relics, the China National Institute of Cultural Property, and the Getty Conservation Institute conducted joint experimental research to control the seepage problem.

Over many years, the Yungang Grottoes Research Institute has undertaken studies and conducted conserva-

FIGURE 1 Weathering of the lower part of the west wall of cave 1 due to groundwater.

FIGURE 2 Tufa-shaped and stalactite-type weathering.

FIGURE 3 Powderlike weathering.

tion work. However, the pervasive problem of water damage has not been completely resolved, and the negative influence of water on the grottoes continues. Statistics from many years of observation show that among the forty-five major grottoes at the site, those that have a record of water seepage are caves 2, 3, 5, 6, 14, 21, 23, and 34.

Main Mechanisms of Water-Caused Deterioration

Powdering of the Sandstone

A layer of white or light yellow powderlike weathered substance forms on the surface of many statues and cave walls. White and hard stalactite-like weathering substances, with protruding granules 1 to 2 millimeters in diameter are also formed. This weathering is especially serious in the lower parts of all the caves and in the caves located in the east section (figs. 2, 3). The weathered products are extremely fragile and fall off at the slightest touch.

Flaking and Scaling

Flaking and scaling result in thin layers of stone lifting from the surface of statues and cave walls. The thickness of the detached layers is dependent on the size of the mineral grains. Flakes from coarse sandstone are about 3 to 4 millimeters thick; those from fine sandstone are about 0.5 to 1 millimeter thick. There is often multilayered exfoliation. Between the layers and between the detached layers and the base rock is white powder. In places with adequate sunlight and good ventilation, such damage is especially serious (fig. 4), and one can often find detached flakes and scaling parallel to the surfaces of the statues and rocks.

Stratigraphic Weathering

Banded weathering occurs on the surfaces of the statues and rocks approximately parallel to the natural layers of rock (fig. 5).

Slablike Weathering

It is often the case that pieces of rock from the ceilings of caves and in the corners and on protruding parts of large statues detach and fall in the form of slabs 2 to 4 centimeters in thickness (fig. 6).

FIGURE 4 Scaling of the statues.

FIGURE 5 Stratigraphic weathering in cave 3.

FIGURE 6 Slab-type weathering and loss at the top of cave 19's side chamber.

Erosion by Wind and Acid Rain

Gamma ray and electrical instrumental tests show that the entrance pillars of caves 9, 10, and 12 are seriously eroded. Erosion of the five front pillars in caves 9 and 10, whose diameters are 80 to 100 centimeters, has reached a depth of 20 centimeters. Our study of weight-bearing safety factors indicates that they are in a dangerous condition. The weathering of these pillars has been caused mainly by wind and rain, especially acid rain, and snow. Due to the high content of SO_2 in the atmosphere in the district, as a result of coal mining and burning, acid rain and snow are prevalent, with serious consequences for the exposed statues. Figures 7a and 7b compare the different degrees of erosion of the same pillars on the outer and inner sides.

Water Sources in the Caves

There are four sources of water in the caves: (1) seepage directly from the ceilings and fissures in the walls; (2) capillary groundwater from the floors; (3) spring water (cave 2); and (4) atmospheric condensation.

There is a perennial spring in cave 2, which was eliminated during a reinforcement project in 1964, when a deep hidden ditch was dug to drain the water. This lowered the outflow level substantially, and as a result the spring no longer affects the cave.

The inside/outside temperature difference in the Yungang Grottoes in summer is large, and the humidity is as high as 100 percent during rain periods. When warm humid air flows into the caves and meets the comparatively cold rocks, the moisture condenses onto the surfaces. In cave 5, for instance, when the humidity inside the cave is 80 percent and the temperature inside is 10°C, the mass of condensed water over twenty-four hours is estimated to be 23 kilograms.

Water Quality and Its Influence on the Grottoes

During the period from 2002 to 2003, the chemical composition of many sources of natural water around Yungang were analyzed, including coal mine water, well water, cave 2 spring water, river water, cave seepage water, rain (snow), and bore hole and seepage water. These were compared with analyses undertaken in the 1960s.

Conclusions from analyses conducted over nearly four decades are as follows:

- Seepage water from cave 3 was found to be the closest to snow water in total mineral content, sulfate,

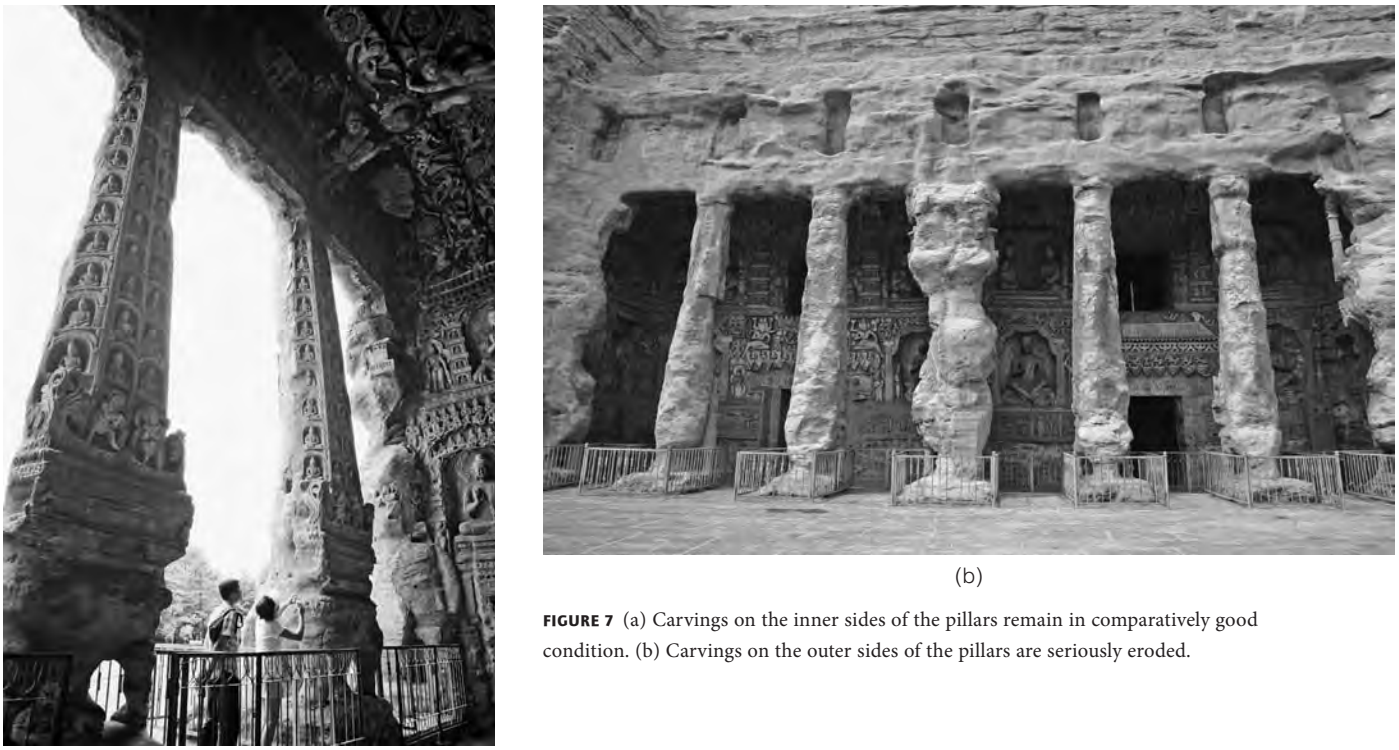

(a) (b)

FIGURE 7 (a) Carvings on the inner sides of the pillars remain in comparatively good condition. (b) Carvings on the outer sides of the pillars are seriously eroded.

and chloride content, which indicates that this water is probably melted snow water.

- The mineralization of all the samples from bores B6, B7, B1, and T3, cave 3 water, and cave 2 spring, as well as snow, water are less than 1,000 milligrams per gram, which means that there is good groundwater circulation, and those areas can be seen as a water containment system.
- The mineralization of water from a well in Yungang village and bore holes B3 and B10 is comparatively high, and water from those places and from the coal mine belong to the same category. They represent deep groundwater, with comparatively weak circulation. They have little to do with precipitation and are mainly influenced by the chemical environment of the deep system.

Based on the chemical analysis of the natural waters around the Yungang Grottoes, the pH, and the concentration of bicarbonate ion (HCO_3^-), a number of charts have been plotted (fig. 8). It is clear that bicarbonate content is higher in spring and seepage water than in snow and rain, while the spring water contains the highest bicarbonate because it has a large area to react with carbonate and dissolve bicarbonate. The seepage water in the caves is rainwater, and it has only a short time to react with the carbonate rock. Therefore, the concentrations of bicarbonate in spring water are between that of seepage water and that of groundwater.

Similarly, the pH value of rain and snow is lower than that of the seepage and spring water. Rain and snow are characterized by their low pH value and high erosion ability. Figure 9 shows that the pH value of cave 2 spring water in 2003 has considerably decreased compared to that in the 1960s, especially in winter, when pollution becomes more severe and sometimes shows acidity. Meanwhile, the content of various ionic substances has increased, and changes in values of potassium, sodium and sulfate, and chloride (K^+, Na^+, SO_4^{2-}, and Cl^-) are especially obvious. The above changes are a consequence of the serious pollution in the Yungang Grottoes area.

Effects of Water on Yungang Sandstone Sculptures

Effects on Rock with Fissures

Infiltration of water through pores and fissures, followed by dissolution of salts and chemical reactions in the rock, results in both physical and chemical deterioration. For example,

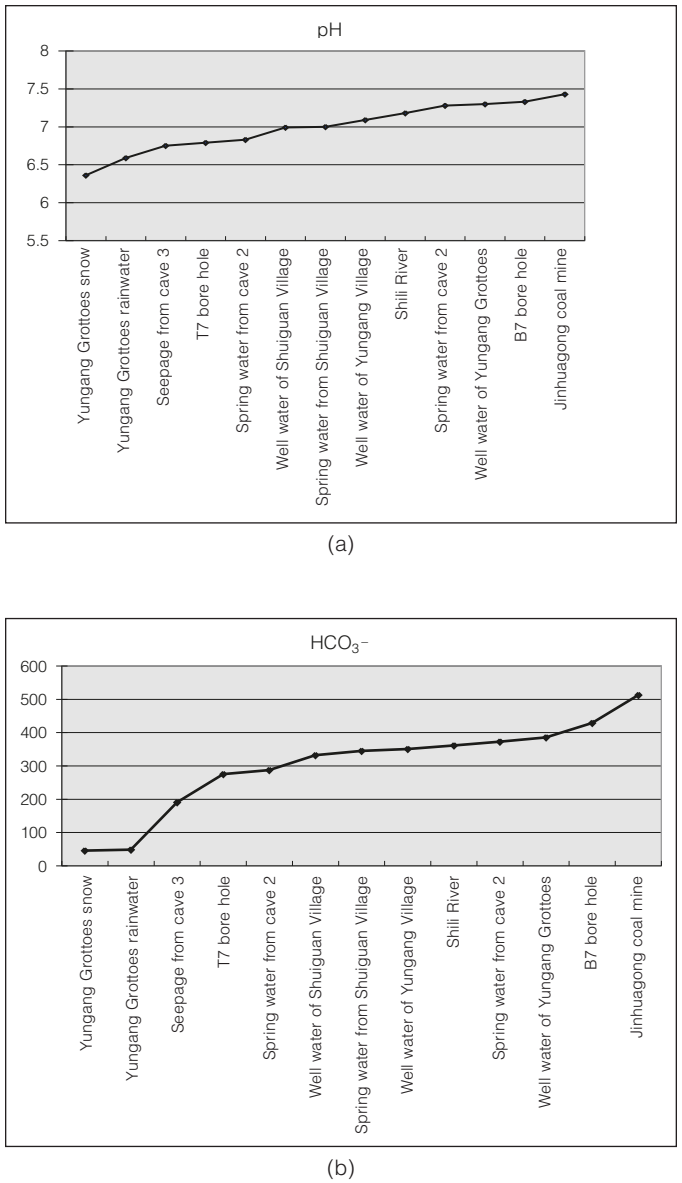

FIGURE 8 (a) The pH of and (b) the concentration of HCO_3^- in water.

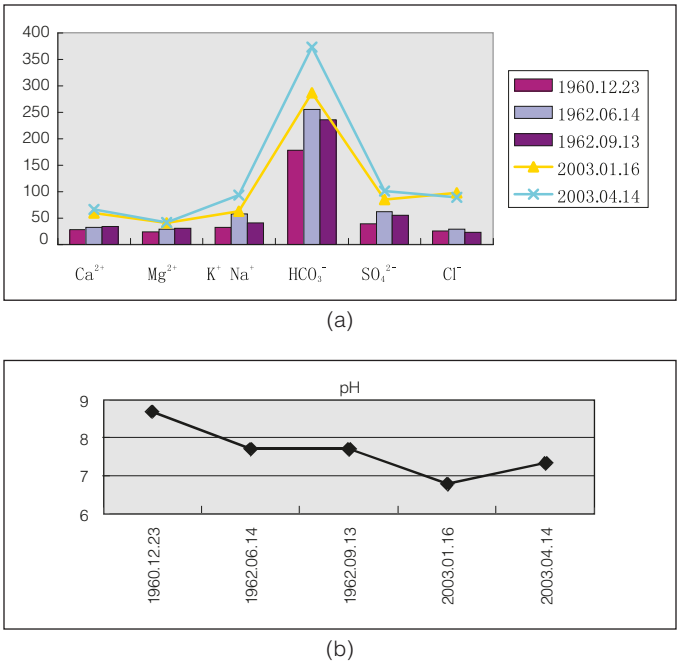

FIGURE 9 (a) Comparison of the cave 2 water quality in the 1960s and in the survey of 2003. (b) Comparison of the pH values of water in cave 2 in the 1960s and in the 2003 water quality survey.

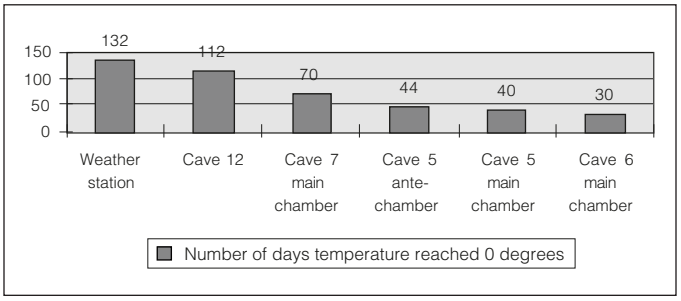

FIGURE 10 Number of days in 2002 and 2003 when the temperature reached 0°C inside and outside the caves.

chemical reaction of water may result in accumulation of clay and mineral substances within fissures. Hydrophilic clay and other minerals expand when water is absorbed and shrink when it is lost. This is why stone fragments have fallen from cave walls after rains that follow a long period of drought. For example, on August 18, 2002, after a period of rain, more than one ton of rock fell in cave 1.

Freeze-Thaw Damage. Freeze-thaw cycles at Yungang are one of the main causes of stone damage. Figure 10 shows the number of days in 2002 and 2003 when the temperature was below freezing inside and outside of caves 12, 7, 5 (front and back chambers), and 6.

Salt Crystallization Pressure. A frequently seen and pervasive weathering phenomenon of carved stone at Yungang is salt crystallization, resulting in powderlike weathering from salt fretting, flaking, and scaling, with loss and subflorescence. When the concentration of salt gets to a certain point, the shear strength of the stone is exceeded. The sand-

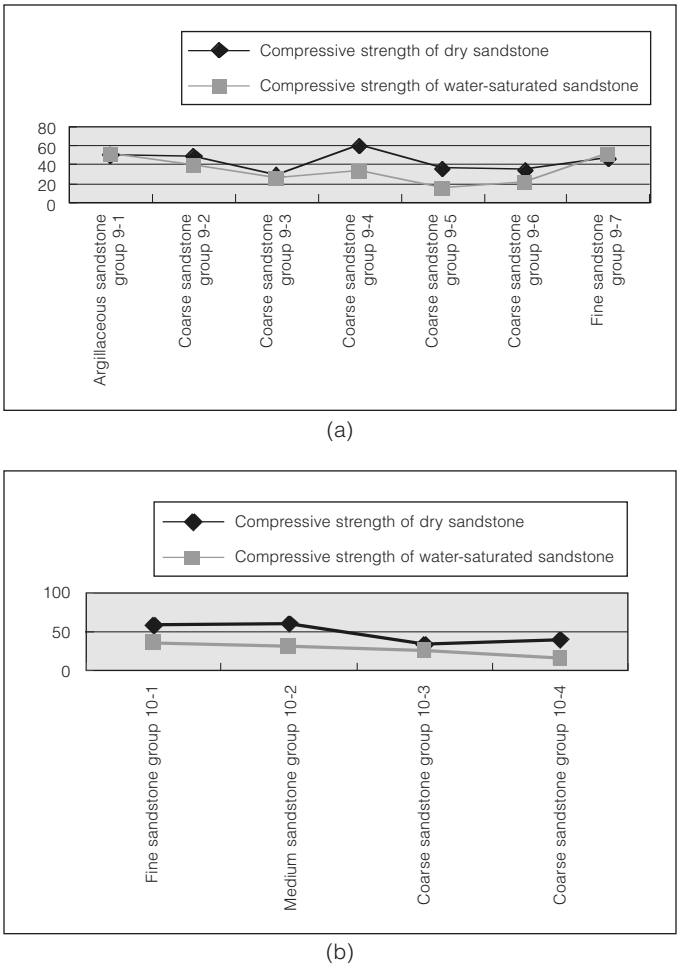

FIGURE 11 Uniaxial compressive strength comparison of dry sandstone and water-saturated sandstone.

stone at Yungang has a compressive stress of 10.8 and a shear stress of 18.7 Nmm^{-2}.

Hydration Pressure. Certain salts, including those found in the Yungang sandstone, react with moisture to form crystals containing lattice water. During this process, the volume of the crystals increases considerably. Although the hydration pressures of different salts containing water of crystallization vary with temperature and humidity and are sometimes considerably different, there is a common consequence for all: hydration pressures are greatest when temperature is low and humidity is high. Such pressures are comparable with the shear strength of the sandstone at Yungang. Figure 11 compares the uniaxial compression strength of the sandstone when it is dry and water saturated.

Chemical Effects of Water-Rock Reactions

A series of water-rock reactions occur during the chemical weathering process of the sedimentary rock of Yungang. Among those reactions, the following are most important: the solution of carbonate cement, the hydrolysis of sedimentary rock, and the formation and transformation of iron oxide and iron hydroxide minerals.

Solution of Carbonate Cement. Carbonate cement exists extensively in the fresh sedimentary rock at Yungang. Its content in coarse and medium sandstone is often between 10 and 20 percent. Therefore, the solution of cement can result in obvious changes in porosity and permeability of the rock. Comparison of the characteristics reveals that as the degree of weathering increases, more carbonate cement will dissolve and the porosity of the rock will increase. Mercury porisimetry on sedimentary rock has shown that rock porosity is also increased and that the radius of the pores of the rocks becomes larger as porosity increases; consequently, water is absorbed by the rock in greater amounts.

Hydrolysis of Feldspar. Feldspar is hydrolyzed in surface weathering. Hydrolysis produces a number of substances. Feldspar in the sedimentary rock at Yungang is mainly microcline, which experienced alternation to kaolinite in the lithogenic process. Therefore, it is comparatively difficult to identify the product of its hypergenesis.

Using microscopy, we have compared microcline in the rocks that are in different phases of weathering and classified the hydrolysis in the process of chemical weathering according to the following phases:

- Argillization: the surface of the feldspar in this phase is "dirty" compared to the clean surface of fresh feldspar. The secondary minerals are of very small size, and it is difficult to determine their composition.
- Illite: In this phase, there are bright, minute minerals inside the feldspar. Given that the interference colors are of a high order, we have identified them as illite.
- Kaolinite: Here the crystal of feldspar has completely weathered into kaolinite, or just a very small amount of it still remains.

When the feldspar has been weathered into illite, kaolinite, and other clay minerals, the mechanical strength of the rock decreases and the power of the destructive expansion of the soluble salt crystals increases. Inevitably, the stone carvings are eroded or weathered.

Conclusion

Water has played an important part in the weathering of the stone carvings at the Yungang Grottoes. All types of deterioration, including loss of stone fragments and cracks, are more or less caused by the mechanical effects of the water-rock reaction.

In terms of water-mediated chemical weathering, the following reactions are important: the solution of carbonate cement, the hydrolysis of sedimentary rock, and the transformation of iron oxide and iron hydroxide minerals. Such reactions decrease the mechanical strength of the stone and result in weathering.

The problem of severe water erosion at Yungang has led to concern from national and international scholars and the Chinese government. Currently, a conservation project to prevent water erosion impact has started, and a comprehensive survey has been completed.

A preliminary plan of water exclusion applied to the area above the caves has been discussed several times by experts. The final plan is in process; in the near future, implementation of the project will minimize the impact of water erosion and greatly slow the deterioration of the Yungang cave temples.

A Chinese-German Cooperative Project for the Preservation of the Cultural Heritage of Shaanxi Province: Conservation of the Polychrome Clay Sculpture and Investigation of Painting Materials in the Great Hall of the Shuilu'an Buddhist Temple

Catharina Blaensdorf and Ma Tao

Abstract: *The Shuilu'an Buddhist temple complex is located near the city of Lantian* ***in Shaanxi province, about 60 kilom****eters west of the provincial capital, Xi'an. The temple may date to the Tang dynasty (618–907 C.E.) or even earlier, to the Sui dynasty (581–618 C.E.). Of the three original structures (halls) in the complex, the one known as the Great Hall, or Shuilu Hall, has always been the focal point of the temple. The walls of Shuilu Hall are decorated with more than a thousand clay figures, including sculptures of Buddhas and bodhisattvas, and lively relief scenes that include architecture, animals, and nature. The sculptures and reliefs are of high artistic quality and retain their original polychromy. For more than one 150 years, water had penetrated through the leaky roof of Shuilu Hall, creating voids in the walls, detaching the clay sculptures and reliefs, and eroding surfaces. Although prior repairs and renovations were carried out, the continued detachment of sculptures and reliefs is a conservation challenge. An increase in both tourism and religious life in the region has brought more attention to the temple complex, making conservation more imperative.*

In 2000 an agreement was reached between the Bavarian State Department of Historical Monuments and the Xi'an Center for the Conservation and Restoration of Cultural Property of Shaanxi Province to conserve Shuilu Hall. The Chinese-German cooperative program, which ended in late 2002, included research on the hall's art history, materials analyses, and tests for the conservation of the clay reliefs and sculptures. This paper presents results on the history of Shuilu Hall and its construction, the modeling and painting techniques used for the clay sculptures and reliefs, the materials used, and the conservation tests and interventions conducted.

Shuilu'an is a Buddhist temple complex that dates to the Tang dynasty (618–907 C.E.) or even earlier, to the Sui dynasty (581–618 C.E.). The temple complex was built on an island in the Qing River, at the foot of the Wangshun Mountains, about 10 kilometers from the city of Lantian in Shaanxi province and about 60 kilometers west of the provincial capital, Xi'an.

The temple complex consists of three original buildings (halls) arranged in a line, flanked by secondary buildings (fig. 1). The entire complex is enclosed within walls. The history of the temple's construction is not completely settled. Although the foundation and early buildings might date to the Tang or Sui dynasty, legend has it that between 1563 and 1568 C.E., during the Ming dynasty, a prince renovated the temple for his family's use as a sacrifice hall. However, an inscription inside the temple names Qing Houli from Lantian as the initiator and benefactor of this renovation. No other records mention the prince or the local donor.

From the temple's entrance, which was added twenty years ago, one reaches the front hall (empty today) and then the middle hall, which was refurbished in 1981 with a clay sculpture of the Buddha Mile fo and wall paintings. Behind this hall lies the Great Hall, or Zhu sheng shui lu dian (Water-Earth Hall of All Saints). This Great Hall, referred to here as Shuilu Hall, has always been the focal point of the temple.

FIGURE 1 Shuilu'an Buddhist temple complex, Shaanxi province. Credit: A. Borchert, University of Heidelberg, 2001

Iconography and History of Shuilu Hall

The walls of Shuilu Hall are covered with exquisite displays of polychrome clay sculpture consisting of complicated scenes in relief, as well as three-dimensional figures, from a few centimeters to 1.6 meters high. The hall also houses twelve larger-than-life-size sculptures of Buddhas and bodhisattvas.

Figure 2 shows the layout of Shuilu Hall, whose entrance faces east. As in many temples, the hall is divided into a larger main section in the front and a smaller rear section by a freestanding middle wall that spans about two-thirds the width of the hall and by two short wall projections. This construction allows worshipers to walk in procession around the middle wall, which is the center of the temple and contains the most important religious images.

Main Section

In front of the middle wall are three large Buddha sculptures representing the "Three Great Teachers" (*san da shi*): Yaoshi fo (Buddha of healing), Sakyamuni (historical Buddha), and Amitabha (Buddha of infinite light). Four additional large Buddha and bodhisattva sculptures are positioned in the corners of the main section: Yaowang pusa (bodhisattva Baisajyaguru, at the southern wall projection), Dizang pusa (bodhisattva Ksitigharba, at the northern wall projection), Yingshen fo (Buddha, at the southern part of the east wall), and Baoshen fo (Buddha, at the northern part of the east wall).

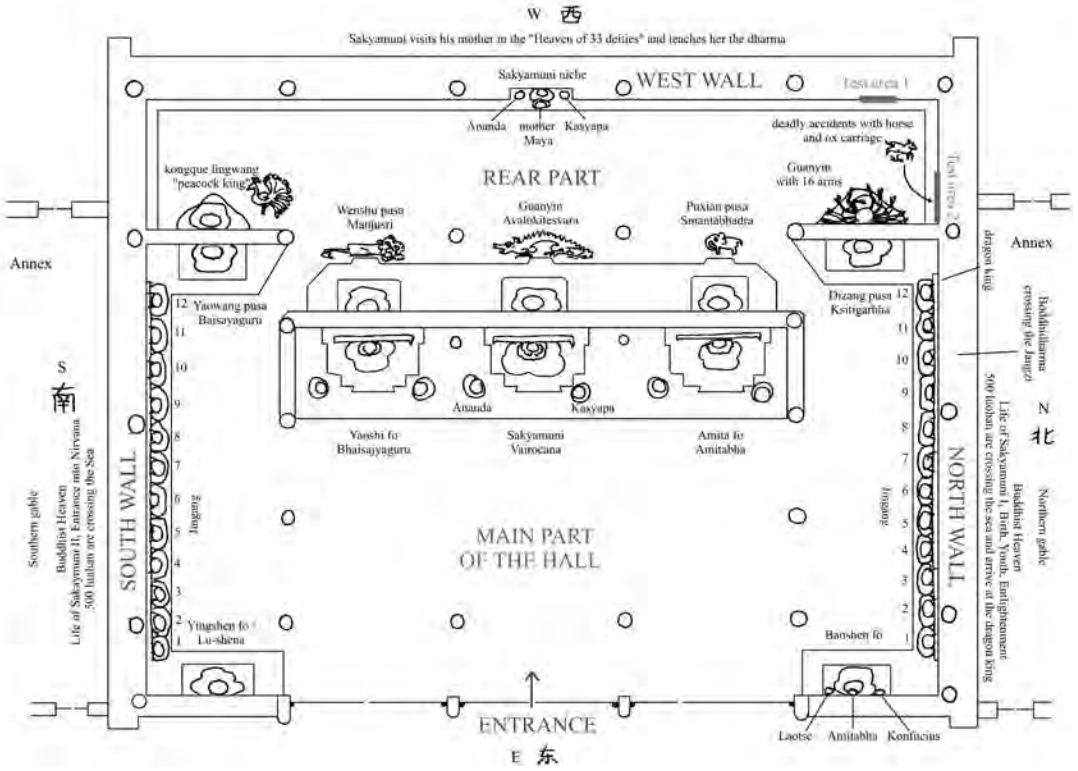

FIGURE 2 Shuilu'an Buddhist temple complex, Shaanxi province. Credit: A. Borchert, University of Heidelberg, 2001

FIGURE 3 Elaborate clay relief on north wall of Shuilu Hall depicting birth and youth of Sakyamuni. Credit: S. Scheder, Bayerisches Landesamt für Denkmalpflege München, 2002

The north and south walls are gabled and decorated with numerous artistic representations arranged on four levels. Along the bottom of each wall there are twelve life-size sculptures of *jingang* (protective deities) from 140 to 160 centimeters high. These sculptures are connected to the wall at their backs. Above them is a relief depicting five hundred *luohan* (enlightened beings) crossing the sea and visiting the Dragon King. Above this scene are large, elaborate reliefs showing the eight stages in the life of Sakyamuni, starting on the north wall with his birth and youth (fig. 3) and steps to his enlightenment and continuing on the south wall with his entrance into nirvana; the central scene depicts mourning disciples at his deathbed. The triangular upper areas of the walls are filled with reliefs showing scenes of Buddhist heaven.

Rear Section

The rear section of Shuilu Hall contains five large bodhisattva sculptures: the three along the rear-facing side of the free-standing middle wall are Puxian pusa (bodhisattva Smantabhadra on an elephant), Guanyin (bodhisattva Avalokitesvara on a dragon), and Wenshu pusa (bodhisattva Manjusri on a white lion). The two sculptures against the short wall projections extending out from the north and south sides of the hall are, respectively, the sixteen-armed Guanyin and the Peacock King (*konque lingwang*, a gold-skinned deity riding a peacock). The reliefs on the west wall and parts of the north and south walls depict "Sakyamuni in the Heaven of the 33 Deities." This scene focuses on a central niche in the west wall showing Sakyamuni's mother kneeling in front of him, surrounded by about three hundred sculptures arranged in four tiers.

The Shuilu Rite

Shuilu refers to the "Water-Land" rite that arose in the tenth century and still exists today. The ceremony is performed to plead for the remission of sins of the deceased, especially those who were not buried in an appropriate way. It is a syncretic ceremony in which the deities of Confucianism, Buddhism, and Daoism and popular beliefs are invoked. Two scenes in Shuilu Hall relate to this rite. The first scene appears above the head of the large Baoshen Buddha flanking the entrance on the north side, where there are three small sculptures of Confucius, the Buddha Amitabha, and Laotse (founder of Daoism), thus assembling the three main religions/philosophies of China. The second scene, a relief near the northwest corner, depicts brutal accidents: a man is trampled by a horse, and another is run over by the wheels of an oxcart. Scenes of deadly accidents are often shown in the context of the Shuilu rite, which involves praying for the unhappy souls of accident victims.

The Chinese-German Cooperative Project to Protect Shuilu Hall

Since 1988, when the Chinese-German Cooperative Project for the Preservation of the Cultural Heritage of Shaanxi Province began, Shuilu Hall had been discussed as a possible site for a joint conservation effort. Consideration of such a project was based on the exquisite quality of the clay reliefs and sculptures, the rareness of this technique in Shaanxi province, and the endangered condition of Shuilu Hall. At that time, the temple complex was located in a military district, cut off from public access and attention and therefore almost forgotten.

Early Repair Efforts

For more than 150 years, water had penetrated through the leaky roof of Shuilu Hall. Rainwater ran down the wooden

pillars, creating voids in the walls, detaching the clay sculptures, and eroding surfaces. This resulted in severe damage to areas below the roof and in the corners.

Starting in the early twentieth century, large-scale repairs and renovations of Shuilu Hall were undertaken. New walls of fired brick were constructed around the building (1919) to protect the original clay walls against further weathering, and the roof was repaired several times (1959 and 1981–85). During the repair campaigns of 1981–85, the clay reliefs were secured by steel anchoring. Many endangered figures in the upper parts of the walls next to the roof were removed at that time and subsequently reattached, although some figures on the west wall were attached in the wrong places. The clay walls on the east side of the hall, flanking the entrance doors, were demolished and rebuilt using fired bricks. The reliefs on these walls were secured to the roof beams with wire. The original small windows in the west wall were sealed; two openings were then cut into the east and west corners of the building, and ventilators were installed to decrease humidity in the summer.

In 1990 the fragile situation became evident when a large part of the peacock feather mandorla behind the head of the Peacock King sculpture collapsed due to vibrations from a passing airplane. In 1994 a report on the situation was compiled by the Xi'an Center for the Conservation and Restoration of Cultural Property of Shaanxi Province (Fan Juan 1994). This report became the basis for all future investigations and conservation measures. Basic work to stabilize the building was carried out until 1997. Today Shuilu Hall appears stable. The roof is watertight, and existing cracks have not become larger over the years. The climatic conditions are fairly stable.

In 1998 the site where the temple complex is located was no longer designated a military zone, and a road was built, allowing public access. Since then the temple complex has enjoyed a revival, culminating in the construction of a new hall in front of the entrance hall that is used for praying and where at least one monk lives. An increase in both tourism and religious life in the region resulted—bringing more attention to the temple complex but also making conservation more imperative.

The Chinese-German Conservation Campaign

In 2000 an agreement was made between the Bavarian State Department of Historical Monuments and the Xi'an Center for the Conservation and Restoration of Cultural Property of Shaanxi Province to cooperate in the research and conservation of Shuilu Hall. The agreement includes research on art history, materials analyses, and tests for the conservation of the clay reliefs and sculptures. The art historical research comprises the history and religious importance of the temple, the iconography, and the style of the reliefs and sculptures. This includes information on building and renovation phases, artists, donors, and religious activity. Materials analyses served to identify most of the pigments used for the sculpture polychromy. Carbon 14 dating of organic material provided data on the history and prior repairs of the building. The style of the sculptures and reliefs in Shuilu Hall indicate that its interior could have been completed in the 1560s. However, the rear section of the hall is quite different in style and looks rather old-fashioned compared to the animated and complicatedly arranged scenes in the main section. It had been thought that the rear section might be considerably older than the main section and thus spared from the Ming dynasty renovation, but the carbon 14 dating of organic additives in the mortars used in that section do not support this theory.[1]

The practical work was carried out during two campaigns of three weeks each: in September–October 2001 and in August 2002. Interventions were carried out on two test areas to determine the best methods for conserving two detached figures and a deformed, partially detached relief, as well as the walls behind them. In preparation for the conservation tests, the German-Chinese research team made maps of Shuilu Hall based on drawings and digital photographs to document in detail the extent of earlier repairs, the methods applied, and the materials used (some of which, such as concrete, were completely inappropriate). The team examined existing damage to the walls and to the at-risk sculpture. With the help of a video-borescope, they also examined conditions inside the walls. During this initial investigation and documentation of the entire wall space in Shuilu Hall, the team determined that there are 1,372 figures.

Building Technique of Shuilu Hall

Shuilu Hall is a classical construction with wooden pillars and walls, about 30 centimeters thick, made of clay and clay bricks. The lower part of the walls up to a height of 150 centimeters is made of rammed earth; the upper part of the walls is built with air-dried clay bricks. The bricks are spaced a few centimeters apart and are connected only with small amounts of mortar between them.

The walls have a 2-centimeter-thick rough cast surface made of clay mortar containing much straw and chaff. This

building technique has been used for many centuries in this region and can still be seen on old houses in Xi'an and in the countryside.

Modeling Technique used for Clay Sculptures and Reliefs in Shuilu Hall

The exquisite display of Buddhist clay sculpture in Shuilu Hall dates from the Ming dynasty, providing rare examples of this technique in Shaanxi province. Clay sculptures and reliefs are often found in Buddhist contexts. The works in Shuilu Hall show a high level of skill in sculpting and painting and were executed with a classical clay modeling technique.

A number of important temples with clay sculptures and reliefs are located in Shanxi, the province northeast of Shaanxi, some dating to the Tang dynasty (ca. 800 C.E.). These early temples have only sculptures and sometimes painted walls, but temples from the Ming dynasty often have clay reliefs covering the walls completely or in part. In this context, an inscription on the pedestal of the main sculpture of Sakyamuni in Shuilu Hall is interesting. It reads:

> Qiao Zhongchao, master of Buddhist sculptures from Shanxi [province], together with four men, has made these reliefs.

Although no record of the artist has been found, this inscription indicates that the technique and the style used in Shuilu Hall indeed came from the neighboring province of Shanxi.

Modeling sculptures in clay is a very old technique in China, described as early as 90 B.C.E. in the *Shiji* (The Grand Scribe's Record) by Sima Qian. The technique has remained relatively unchanged since then and includes the following:

1. wooden support structure;
2. hemp rope or strings wound around the wooden support to provide an attachment surface for the clay;
3. rough modeling layer with clay containing straw;
4. finely detailed modeling;
5. fine clay finish containing fibers such as hemp, silk, or cotton;
6. partial or complete paper coating followed by white primer and sizing;
7. application of decorative *pastiglia* (in Chinese, *lifen*)[2] and gilding; and
8. painting of the sculpture.

FIGURE 4 Severely damaged clay figure showing internal support structure. Credit: S. Wallner, Bayerisches Landesamt für Denkmalpflege München, 2001

This technique was also used in Shuilu Hall. All sculptures and reliefs were modeled in place in the temple. Dowels attached the art to the walls. The dowels were inserted at an oblique angle to keep the sculpture in position by its own weight, even if the dowel loosened to a certain degree.

The support structure inside the sculptures and reliefs is made of bamboo sticks or wood. For the smaller figures (up to about 50 cm high), the support often consists of only one or two vertical bamboo sticks for the body (fig. 4), with small twigs inside the forearms and wrists. The larger figures, up to about 5 meters high, have a more complicated support structure of wooden sticks and panels, reed, and wire that forms a more or less detailed outline of the sculpture. Long parts of figures such as fluttering scarves, strands of hair, or decorations on headwear are supported by a wire core. Reed bundles form the internal support for architecture and landscape reliefs.

A rough modeling layer was applied over the support structure and consisted of a coarse clay with the same composition as the clay mortar (clay with chaff and straw) on

the walls. The fine clay finish (about 3–5 mm thick) contains hemp fibers as well as sand. It was applied on the sculptures and the walls at the same time, so the same material covers all surfaces of Shuilu Hall.

Some smaller elements that were needed in large quantities were made using molds and attached with clay slip. This technique was used for such ornamental elements as clouds, railings, and roof tiles of pavilions, as well as for the faces of the smaller wall sculptures such as those on the west wall.

The clay modeling in Shuilu hall is very fine and shows detailed structures even on the smallest figurines. The fine clay finish is adapted to what will be depicted; for example, it is very smooth in preparation for architectural scenes but sandy and rough where landscapes or clouds were planned.

The twenty-four life-size *jingang* possess black glass eyes. Today all these glass eyes are broken, but several that are held in the palms of the sixteen-armed Guanyin have survived intact.

Painting Technique

The dominant colors used on the Shuilu Hall sculpture are green, red, white, and gold, often in sharp contrast. Walls, reliefs, and sculptures were painted at the same time, so the polychromy of the sculptures is the same as that of background scenes painted as murals. The polychromy is carefully applied down to the smallest details. The smallest figurines and elements (a few centimeters tall) are finely painted, even if they are barely visible.

Preparatory Layers. These started with a sizing layer, possibly of animal glue, followed by a white ground layer and another thin layer of sizing. The white ground layer consists of a white earth (the main component is muscovite mica, not kaolinite). The ground layer was grayed with charcoal black when used for painted landscapes. Joints in the modeling were covered with thin strips of paper before or during addition of the ground.

Underpainting. These preliminary paint layers were colored according to the color of the final coat. For example, gray underpainting was used for a final coat of blue, light green for greens, or orange for red. Underdrawings of orange and green demarcated areas of different color.

Overpainting. The final colors were translucent and applied in several layers, thus making them increasingly opaque with each additional layer, a technique similar to watercolor painting. The effect of this technique is highly visible on the multicolored trimmings of robes, where at least four layers were applied, making the color darker and brighter with each layer.

Binding Medium. The binding medium has not yet been identified. The paint layers today appear matte and are highly sensitive to water, so an aqueous binding medium such as plant gum or animal glue might have been used for both the primer and the colors.

Pigments. The pigments identified so far are white earth (in robes, architecture, clouds); a mixture of lead white and shell white (in white lines and faces); cinnabar, often with an underpainting of minium (red lead); hematite and orpiment (to create brown colors); atacamite; indigo; and charcoal black. Pink consists of white earth mixed with red iron oxide when used for clouds or garments but mixed with cinnabar when used for faces.

Special colors in this palette are the greens and the blues. Instead of malachite and azurite, the pigments normally used for these colors, atacamite and indigo were found. The atacamite is artificial, as seen in its morphology. The indigo was extended with natural chalk, a material that was not found in any other place in Shuilu Hall.

Gilding. Gilding was applied with an aqueous medium and was not burnished. On smaller decorations, gold leaf cut into tiny squares, often only 5 by 5 millimeters, was applied. In contrast to the usual order of creating traditional Chinese clay sculpture, this gilding was executed after the painting.

Decoration Techniques. For decorations on garments with flower or geometric patterns, different techniques were used. The garments of the larger sculptures are decorated with elaborate patterns of painted or gilded *pastiglia*. *Pastiglia* and painted decorations are often combined (fig. 5). On the pedestals of the large Buddhas, very fine clay decorations made in molds were used instead of *pastiglia*. Four small scenes of flying cranes and landscapes were created in fine gold *sgraffiti*.[3]

Mordant gilding, in which a sticky, viscose material was used to adhere gold leaf to the paint layer, was used for geometrical decorations on the robes of smaller figures.

Conservation Challenges of Shuilu Hall

The biggest conservation problem for Shuilu Hall is the continued detachment of sculptures and reliefs, especially from the west wall and the adjacent parts of the north and south walls. The sculptures and relief sections tilt away from the wall under their own weight. The dowels attaching the sculptures and reliefs to the walls are pulled into a horizontal

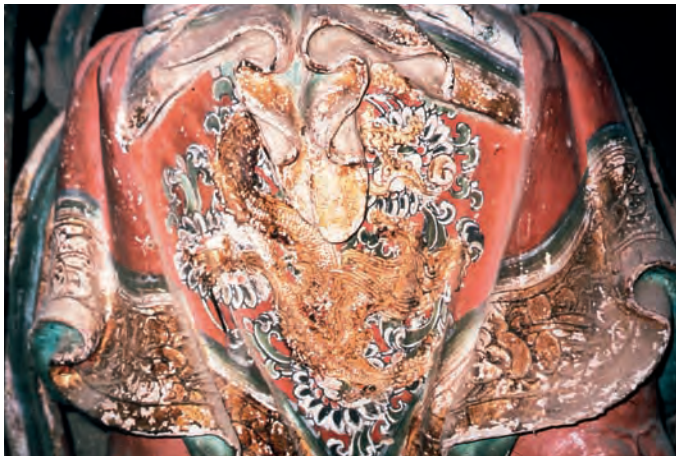

FIGURE 5 Gilded *pastiglia* dragon and painted flowers on the robe of a *jingang* sculpture. Credit: S. Wallner, Bayerisches Landesamt für Denkmalpflege München, 2001

position and can no longer hold up the art. Some reliefs have deformed considerably because of this process. On the west wall, in particular, many of the figures, about 50 centimeters high and weighing 3 kilograms, now hang only at the tip of a single dowel. Consequently, the figures tend to fall from the walls. Temporary fixes—for example, securing the sculpture with wire attached to nails in the wall—are not sufficient and are visually objectionable (fig. 6).

The visual appearance of the walls is especially affected by surface damage. Parts of the wall sculptures are severely eroded by water or are missing completely. Water damage has caused the paint layer to lose its cohesion and turn into powder. Heads, small figures, and parts of architecture are often missing in areas that were easily reachable by visitors, before barriers were installed. All surfaces are covered with dust, a problem that has increased because of the added ventilation system. The ventilators draw in dusty air from the courtyard. There are screens in front of the ventilators to exclude birds, but these are not fine enough to prevent the entrance of dust. The areas below the ventilators are especially dusty.

Many white painted areas, especially in faces, appear slightly gray today due to discoloration of the lead white in the paint layers caused by sulfur from the air. Interestingly, minium (red lead), which as a lead oxide can also be affected by sulfur, does not show any recognizable changes.

Conservation Tests

The Chinese-German team began work on Shuilu Hall in 2001. Two test areas were selected for conservation in the northwest corner to be representative of the severer damage (see fig. 2).

FIGURE 6 Test area 1 prior to conservation, showing two detached clay figures held in place by wire and nails. Credit: S. Scheder, Bayerisches Landesamt für Denkmalpflege München

FIGURE 7 Test area 1 after conservation. Credit: C. Blaensdorf, Bayerisches Landesamt für Denkmalpflege München

FIGURE 8 Test area 2: "Deadly accident" relief after conservation. Credit: Technical Center for Conservation, Xi'an, China

Test area 1 consists of two figures detaching from the west wall; they were held in place by only a few nails and wires as the dowels had completely loosened from the wall. Figure 6 shows these figures before conservation; figure 7 shows them after conservation. One detached sculpture was used for tests to stabilize the clay layers.[4]

Test area 2 was the relief of the "deadly accident" scenes described earlier. This is a large relief, measuring about 2 square meters (fig. 8).

The two test areas were used to determine the best methods for the following:

- cleaning the surfaces;
- consolidating the powdery paint layers;
- removing poorly or erroneously attached sculptures from the walls;
- repairing the walls behind the reliefs and sculptures;
- structurally stabilizing the wooden support structure and clay layers of the figures;
- resecuring the sculptures or reliefs to the walls; and
- completing missing pieces of the clay sculpture (only if necessary for their stabilization).

Conservation Interventions

The primary goal of the conservation effort was to keep interventions to a minimum and to stabilize the walls and sculptures in their current condition. The following describes the initial actions taken for the two test areas.

Paint Layer. After several tests with different adhesives, the surface of the paint layers was dry-cleaned and consolidated with polyvinyl alcohol (Mowitol 4-88; 2% and 5% diluted with water).

Clay Layers of Walls and Sculpture. The best results for stabilizing the clay layers and grouting voids were achieved by applying the same type of material that had been used for the fine clay finish. This consisted of clay from local deposits mixed with hemp paper and sand.[5] Grouting was used for the smaller voids inside the wall in test area 1.

Deformed Clay Relief. The deformed "deadly accident" relief in test area 2 was no longer in contact with the eroded wall; it was standing on a ledge along its lower edge and was partially attached to another relief along its upper edge. Behind the lower part of the deformed relief, the gap measured about 6 centimeters. Investigations with the videoborescope showed that the dowels originally used to attach the relief had slipped out of the wall and, unable to carry the relief's weight, had broken off. After a long discussion, it was decided to remove the deformed relief. This is a highly invasive action, and it is not planned on a larger scale for the rest of Shuilu hall. The detached relief was reshaped into its original form by placing it facedown on a soft but stable support and moistening the back side. The moisture softened the relief slightly so that it straightened out under its own weight. After the wall had been stabilized and a new layer of clay mortar applied, the relief was reattached. Two years later, no new damage has occurred, except for recent layers of dust covering the surfaces.

Conclusion

The exemplary conservation work done in Shuilu Hall, executed in two campaigns of only three weeks each, demonstrates that conservation of the entire hall will be possible with promising results at a rather low cost. Although the reliefs and sculptures in Shuilu Hall are fragile in places and minor areas cannot be reconstructed, the building is stable and important parts of sculptures and reliefs are still preserved and can be rescued. Thus it is still possible to understand the temple's special iconographic program, that is, its imagery or symbolism, associated with tantric Buddhism in relation to the syncretic Shuilu rite, and to enjoy its artistic quality.

The Chinese-German conservation effort concluded in late 2002, when funding from Germany ended. During winter 2002–3, seven more figures at risk of falling had to be removed from the walls. This illustrates the dangerous situation of the sculpture in Shuilu Hall and the urgency of the conservation work. The Xi'an Center for the Conservation and Restoration of Cultural Property of Shaanxi Province has applied for financial support from the Shaanxi Cultural Relics Bureau for the conservation of the entire Shuilu'an temple complex. We hope to find a way to continue this urgent task.

Acknowledgments

The authors wish to extend special thanks to Director Hou Weidong and Yang Qi of the Xi'an Center for the Conservation and Restoration of Cultural Property of Shaanxi Province; to Fan Juan, formerly with the Technical Center; and to Rolf Snethlage, of Bayerisches Landesamt für Denkmalpflege, head of the German side of the project. We also wish to thank Zhang Xiaorong, Liu Linxi, Yang Qiuying, and Dang Xiaojuan of the Xi'an Center for the Conservation and Restoration of Cultural Property of Shaanxi Province, all of whom worked on the conservation campaign. Zhen Gang, photographer at the Xi'an Center for the Conservation and Restoration of Cultural Property of Shaanxi Province, provided the first professional detailed photographs of the reliefs. Siegfried Scheder, freelance conservator from Ochsenfurt, carried out the practical work, from mapping to conservation, in the Shuilu'an temple complex, along with student assistant Stephanie Wallner. Vojislaw Tucic and Rupert Utz, of Bayerisches Landesamt für Denkmalpflege, conducted additional analyses; Angelika Borchert, of the University of Heidelberg, Department of East Asian Research, researched the Shuilu'an temple complex's history and iconography and the Shuilu rite as part of her Ph.D. dissertation; Lucien Van Valen, with the Research School of Asian, African, and Amer-Indian Studies, Leiden, contributed additional information on painting techniques and materials.

Notes

1 The results of seventeen samples indicate a date between 1440 and 1630 C.E. (except for one sample from the west wall dated at 1030–1380). The ^{14}C-AMS (accelerator mass spectrometry) dating was done by Gerhard Morgenroth, University of Erlangen, Germany, and Georges Bonani, Institute for Particle Physics, Swiss Federal Institute of Technology (ETH), Zurich.

2 *Pastiglia* are raised decorations made by the application of a priming material on the white primer or between priming layers. The composition of the decoration material is different from the primer and usually is white, ocher yellow, or reddish.

3 *Sgraffito* is a method for creating a design by incising one layer of color to reveal another color underneath. To create the scenes of flying cranes and landscapes, a plain area was first gilded and burnished and then covered with a translucent paint layer. A fine pointed tool was used to scratch off the color in the desired design, creating a golden scene on a colored background.

4 The sculpture had been stored in the office of the temple director, and its original location in the hall was not recorded.

5 Following a recipe provided by local workers, a layer of clay mixed with water was placed in a bucket and covered with a layer of paper made of hemp. This was followed by several more layers of clay and paper as well as sand. After twenty-four hours, the contents of the bucket were stirred, causing the paper to separate into fibers.

References

Fan Juan. 1994. Shaanxi sheng Lantian Shuilu'an, nizhi caihui bisu fenghua jilu ji jia gu jishu yanqiong (Studies on the weathering mechanisms of the painted clay sculptures in Shuilu'an temple). Internal report in Chinese. Partial translation into German in the Bayerisches Landesamt für Denkmalpflege, Munich.

Sima Qian. 1936. *Shiji (The Grand Scribe's Record) ca. 90 B.C.E.* Shanghai: Shang wu yin shu guan.

Two Methods for the Conservation of the Polychromy of the Terracotta Army of Qin Shihuang: Electron Beam Polymerization of Methacrylic Monomers and Consolidation Using Polyethylene Glycol

Daniela Bathelt and Heinz Langhals

Abstract: *The life-size sculptures of the Terracotta Army of the first Chinese emperor, Qin Shihuang, are among the most famous archaeological monuments in the world. The site, located in Lintong, about 45 kilometers northeast of Xi'an, is still being excavated. Rows of soldiers are on display in the site museum. The sculptures, gray-brown in color, originally were painted vividly, then buried for 2,200 years in humid soil. Soon after excavation and exposure to a dry environment, the polychromy of the terracotta sculptures flaked off rapidly as water was lost from the ground layer, which is made of East Asian qi-lacquer. For this reason, after excavation and before conservation begins on other terracotta pieces, the objects are maintained in a humid environment to prevent detachment of the paint layer. Our project concerns the development and testing of special conservation methods to preserve the polychromy of the Terracotta Army. This work is being carried out in both Germany and China.*

The problem facing conservation of the terracotta figures is stabilizing the lacquer layer in such a way that it no longer shrinks when it loses water. None of the substances usually used for restoration give positive results. This paper discusses two new strategies that have been developed for conserving the polychromy: polyethylene glycol (PEG) consolidation and electron beam polymerization of 2-hydroxyethyl methacrylate (HEMA). Both PEG consolidation and electron beam polymerization have proven capability to serve the conservation needs of the Terracotta Army. Both have clear advantages, but each also has room for improvement.

The Terracotta Army is among the most famous archaeological monuments in the world and one of China's greatest tourist attractions. Almost everyone has seen pictures of the rows of life-size soldiers, gray-brown in color, like the earth around them (figs. 1, 2). But it is not well known that

FIGURE 1 View of the Terracotta Army in pit no. 1.

FIGURE 2 Colored kneeling archers in pit no. 2.

these figures were originally painted vividly; the colors were lost after the figures were excavated (Rogner et al. 2001). This paper discusses the problem encountered in trying to preserve the polychromy on other terracotta figures and the solutions we have developed.

The Terracotta Army

When the Terracotta Army was discovered on March 29, 1974, in Lintong, about 45 kilometers northeast of Xi'an, it quickly became a sensation. Approximately eight thousand life-size terracotta warriors and horses had been entombed in four pits about 1.5 kilometers from the tomb of the first emperor of China, Qin Shihuang (259–210 B.C.E.). The Terracotta Army is said to protect the "city" of the "sleeping emperor," whose mausoleum has not yet been excavated. There are about one hundred other pits in the burial complex, containing not only terracotta figures but also life-size horses, weapons, carriages, and birds made of bronze and armor carved out of limestone. In 1987 UNESCO added the Terracotta Army and the Tomb of the First Qin Emperor to the World Heritage List.

When the emperor died, the burial complex was pillaged. The weapons of the terracotta warriors were stolen, and the underground wooden structures that protected the warriors were set on fire. The structures collapsed, burying the figures in water-saturated soil for two millennia and creating challenges for the conservation of the polychromy on the figures.

Polychromy

Structure

As shown in figure 3, the polychromy on the terracotta figures consists of

- a base, or ground, of qi-lacquer (Kryo-SEM [scanning electron microscopy] clearly shows that the qi-lacquer was applied as a double layer, each layer 20 microns [µm] thick; fig. 4); and
- a pigment layer. The binding media could not be identified.

Although analysis has not identified an isolation layer below the base, this third layer must have existed to prevent the qi-lacquer from penetrating the terracotta.

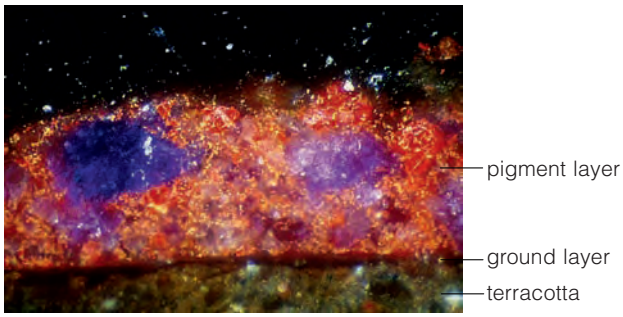

FIGURE 3 Polychromy structure.

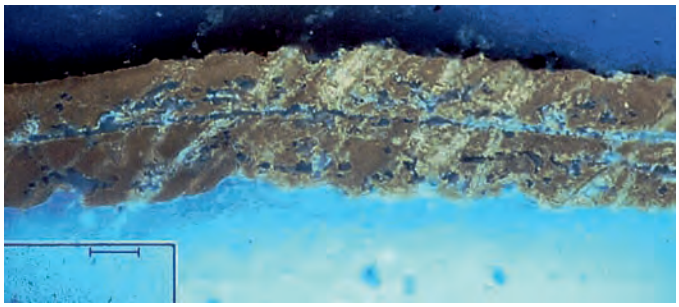

FIGURE 4 Double layer of qi-lacquer ground.

Qi-lacquer is a hydrophobic material (Thieme et al. 1995) obtained from the East Asian lacquer tree *Toxicodendron vernicifluum*. In addition to water, the main components of the raw material are polysaccharides, glycoproteins, and benzcatechin derivatives, which polymerize to form a black lacquer.

The painted figures of the Terracotta Army had been buried for 2,200 years in damp soil. As long as the figures are kept in a humid environment, water remains incorporated in the lacquer layer. But after excavation and exposure to a dry environment, the lacquer quickly loses water (fig. 5). This layer soon shrinks, develops a detailed cracking pattern, shows deformation, loses its adhesion to the terracotta, and falls off.

If flaking occurs, conservation is problematic; there is no satisfactory way to reaffix the detached layers to the terracotta. For this reason, after excavation of new pieces and before conservation begins, the objects are maintained in a saturated atmosphere—100 percent relative humidity (% RH)—to prevent detachment of the paint layer.

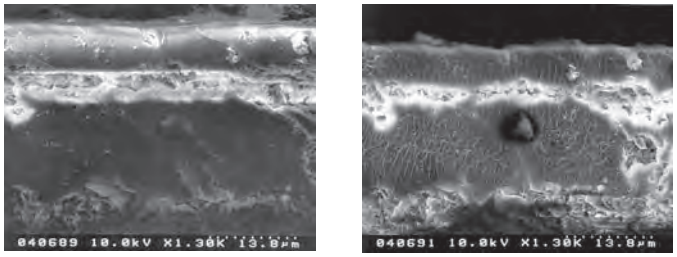

FIGURE 5 Kryo-SEM images of the qi-lacquer ground saturated with water (left) and dry (right).

Stabilization and Consolidation

In order to conserve the terracotta figures, the lacquer layer must be stabilized in such a way that it no longer shrinks when it loses water. Previous conservation attempts and analysis of the lacquer's structure indicate that the lacquer layer can be stabilized by substituting a hydrophilic consolidant for the water in the lacquer. This substitution must be undertaken in several steps, with increasing concentration of the consolidant. If the substitution is done too quickly, cracks form.

The material used as consolidant and adhesive has to have good long-term stability and be at least partially reversible. Further, it must tolerate seasonal climate changes (winter, down to 2°C, as low as 20% RH; summer, up to 37°C, as high as 85% RH) since the exhibition halls where the Terracotta Army is on display are not climate controlled to museum conditions.

Our group tried many times to find a way to stabilize and consolidate the lacquer, but none of the substances usually used for restoration gave positive results. Two new possibilities have been developed to conserve the polychromy: PEG consolidation and electron beam polymerization.

PEG Consolidation

PEG consolidation uses short-chain polyethylene glycol 200 (PEG-200), which is well known for conserving waterlogged wood. The PEG-200 consolidant is applied as a poultice in three steps to slowly substitute for 30, 60, and 80 percent of the water in the lacquer base. Each step takes two days. An adhesive dispersion is added in the first step to stabilize the layer. We have used a polyurethane dispersion, which shows good adhesion. For better long-term stability, however, a polyacrylate dispersion should be used.

Electron Beam Polymerization

With electron beam polymerization, one substance takes over the tasks of stabilization and consolidation. The object being treated is first soaked in a monomer that replaces the water in the lacquer layer. Afterward the object is irradiated by an electron beam. The irradiation creates free radicals of the monomers, which start a chain reaction that builds up the polymer in situ, at the important interface between the terracotta and the lacquer. As with PEG consolidation, a poultice is used to apply the monomer in three steps for 30, 60, and 80 percent water substitution. Each step lasts at least forty-eight hours.

The monomer used for this method has to be highly miscible with water and, on irradiation, form a polymer with a low glass transition point and good aging characteristics. A monomer that has these properties and has already been used to conserve waterlogged materials is 2-hydroxyethyl methacrylate, a derivative of methacrylic acid (Rogner 2000). With its OH-function, it is very hydrophilic. HEMA is miscible with water in any ratio, has a glass transition temperature of about 11°C, and has acceptable aging properties. For these reasons, HEMA was used for initial tests to stabilize the polychromy.

Polymerization can be initiated once the final concentration of monomer in the object has reached 80 percent. Various techniques were considered, but most of them failed:

- UV/visible light of any wavelength cannot penetrate the black lacquer.
- X-rays and γ-rays either damage the terracotta or do not generate enough radicals (Rogner 2000).
- High temperature damages the lacquer.

Molecular radical initiators cannot be applied at the interface between lacquer and terracotta. The only possibility left is electron beam irradiation. The accelerated electrons can penetrate the terracotta down to about 2 millimeters. They generate reactive radicals of the HEMA monomer, which themselves react with other monomers to form a relatively homogeneous polymer that stabilizes and consolidates the polychromy (fig. 6). The polymerization takes place mainly in the upper layer of the terracotta, where the electrons are absorbed, and it does not cause any side reactions with the pigments, which remain stable during irradiation (Barcellona Vero et al. 1976; Bathelt 2002; Serra 1972).

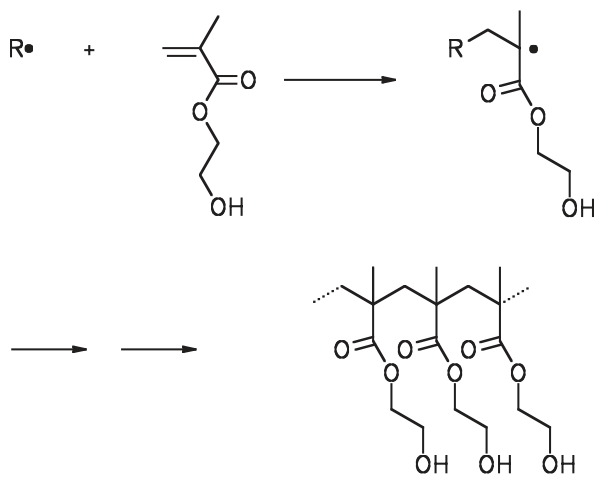

FIGURE 6 Polymerization reaction of HEMA.

HEMA itself does not form a sufficiently adhesive polymer in the terracotta. Therefore, a polyfunctional monomer has to be added to the mixture to cause cross-linking in the polymer. The cross-linking inhibits migration of the polymer and effects better adhesion of the polychromy to the terracotta.

For the cross-linking agent, polyethylene glycol dimethacrylate 550 (PEG-DMA 550) was used. During the first attempts at cross-linking, a high ratio of PEG-DMA 550 (15 w% of acrylate in the aqueous consolidation mixture) was used. This high ratio resulted in a highly brittle polymer that is sensitive to environmental changes. Therefore, the ratio of cross-linking agent was reduced.

Not all the monomer molecules in the consolidant are polymerized by electron beam irradiation. Most of them are still unreacted after irradiation and remain in the terracotta. HEMA evaporates after a while, but PEG-DMA 550 does not. This kind of cross-linking agent remains in the terracotta and undergoes delayed polymerization via metal catalysis, mostly promoted by copper-containing pigments. The copper-containing pigments used for the statues in the Terracotta Army are Han purple, $BaCuSi_2O_6$; malachite, $Cu_2CO_3(OH)_2$; and azurite, $Cu_3(CO)_3(OH)_2$.

Metal-catalyzed polymerization, especially with copper-containing pigments, produces shiny spots on the surface of the polychromy. The spots emerge months after treatment; they are soft in the beginning and become harder with time. Fourier transform infrared spectroscopy reveals that the spots consist of polymerized PEG-DMA.

To avoid these effects, the cross-linking monomer has been changed to a shorter chain: ethylene glycol dimethacrylate (EG-DMA). EG-DMA is able to cross-link HEMA in a way similar to that of PEG-DMA, and it evaporates more easily at normal room climate. In contrast to PEG-DMA, EG-DMA is applied in a lower ratio, producing a less rigid polymer. In this way, it should be possible to avoid shiny spots.

Physical Setup for Electron Beam Polymerization

Electron beam polymerization is easily done, but it requires access to an electron beam facility, which is not usually available. Fortunately, we have access to one at the Institute for Polymer Research in Dresden, Germany, as well as at the Xi'an Radiation Research Center in Lintong, China.

At the Dresden facility, the object to be irradiated is placed on a tray that passes through several shielding gates on its way to the outlet of the electron accelerator. Electrons are generated in a vacuum by a heated cathode, and the emitted electrons are accelerated in an electrostatic field applied between cathode and anode. Acceleration takes place between the cathode, which is at high negative voltage potential, and the grounded accelerator vessel (anode). The energy gain of the electrons is proportional to the accelerating high voltage. After moving past the outlet of the accelerator, the tray passes through several additional shielding gates to the exit. The shielding is necessary because of the X-rays (Bremsstrahlung) that are generated during the production of the electron beam. One should also be aware of the large amount of ozone that is a by-product.

Electron beam polymerization was developed in cooperation with the Institute of Polymer Research in Dresden, where an ELV-2, INP Novosibirsk accelerator is used. The energy of the electron beam at the Dresden facility can be varied between 0.6 million electron volts (MeV) and 1.5 MeV; the maximum current is 25 milliamps (mA). This polymerization method has also been adapted to the ELV-8, INP Novosibirsk accelerator used at the Lintong facility.

To determine the best irradiation values to use for treating an object, the following parameters have to be taken into account:

- the distance from the tray to the outlet of the accelerator, since oxygen in the air slows down accelerated electrons; and
- the electron beam radiation dose, since heat develops in the object and increases enormously with increasing dose.

Various tests showed that the best values for irradiating objects are 1 MeV, 2 mA, and 60 kGy (radiation dose). At a dose lower than 60 kGy, the polymer does not harden enough to consolidate. At a higher dose, the heat generation is so high that the polychromy becomes seriously damaged.

Conclusion

Both PEG consolidation and electron beam polymerization have proven capability to serve the conservation needs of the Terracotta Army. Both have clear advantages, but each also has room for improvement.

Electron Beam Polymerization. Objects treated with this method retain what was probably the original matte appearance of the pigments. However, cracks and shiny spots have developed in the polychromy of some treated objects. Further research is needed to improve the resulting polymer, for example, by using a shorter chain cross-linker such as EG-DMA. In addition, it will be necessary to build a device to treat round objects under the electron beam.

PEG Consolidation. This treatment can be applied in situ, while objects are still in the pit immediately after excavation, as well as on objects that already show damage from drying. Treated objects do not develop cracks and shiny spots, but they look much darker after treatment and stay wet. Their appearance is duller than with electron beam polymerization, and they tend to attract dust.

Acknowledgments

The authors would like to thank Wu Yongqi, Zhou Tie, Zhang Zhijun, Rong Bo, Xia Yin, and Zhang Shangxin of the Museum of the Terracotta Army of Qin Shihuang, Lintong, Shaanxi, China; Ingo Rogner, Cristina Thieme, Christoph Herm, and Rupert Utz, former coworkers on the China Project at the Bavarian State Department of Historical Monuments, Munich, Germany; Sandra Bucher, Felix Horn, Catharina Blänsdorf, and Rolf Snethlage, current coworkers on the China Project at the Bavarian State Department of Historical Monuments, Munich, Germany; Herbert Juling of MPA Bremen, Germany; Gerd Gülker, Arne Kraft, and Akram El Jarad of the University of Oldenburg, Germany; and BMBF for financial support.

References

Barcellona Vero, L., G. Magaudda, Rota Rossi-Doria, and M. Tabasso Laurenzi. 1976. Radiosterilizzazione di tavole dipinte: Azione sui microrganismi ed effetti collaterali sulla colla di congilio e su alcuni pigmenti. In *International Conference, Applications of Nuclear Methods in the Field of Works of Art (Rome-Venice, 24–29 May 1973) = Congresso internazionale, applicazione dei metodi nucleari nel campo delle opere d'arte (Roma-Venezia, 24–29 maggio 1973),* ed. R. Cesareo. Atti dei convegni lincei. no. 11. Roma: Accademia nazionale dei Lincei.

Bathelt, D. 2002. *Forschungsbericht 2001–2002 des Projektes "Eprobrung und Optimierung der Konservierungstechnologien für Kunst- und Kulturgüter der Provinz Shaanxi, VR China" = Work Report of 2001 and 2002 for the "Project Testing and Optimising of Conservation Technologies for the Preservation of Cultural Heritage of the Shaanxi Province, PR China."* Munich: Bayerisches Landesamt für Denkmalpflege.

Rogner, I. 2000. Festigung und Erhaltung der polychromen Qi-Lackschichten der Terrakottakrieger des Qin Shihuangdi durch Behandlung mit Methacryl-Monomeren und Elektronenbestrahlung (Teil 1): Untersuchungen zu Synthese der 6,6'-Bis (diorganylamino)-oxindingos (Teil 2). Ph.D. dissertation, Ludwig-Maximilians-Universität München. http://edoc.ub.uni-muenchen.de/309/1/Rogner_Ingo.pdf.

Rogner, I., H. Langhals, Zhou Tie, Zhang Zhijun, Rong Bo, and C. Herm. 2001. Consolidation and preservation of the polychrome qi-lacquer layers of the Terracotta Army of Qin Shihuang by treatment with methacrylic monomers and electron beam curing. In *Die Terrakottaarmee des ersten chinesischen Kaisers Qin Shihuang = The Terracotta Army of the First Chinese Emperor = Qin Shihuang ling bingmayong,* ed. C. Blänsdorf, E. Emmerling, and M. Petzet, 594–617. Arbeitshefte des Bayerischen Landesamtes für Denkmalpflege, vol. 8. Munich: Bayerisches Landesamt für Denkmalpflege.

Serra, M. 1972. Controllo dei colori sottoposti a radiazioni gamma. *Quaderno de la Ricerca Scientifica* 81: 50–54.

Thieme, C., E. Emmerling, C. Herm, Wu Yongqi, Zhou Tie, and Zhang Zhijun. 1995. Research on paint materials, paint techniques and conservation experiments on the polychrome Terracotta Army of the first emperor Qin Shi Huang. In *The Ceramics Cultural Heritage: Proceedings of the International Symposium, The Ceramics Heritage, of the 8th CIMTEC—World Ceramics Congress and Forum on New Materials, Florence, Italy, June 28–July 2, 1994,* ed. P. Vincenzini, 591–601. Monographs in Materials and Society, no. 2. Faenza: Techna.

The Stone Armor from the Burial Complex of Qin Shihuang in Lintong, China: Methodology for Excavation, Restoration, and Conservation, including the Use of Cyclododecane, a Volatile Temporary Consolidant

Sandra Bucher and Xia Yin

Abstract: *In 1998 more than eighty sets of ceremonial stone armor, including forty helmets for soldiers and horses, were discovered near the mausoleum at Lintong of Qin Shihuang, the first Chinese emperor, through the systematic work of Chinese archaeologists. The armor was made from limestone plates connected with bronze wires. The material showed a wide spectrum of conditions. Some parts were well preserved; others were severely damaged by a fire set during the succeeding dynasty.*

In May 2000 a Chinese-German partnership between the Museum of the Terracotta Warriors and Horses in Lintong and the Bavarian State Department of Historical Monuments in Munich began to investigate ways to preserve the stone armor. The limestone and the bronze were analyzed by instrumental techniques. In addition, petrographic analyses determined water uptake, and tensile strength and porosity of the armor were measured. The investigations yielded information about production techniques, materials used, conditions of the materials, and the decay process affecting the stone plates and its physical and chemical causes. Based on these results, a conservation plan is being developed for the armor.

A new method was tested for preventing the deterioration of the material during excavation. With the use of cyclododecane (CDD), a volatile binding medium, as a reversible consolidant, good results were achieved. CDD has been used in conservation mainly for stabilizing wall paintings. More recently, it was adopted for use in the conservation of archaeological objects. This paper reports the successful removal of a complete set of armor using CDD.

In 1998 Chinese archaeologists systematically exploring a 120-square-meter area near the mausoleum of Qin Shihuang, the first Chinese emperor, made a spectacular discovery: about eighty sets of ceremonial body armor for warriors, including forty helmets, as well as armor for horses, all made of small limestone plates. The stone armor was discovered in a burial chamber in the southeast section of the mausoleum, 1.5 kilometers west of the Terracotta Army.

Each set of armor consists of at least six hundred individual small limestone plates connected with bronze wire in a highly complicated system that allowed the armor to move (fig. 1). Although life-size, this armor was never intended for use. Rather, it represents copies of real armor that was made of iron or leather, and the different types vary in design in accordance with a warrior's rank. The two main types of armor were (a) copies of leather armor made with rectangular plates and (b) copies of metal armor whose plates resembled fish scales (Sheng kao gu yan jiu suo and Qin shi huang bing ma yong bo wu guan 2006: 271).

The current situation in the excavation pit is very complex. The sets of armor lie on top of one another in several layers (fig. 2). In some places the individual plates are still connected; in other places they lie in jumbled disorder. The result resembles 80 different puzzles, each with about 600 pieces thrown together in a pile. Some sets of armor are well preserved; others were severely damaged by a fire set during the succeeding dynasty.

It is unclear how the armor and the helmets were originally displayed in the pit. Based on the position of the plates today, it is surmised that the armor was hung from the ceiling of the burial chamber. However, nothing is preserved of any wooden substructure, if one existed.

In May 2000 a team of Chinese and German researchers, representing a partnership between the Museum of the

FIGURE 1 Set of stone body armor and helmet. Reproduced by permission of the Museum of the Terracotta Warriors and Horses of Qin Shihuang, Lintong, China

FIGURE 2 Current condition of stone armor in the excavation pit. Reproduced by permission of the Museum of the Terracotta Warriors and Horses of Qin Shihuang, Lintong, China

Terracotta Warriors and Horses in Lintong and the Bavarian State Department of Historical Monuments in Munich, began a project to investigate ways to preserve the stone armor. During the course of this study, numerous analyses were conducted to determine the characteristics of the limestone and the bronze. The materials were analyzed in cross section and thin section using X-ray fluorescence, X-ray diffraction, infrared spectroscopy, mass spectrometry, and optical emission spectroscopy. In addition, specific petrographic analyses were conducted to determine water uptake and tensile strength. Ultrasonic and porosity measurements (by mercury intrusion) were made to determine damage caused by the fire. The investigations yielded fundamental information about the production techniques and materials used for the stone armor, the condition of the materials, and the physical and chemical alterations experienced by some of the armor during the fire (Bucher and Weichert 2002; Langhals, Bathelt, and Bucher 2005). Based on these results, a conservation treatment plan is being developed.

Stone Armor Production Techniques

To produce the stone armor, craftsmen sawed and split many thousands of individual plates from a dark limestone, filing and polishing them into perfect form. The majority of the plates are rectangular in shape and measure approximately 5 by 4 by 0.5 centimeters. There are also square, trapezoidal, scaled, and irregular shapes.

Recently, tools that were used to produce the limestone armor were found in a well from the Qin period close to the grave site. With the tools were several unfinished or broken limestone plates, probably discarded waste material. Various sandstone grinding and polishing stones used to

treat the surfaces of the plates were also found. The discovery of tools, as well as traces of the workmanship left on the stone plates, documents that making the armor was a laborious undertaking.

Connecting Wires

A clay mold was discovered that provides insight into how the bronze connecting wires were made. The mold, approximately 10 centimeters long and 4 centimeters in diameter, is perforated along its length. The holes are close together, and their cross section reveals the square shape and size of the original wires. Thus it seems likely that the wires were cast and mass produced at almost industrialized speed, not drawn, as was usual in Europe. Metallurgical investigations of the cross sections of the wires, using a scanning electron microscope, reveal the typical crystal form of cast metal.

Drilling Technique

In order to be connected with one another, each of the armor plates had to be drilled through several times. Technical aspects of this drilling technique were investigated, including the form and material of the drill point, the abrasiveness of the drill, the optimal pressure placed on the drill, and the kind of supports used during drilling. The relevant literature, substantiated by scientific investigations, leads to the conclusion that a spiral hand drill was used on the limestone plates. X-ray diffraction of a metal particle discovered in one of the drill holes identified it as iron, thus suggesting that the holes were made with an iron drill. Practical experiments with a spiral hand drill showed that a maximum of three minutes were necessary to drill one hole. Based on this rate, and the fact that each plate contains between six and fourteen holes, we calculated that about 350 working hours were needed merely to drill the holes in the plates for a single set of armor.

Condition of the Stone Armor

The armor and helmets not affected by the fire are astonishingly well preserved, whereas the damage to those pieces exposed to the fire is disastrous. The affected limestone plates, originally dark gray, had turned white as the bituminous component of the stone escaped when the temperature from the fire reached 600°C.

Initially the limestone was chemically altered into calcium oxide. Then, in combination with air and moisture from the ground, this was slaked to calcium hydroxide (lime). All phases of the chemical alteration of the limestone were documented through X-ray diffraction, thin section analysis, and scanning electron microscopy.

When the pit was opened, the fire-damaged plates initially displayed their original shape. However, once in contact with air, within some weeks the plates recarbonated and swelled to about nine times their volume. They became severely cracked and friable. Many plates decomposed completely into powder.

The bronze connecting wires of the fire-damaged plates were also corroded. Some of them were broken, or they had become so deformed that in some parts of the pit the armor can no longer be put back together.

Restoring the Stone Armor

After the condition of individual armor plates and wires was documented, attention turned to removing and conserving the armor.

Removal

The stone armor was fragile, even those pieces not burned, and its removal from the pit posed a special challenge. During initial salvage efforts, it was not possible to remove a complete set of armor together with its bronze connecting wires. Instead, the wires had to be cut and removed, and then the plates were individually extracted from the ground and reconnected using new wires. Unfortunately, cutting the wires irretrievably lost precious original material, and removing the plates individually lost important information concerning their production. Some other way had to be found to remove the armor intact, without altering the arrangement of the individual plates.

To avoid future losses, trials were conducted using cyclododecane (CDD) as a reversible consolidant. CDD is a nonpolar hydrocarbon compound that is solid at room temperature. It melts at 58–61°C, and it can be applied as a liquid to an object, after which it solidifies quickly into a waxlike coating. Its high vapor pressure causes it to sublime at ambient temperature (20–23°C) at a rate of 4.5 milligrams per day, leaving practically no trace behind, thus making it particularly gentle for use on fragile objects (Geller and Hiby 2002: 15).

Because of its special properties, CDD has been increasingly used in the restoration field. The material has been successfully used to temporarily stabilize fragile objects, from sculpture to wall paintings, during transport

FIGURE 3 Close-up of cyclododecane-coated stone armor plates with lifting straps. Reproduced by permission of the Bavarian State Department of Historical Monuments, Munich, Germany

FIGURE 4 Brush application of cyclododecane over cotton gauze on test section of armor. Reproduced by permission of the Bavarian State Department of Historical Monuments, Munich, Germany

and consolidation (Brückle et al. 1999; Hangleiter 1998; Hiby 1999; Scharff and Huesmann 1998; Stein et al. 2000). CDD is also used as a hydrophobic coating. Only recently has the material been used, on a limited basis, to remove archaeological objects safely.

Cyclododecane Trials

An initial experiment was conducted in 2002 to stabilize a section of armor containing about one hundred plates with CDD. A hot wax gun was used to spray the material onto the armor. The resulting waxlike layer, about 3 millimeters thick, held the individual plates and their connecting wires together, and the entire section was removed from the ground using attached straps (fig. 3). After the CDD evaporates (the time can be shortened significantly by raising the room temperature and increasing air circulation), restoration work can be undertaken.

This was the first time that CDD had been used to remove an interconnected armor segment in preparation for conservation. Because a CDD coating is weak, however, it has a tendency to break. This posed a risk for the removal of a complete set of armor, which weighs about 20 kilograms. For this reason, further improvements in the procedure were sought, and a new method was tested.

After a series of tests using an exact dummy of a set of armor, a new salvage experiment was initiated in summer 2004 on an intact segment of armor. The individual steps of the operation, described below, were more complicated than those of the initial experiment, but this guaranteed that the weight of a complete set of armor could be removed without any problem.

- *Step 1:* The melted cyclododecane was mixed with 10 percent of heptane, thus making it possible to apply it with a brush. The cyclododecane was applied to several layers of cotton gauze placed over the armor (fig. 4). This produced a solid protective layer.
- *Step 2:* After a wait of about twenty-four hours to be sure that the heptane had evaporated, the treated armor was encircled with a cardboard frame. This was filled with a layer of polyurethane foam, about 10 centimeters thick, and a wooden reinforcement grid and lifting straps were embedded in the foam (figs. 5, 6).
- *Step 3:* After the foam hardened completely, it was possible to raise the unit out of the ground with the lifting straps. The armor released cleanly from the ground without leaving behind any pieces. Turning the unit upside down revealed the side of the armor that originally had been facedown on the ground (fig. 7).

FIGURE 5 Removal unit with wooden reinforcement grid and lifting straps before addition of polyurethane foam. Reproduced by permission of the Bavarian State Department of Historical Monuments, Munich, Germany

FIGURE 6 Removal unit with lifting straps embedded in polyurethane foam. Reproduced by permission of the Bavarian State Department of Historical Monuments, Munich, Germany

FIGURE 7 Underside of removal unit, revealing intact armor plates. Reproduced by permission of the Bavarian State Department of Historical Monuments, Munich, Germany

Cleaning

The exposed stone plates and wires were carefully cleaned, and any loose stone elements were glued in place with polybutyl-methylacrylate (Mowital B30 H15).[1] After cleaning, a plastic layer was applied over the exposed armor and a negative mold of the surface was made out of gypsum plaster, making it possible to turn over the armor. The plaster layer then became a support. Next, the polyurethane foam and layers of CDD-impregnated cotton gauze, now on top, were removed. This removal was done with a bath of heptane that penetrated the gauze and dissolved the CDD. The now-loosened fabric and foam were removed, revealing the side of the armor that had been faceup on the ground. Now this side could be cleaned. The restored test section of armor is shown in figure 8.

Promise for the Future

The promising results using CDD-based stabilization to salvage a test section of stone armor meant that researchers could confidently proceed with the removal of a complete set of armor. In May 2005 we did so, successfully lifting and transporting a complete set of armor from the burial pit to the conservation workshop, where it will be restored

FIGURE 8 Restored test section of stone armor. Reproduced by permission of the Bavarian State Department of Historical Monuments, Munich, Germany

and prepared for exposition to the general public. The final plans for the ceremonial stone armor of Emperor Qin's army include construction of a museum around the pit where the armor was found. This museum will join the Terracotta Army museum and other excavations at the site of Qin's mausoleum, providing scientists and visitors with the opportunity to see the armor in its historical context.

Acknowledgments

The authors extend special thanks to Yang Mangmang, Archaeological Institute of Shaanxi Province, Xi'an, China; Wang Dongfeng, Wang Weifeng, and Li Hua, Museum of the Terracotta Warriors and Horses of Qin Shihuang, Lintong, China, for their help during excavation; German conservator Hans Hangleiter and trainee Leonie Salzmann for ideas about a more stable excavation method and for help in conducting one of the project tests; Vojislaw Tucic, Bavarian State Department of Historical Monuments, Munich, and Herbert Juling, Materialprüfanstalt, Bremen, for metal and stone analysis; and Maya Weichert, conservator and former member of the team, for her contributions to the work and for conducting one of the project tests.

Materials List

Cyclododecane
Dr. Georg Kremer, Dipl.-Chemiker, Farbmühle
Hauptstrasse 41–47, D-88317 Aichstetten/Allgäu
Tel. + 49 (0)7565-1011 oder - 91120; Fax + 49 (0)7565-1606
e-mail: kremer-pigmente@t-online.de

Kremer Pigments, Inc.
228 Elizabeth Street
New York, NY
Tel. + 1 212 219 2394; Fax. + 1 212 219 2395
e-mail: kremerinc.@aol.com

Mowital B30 H15
Clariant (Germany) GmbH
Wiesentalstrasse 27
Postfach 2280
D-79512 Lörrach, Germany
Tel. + 49 7621 417 0; Fax + 49 7621 417 150

Notes

1 Mowital B30 H15 was used for gluing, instead of Paraloid® B72, because of its higher glass transition temperature (65°C). In summer, the temperature in Lintong can quickly rise above 40°C, and in the past this has led to problems with Paraloid®. The material becomes soft and sticky, with severely diminished adhesion, and particles of dirt remain stuck to objects. Tests of Mowital's bonding strength on limestone produced sufficiently good results.

References

Archaeological work report of the mausoleum of Qin Shihuang. 2000. Archaeological Institute of Shaanxi Province and the Museum of the Terracotta Warriors and Horses, Beijing.

Brückle, I., J. Thornton, K. Nichols, and G. Strickler. 1999. Cyclododecane: Technical note on some uses in paper and objects conservation. *Journal of the American Institute for Conservation* 38 (2): 162–75.

Bucher, S., and M. Weichert. 2002. Konservierung und Restaurierung der Kalksteinpanzer = Analysis of deterioration processes of the burnt limestone plates. In *Forschungsbericht 2001-2002 des Projektes "Eprobrung und Optimierung der Konservierungstechnologien für Kunst- und Kulturgüter der Provinz Shaanxi, VR China" = Work Report of 2001 and 2002 for the "Project Testing and Optimising of Conservation Technologies for the Preservation of Cultural Heritage of the Shaanxi Province, PR China,"* 112–30. Munich: Bayerisches Landesamt für Denkmalpflege.

Geller, B., and G. Hiby. 2000. *Flüchtige Bindemittel in der Papierrestaurierung sowie Gemälde- und Skulpturenrestaurierung.* Kölner Beiträge zur Restaurierung und Konservierung von Kunst- und Kulturgut, no. 10. Munich: Siegl.

Hangleiter, H. M. 1998. Erfahrungen mit flüchtigen Bindemitteln. Teil 2: Vorübergehende Verfestigung, schützende oder verdämmende Versiegelung von Oberflächen an Gemälden, Stein oder Wandmalereien. *Restauro* 7: 468–73.

Hiby, G. 1999. Cyclododecan als temporäre Transportsicherung: Materialeigenschaften des flüchtigen Bindemittels bei Bild- und Fassungsschichten. *Restauro* 5: 358–63.

Langhals, H., D. Bathelt, and S. Bucher. 2005. The tomb of the first Chinese emperor: A challenge for conservation = Das Grabmal des ersten chinesischen Kaisers: Eine konservatorische Herausforderung. *Chemie in Unserer Zeit* 39 (3): 196–211.

Scharff, W., and I. Huesmann. 1998. Conservation of archaeological metal artifacts: Thermal treatment methods for iron objects and temporary consolidation of fragile corrosion products with volatile binders. In *Metal 98: Proceedings of the International Conference on Metals Conservation = Actes de la conférence internationale sur la conservation des métaux: Draguignan-Figanières, France, 27–29 May 1998,* ed. W. Mourey and L. Robbiola, 155–61. London: James & James.

Shaanxi Sheng kao gu yan jiu suo and Qin shi huang bing ma yong bo wu guan. 2006. *Qin shi huang di ling yuan kao gu bao gao (2000) = Report on Archaeological Researches of the Qin Shihuang Mausoleum Precinct in 2000.* Ed. Di 1 ban. Beijing: Wen wu chu ban she.

Stein, R., J. Kimmel, M. Marincola, and F. Klemm. 2000. Observations on cyclododecane as a temporary consolidant for stone. *Journal of the American Institute for Conservation* 39 (3): 355–69.

The Development of Ancient Synthetic Copper-Based Blue and Purple Pigments

Heinz Berke, Armin Portmann, Soraya Bouherour, Ferdinand Wild, Ma Qinglin, and Hans-Georg Wiedemann

Abstract: *Mineral sources for stable blue and purple pigments were rare in antiquity. Efforts to improve availability of such pigments began more than five thousand years ago, in predynastic Egypt, with the synthesis of Egyptian blue, a defined chemical compound of the composition* $CaCuSi_4O_{10}$*. This synthetic pigment became widespread, and archeometric studies have shown that it was definitely used in the Mesopotamian, Greek, and Roman civilizations.*

In China, where the lack of mineral blue pigments also became a challenge, the synthetic pigments Chinese blue and purple, also known as Han blue and purple, were developed. It is known that they existed by the late Western Zhou dynasty, around 800 B.C.E. Artifacts containing Chinese blue or purple that we have investigated so far include beads, earrings, and octagonal sticks. These pigments were also found in pigment layers of the Terracotta Army from the Qin dynasty (221–207 B.C.E.) and on wall paintings of Han dynasty tombs (206 B.C.E.–220 C.E.). In two beads we studied, ultramarine blue was found along with Chinese blue or purple. It is plausible that the ultramarine blue was of synthetic and not mineral origin (from lapis lazuli). Chinese blue and purple are even more complex than Egyptian blue, and their production is more sophisticated because of the higher temperatures required and the need to carefully control component quantities and the physical conditions of the synthesis. These difficulties, along with the chemical similarities to Egyptian blue, suggest that the Chinese pigments were likely to have been improvements on the Egyptian predecessor rather than independent developments. The question remains as to how knowledge about Egyptian blue spread to China. A technology transfer might have occurred along the Silk Road, but this is a matter to be addressed by future archeometric studies.

Colors had great meaning to people in prehistoric times and in antiquity. Earth colors were readily available as they could be obtained directly from soil. Some colors, such as blue and purple, however, depended on mineral sources that were exceptionally rare in antiquity and not always accessible. Lapis lazuli and azurite were the main pigment minerals for blue color as well as for purple,[1] which was achieved by mixing blue pigment with red (iron oxides, vermilion). Azurite is quite abundant but not very stable, whereas lapis lazuli, which was highly valued in antiquity, is rare and restricted in use. Thus, although earth colors were used in prehistoric cave paintings (Ball 2001), blue colors are strikingly absent. Later civilizations, even highly developed ones, also suffered from frequent shortages of stable blue pigments, and this probably accounted for their high idealistic and materialistic esteem. This situation did not change until the nineteenth century, when industrialization led to the chemical mass production of dyes and pigments.

The limited availability and stability of natural blue pigments in antiquity presumably stimulated the invention of appropriate synthetic materials. The Egyptians created Egyptian blue, the Chinese invented Chinese (or Han) blue and purple, and the Maya synthesized Maya blue (Chiari, Giustetto, and Ricchiardi 2003: 21–33). Various civilizations also made a blue pigment (smalt) by grinding cobalt-containing glass and glazes (Berke 2004: 401–5). The different types of ancient man-made blues and purple are listed in table 1 together with their chemical compositions and brief historical data.

This paper focuses on the chemical development of the important synthetic pigments of antiquity: Egyptian blue, Chinese blue, and Chinese purple (Berke 2002). These

Table 1 Compilation of Various Synthetic Blue and Purple Pigments Produced in Antiquity (Berke 2004: 401–5)

Name	Composition	Material Type	Approximate Time of Appearance
Egyptian blue	$CaCuSi_4O_{10}$	Alkaline-earth copper silicate	3600 B.C.E.
Smalt (cobalt blue)	$CoO(SiO_2)_n$	Cobalt oxide in a glass matrix	1000 B.C.E.
Chinese (Han) blue	$BaCuSi_4O_{10}$	Alkaline-earth copper silicate	800 B.C.E.
Chinese (Han) purple	$BaCuSi_2O_6$	Alkaline-earth copper silicate	800 B.C.E.
Ultramarine blue	$Na_{0.9}[Al_{5.6}Si_{6.4}O_{24}]S_{2.0}$	Sodalite cages filled with S_n^-	800 B.C.E.
Maya blue	$(C_{16}H_{10}N_2O_2)_y \cdot [(Mg,Al)_4Si_8(O,OH,H_2O)_{24}]_m \cdot x\ H_2O$	Indigo as a host molecule in white clay	400 B.C.E.

pigments were developed through complex experimentation based on a related alkaline-earth copper silicate chemistry (*alkaline-earth* refers to such elements as calcium and barium). This paper also discusses a recently detected ultramarine blue pigment, which appears to be the serendipitous outcome of experimentation with alkaline-earth copper silicate chemistry in antiquity.

Alkaline-Earth Copper Silicate Pigments

Azurite is an abundant mineral source for natural blue pigment, but the color is not very stable. In antiquity, Egyptians and Chinese learned how to use azurite or another copper mineral as the starting component for the synthesis of stable blue and purple copper silicate pigments.

Egyptian Blue

Egyptian blue is the oldest man-made pigment, developed in predynastic Egypt more than five thousand years ago (Chase 1971: 80–90).

Chemistry. Egyptian blue is a defined chemical compound with the formula $CaCuSi_4O_{10}$. Figure 1 is a schematic representation of this pigment's chemical structure.[2] The copper ions in Egyptian blue function as chromophores (structures that give color to the pigment).

Synthesis. In ancient times, Egyptian blue was prepared by heating ground limestone, quartz (sand), and a copper mineral such as malachite, azurite, kinoite, or even copper metal to 800 to 900°C in the presence of a flux (Bayer and Wiedemann 1976: 20–39). Certain other physical and chemical conditions, such as an excess of air and control over stoichiometric ratios of the starting materials, also had to be satisfied to obtain products of high quality. Apparently ancient Egyptians had knowledge of the necessary ratios for mixing the ingredients, since the various elemental constituents were kept relatively constant over more than two thousand years, as shown in table 2 (Wiedemann and Berke 2001).

Distribution. Egyptian blue became widespread in the Mediterranean region, especially later, during the Greek and Roman civilizations (Riederer 1997: 23–45). It continued to

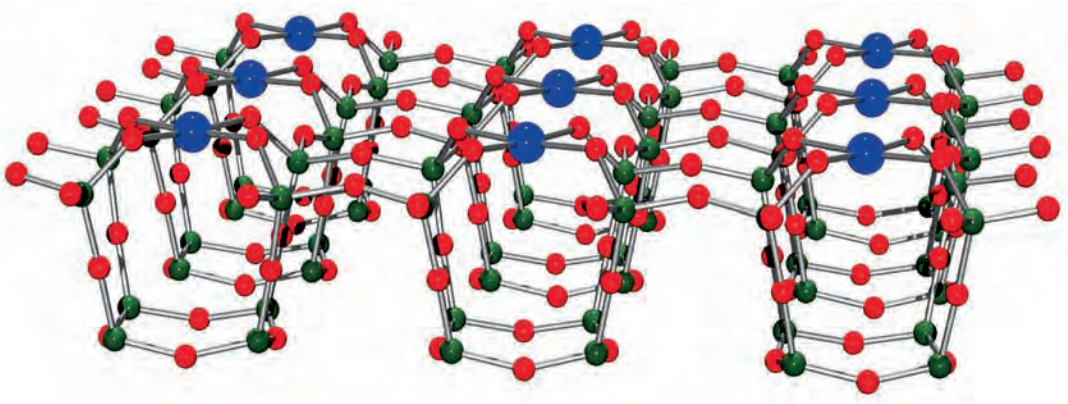

FIGURE 1 Schematic representation of the silicate sheet framework for both Egyptian blue ($CaCuSi_4O_{10}$) and Chinese blue ($BaCuSi_4O_{10}$). The calcium (Ca) or barium (Ba) ions are located between layers but are omitted here for clarity. The copper (Cu) ions, which give the pigments their color, are shown in blue. Silicon (Si) is shown in green; oxygen (O), in red.

Table 2 Ancient Egyptian Artifacts Containing Egyptian Blue Pigment and Its Respective Elemental Composition (Wiedemann and Berke 1999: 154–70)

Artifact and Location	Dynastic Period	Time	Composition (in oxide percent)		
			Ca	Cu	Si
Mastaba of Mereruka, Saqqara, Egypt	Old Kingdom	2575–2134 B.C.E.	15.2	21.3	63.0
Tomb of Intef*, Thebes, Egypt	Middle Kingdom	2040–1640 B.C.E.	14.9	21.5	63.8
Akhenaten Temple, Talatat Stones, Amarna, Egypt	New Kingdom	1353 B.C.E.	24.0	22.5	53.5
Nefertiti, Berlin, Germany	New Kingdom	1340 B.C.E.	17.4	30.2	52.3
Bes amulet, unknown location	Late Period	712–332 B.C.E.	13.6	28.5	58.3
Mummy coffin, unknown location	Greek-Roman	332 BCE–395 C.E.	18.4	22.5	59.2
		Average composition	17.3	24.4	58.4
		Theoretical composition	18.6	29.4	52.0

*General Intef, Middle Kingdom, 11th dynasty, reported to Mentuhotep II

spread east into Mesopotamia and Persia. Completing the distribution map of Egyptian blue remains a great challenge. At present it is not certain how far east and north this synthetic pigment spread and whether its geographic distribution also followed the Silk Road into central Asia and the Far East. Any new Egyptian blue finds in these eastern regions could help to establish whether the chemical experimentation that led to the development of Egyptian blue had also influenced the development of the chemically related Chinese blue and purple or if an independent synthesis was found for them. Samples of Egyptian blue as well as Chinese blue and purple made by contemporary synthesis are shown in figure 2. With comparable particle size, Egyptian blue and Chinese blue are nearly identical in color. The pigments appear different in figure 2 because the Chinese blue particles are coarse and the Egyptian blue is finely ground, producing a lighter tone.

FIGURE 2 Left: Egyptian blue ($CaCuSi_4O_{10}$); middle: Chinese purple ($BaCuSi_2O_6$); right: Chinese blue ($BaCuSi_4O_{10}$).

Chinese (Han) Blue and Purple

Chemistry. Chinese blue and purple are distinct chemical compounds with the compositions $BaCuSi_4O_{10}$ and $BaCuSi_2O_6$, respectively. As alkaline-earth copper silicates, they are closely related chemically to each other and to Egyptian blue. Chinese blue differs very little from Egyptian blue: the calcium in Egyptian blue is replaced by the chemically similar element barium to create Chinese blue. Consequently, Chinese blue has a chemical structure closely related to Egyptian blue and likewise belongs to the class of sheet silicates (see fig. 1).

Although Chinese purple is chemically similar to Chinese blue and Egyptian blue, this pigment has a unique layered structure (Janczak and Kubiak 1992), as shown in figure 3.[3] This unique structure gives Chinese purple physical and chemical properties that differ from those of the two blue pigments—not only its purple color, but its lower thermal stability and low chemical resistance to acidic agents.

Synthesis. Chinese blue and purple are more difficult to make than Egyptian blue. These pigments are synthesized at higher temperatures (900–1,000°C)—about 150°C higher than for Egyptian blue. In ancient times, this temperature range was technologically more difficult to achieve. In addition to quartz and a copper starting mineral, a barium source was needed. Barium minerals are generally much less abundant than the limestone used for Egyptian blue, although they are nevertheless common in some areas of China. Either barite ($BaSO_4$) or witherite ($BaCO_3$) was used in antiquity, and both

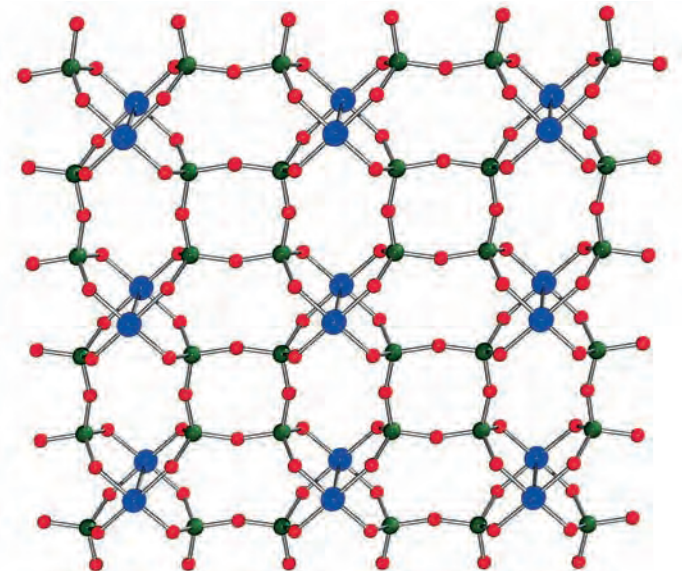

FIGURE 3 Schematic representation of the silicate structure of Chinese purple ($BaCuSi_2O_6$). The barium (Ba) ions, which are located between layers, are omitted for clarity. Silicon (Si) is shown in green; oxygen (O), in red; and copper (Cu), in blue.

require comprehensive mineralogical knowledge for their utilization. For example, when the more abundant barite was used, lead salts had to be added to obtain satisfactory pigment qualities. The lead salts had two chemical functions—that of a catalyst to break down the barite and that of a flux. Thus the production of the Chinese pigments was developed based on more sophisticated technologies and was on the whole a more complicated process than that involved in the production of Egyptian blue (Wiedemann and Bayer 1997; Wiedemann, Bayer, and Reller 1997).

Historical Use. Blue pigment played an important role in China's historical development (Ma Qinglin et al. 2001), apparently beginning in the late Western Zhou dynasty, about 800 B.C.E. Whether this date really marks the earliest appearance of Chinese blue and purple is open to speculation. New discoveries are expected from still older archaeological sites, and the earliest date of the historical appearance of the pigment may perhaps be about 900 to 1000 B.C.E. This period would coincide with the beginning of an important technological era in ancient northwestern China.

Samples of Chinese blue and purple that we investigated cover a range of one thousand years of use. The pigments were found in decorative objects, such as glazed blue beads and earrings from the late Western Zhou dynasty and the Spring and Autumn period of the Eastern Zhou dynasty (800–475 B.C.E.) and octagonal sticks probably used as a commodity for paint applications or decoration from the Warring States period of the Eastern Zhou dynasty (475–221 B.C.E.), from the Qin dynasty (221–207 B.C.E.), and from the Western and Eastern Han dynasties (206 B.C.E.–220 C.E.) (FitzHugh and Zycherman 1983, 1992).

Figure 4 presents a selection of recently studied Chinese objects containing blue and purple pigments from the earlier periods (Ma Qinglin et al. 2006). Bead 1 has a glassy surface containing Chinese purple and ultramarine blue with a white inner core and dated to 777–766 B.C.E. (Dai Chunyang 2000). Bead 2 has a glassy outer layer containing primarily Chinese blue and ultramarine blue with a colored inner core and dated to the eighth–sixth century B.C.E. Both beads were recovered from northwestern China. Bead 3 consists of a heterogeneous compact blue body containing Chinese blue and dated to the sixth–fourth century B.C.E. (Archaeology Team of Baoji City 1993). The octagonal stick is uniformly colored with Chinese purple and consists of partly crystalline, partly vitreous sinter material with high lead and barium content with a weathered whitish outer layer, dated to the fifth–third century B.C.E. (Archaeology Team of Luoyang City 1999; Ma Qinglin et al. 2006; Zibo Museum 1997).

FIGURE 4 Chinese artifacts containing synthetic blue and purple pigments.

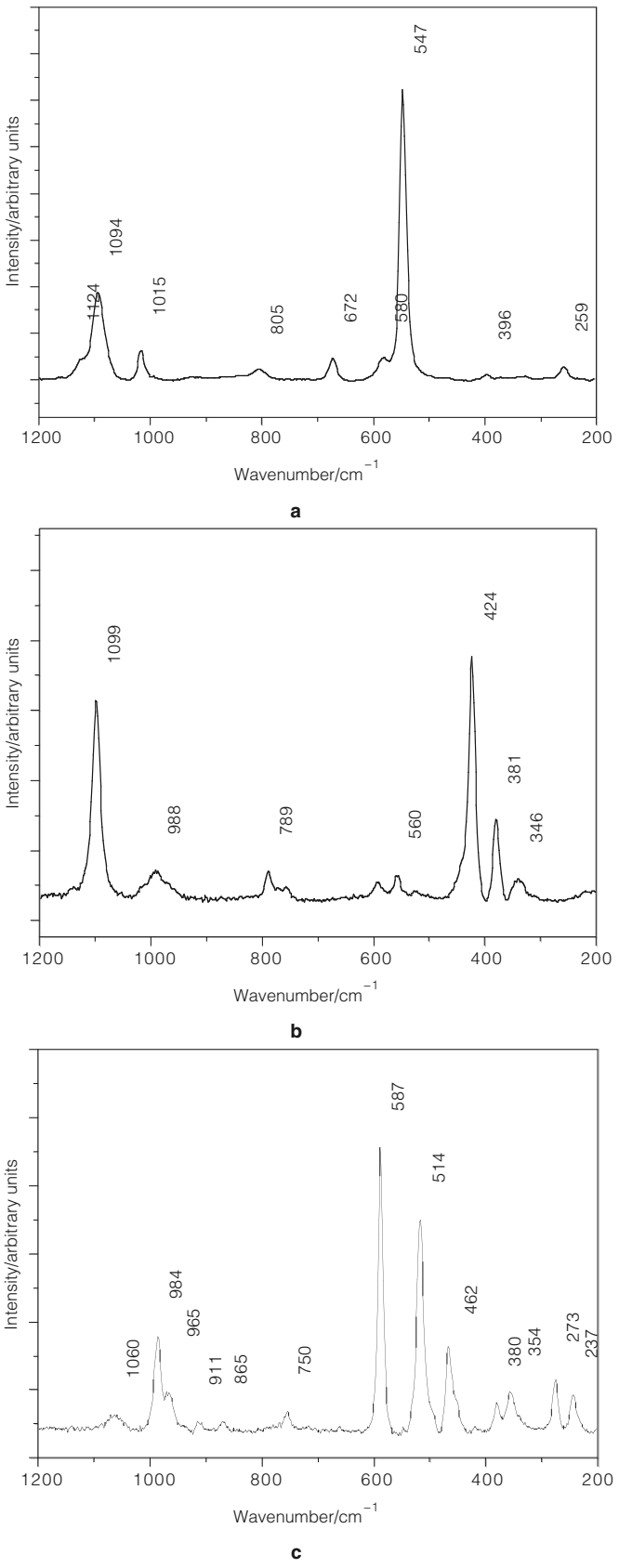

FIGURE 5 Raman spectra of ultramarine blue in bead 1 (a); of Chinese blue in bead 3 (b); and of Chinese purple in the octagonal stick (c) in the range 1200–200 cm^{-1}.

Detailed archeometric investigations of these objects by Raman spectroscopy and scanning electron microscopy (SEM/EDX) revealed that Chinese blue was more frequently present in the earlier objects. In contrast, Chinese purple was the predominant pigment in objects from later periods, not only in the octagonal sticks we studied, but in pigment samples from the Terracotta Army of the Qin dynasty (221–207 B.C.E.) (Thieme 2001; Thieme et al. 1995; Zhou Tie 2001) and in wall paintings in tombs of the Eastern Han dynasty. It should be noted that all the Chinese blue and purple samples always contained considerable amounts of lead. As described earlier, lead additives in these pigments act as catalyst and flux.

Ultramarine Blue

In two of the beads we studied (fig. 4, beads 1 and 2) from the late Western Zhou dynasty and the Spring and Autumn period, Raman spectroscopy detected ultramarine blue particles in the glassy surface in conjunction with either Chinese blue or Chinese purple (fig. 5).

Natural ultramarine blue pigment was originally prepared from lazurite (the primary blue mineral component of lapis lazuli). However, natural ultramarine blue was rarely used in ancient China (Berke and Wiedemann 2000); when it was used, it was applied in much later periods, for example, in the Kizil Grottoes dating from the second and third centuries C.E. (Su Bomin, Li Zuixiong, and Hu Zhide 1999; Su Bomin et al. 2000).

Finding ultramarine blue in these older beads is as yet unprecedented. Although the origin of the pigment—synthetic or mineral—in these objects is still open to question, we suggest that it is a synthetic product, formed serendipitously during the firing process at temperatures ranging from 800 to 1000°C when Chinese purple or Chinese blue was actually being synthesized. A modern synthesis of ultramarine blue uses silica, kaolin, soda or sodium sulfate, sulfur, and charcoal (Seel et al. 1974). At temperatures around 800°C and reducing conditions, sodalite forms and hosts the sulfur molecules, which play the key role in coloring the pigment (see below). These conditions are quite close to the manufacturing process of Chinese blue and Chinese purple, with the charcoal and reducing conditions coming

from the kiln. Only kaolin has to be added, either voluntarily for making a glaze or accidentally as a by-product of the other minerals.

Chemistry. The mineral lazurite—with the empirical formula $Na_3CaAl_3Si_3O_{12}S_4$—from which natural ultramarine blue was prepared—and synthetic ultramarine pigment—with an empirical formula $Na_{6.9}[Al_{5.6}Si_{6.4}O_{24}]S_2$ (Reinen and Lindner 1999)—both contain sulfur molecules consisting of two or three sulfur atoms trapped in a cage of sodalite. Sodalite is the principal constituent of both lazurite and synthetic ultramarine and has the formula $(Na_8[Al_6Si_6O_{24}]Cl_2)$.[5] The typical blue color of both the natural and synthetic pigments comes from blue sulfur radical ions (S_3^-) substituting for sodalite's chloride ions. In synthetic ultramarine, a yellow sulfur ion (S_2^-) often accompanies the blue sulfur ion in varying amounts, resulting in a green (blue plus yellow) variety of this pigment.

In the beads we studied, the radical sulfur anions $S_2^{-\bullet}$ and $S_3^{-\bullet}$ were identified simultaneously by Raman spectroscopy (Clark 1995; Clark and Cobbold 1978; Colomban 2003), but the Raman analysis cannot distinguish if the ultramarine pigment is of synthetic or natural origin. However, given the notable absence of pyrite (FeS_2) and the very low content of iron in the ultramarine blue found in the beads, this pigment could not be attributed to the mineral lazurite obtained from lapis lazuli, which has pyrite as a minor component. Rather, it had to be assigned to a synthetic variant.

As mentioned earlier, ultramarine blue particles were found embedded in the glaze of the beads, and this glassy layer would provide all the necessary ingredients for the pigment formation. Other major conditions for the formation of synthetic ultramarine blue are the presence of basic ingredients, such as carbonate (CO_3^{2-}) from plant ash or from witherite ($BaCO_3$) and sulfur presumably present as sulfate (SO_4^{2-}) from barite, as well as the presence of a reducing agent, here carbon black particles presumably resulting from the operating conditions of a wood-fired kiln.

Thoughts on the Historical Development of the Alkaline-Earth Copper Silicate Pigments

It is still too early to put forth any definitive theory on whether the blue and purple pigments were developed independently of each other or through technology transfer. Some of the evidence for both sides is discussed below.

Evidence for Independent Development

The development of the barium copper silicate pigments—Chinese blue and purple—and serendipitously that of ultramarine blue represents a great ancient Chinese "high-tech" achievement. These blue and purple pigments were used in a relatively confined geographic area of ancient China—the regions of today's Gansu, Shanxi, Shaanxi, and Henan provinces in northwest China, the easternmost part of the Silk Road (Dai Chunyang 2000; Archaeology Institute of Henan Province 1987; Department of Archaeology of Beijing University 1994). To our knowledge, there was no further geographic spread of these Chinese pigments or geographic overlap with the distribution of Egyptian blue. This would suggest that no transmission of the technical know-how for making these very similar pigments took place. However, the picture of the distribution of Egyptian blue in central Asia and that of the Chinese pigments is still incomplete.

Other evidence for the independent origins of the blue and purple pigments comes from the development of vitreous materials (some of the Chinese objects that were investigated for their pigment, including the octagonal sticks, consist partly of vitreous phases). The development of vitreous materials in Egypt and Mesopotamia was widespread and took advantage of the lighter alkaline and alkaline-earth elements, such as calcium, as glassing agents (Tite, Shortland, and Paynter 2002). In contrast, the development of vitreous materials in northwestern China was quite localized. Also, heavy elements such as barium and lead were predominantly used (Brill 1993; Brill, Tong, and Dohrenwend 1991; Brill, Barnes, and Joel 1991; Brill, Tong, and Zhang Fukang 1989). Figure 6 summarizes the hypothesized developments that eventually led to the production of blue and purple pigments in the Western and Eastern worlds.

The chemistry involved in the production of vitreous materials in Mesopotamia or Egypt could have led to the development of Egyptian blue. Likewise, in ancient China, the production of early glassy materials such as glazed stones and faience that used barium and lead could also have led to the development of Chinese blue and purple. These developments of glassy or vitreous materials occurred independently of each other, thus arguing for the independent development of the blue and purple pigments.

Evidence for Technology Transfer

The chemical similarities between Egyptian blue and the Chinese pigments are both striking and intriguing, sug-

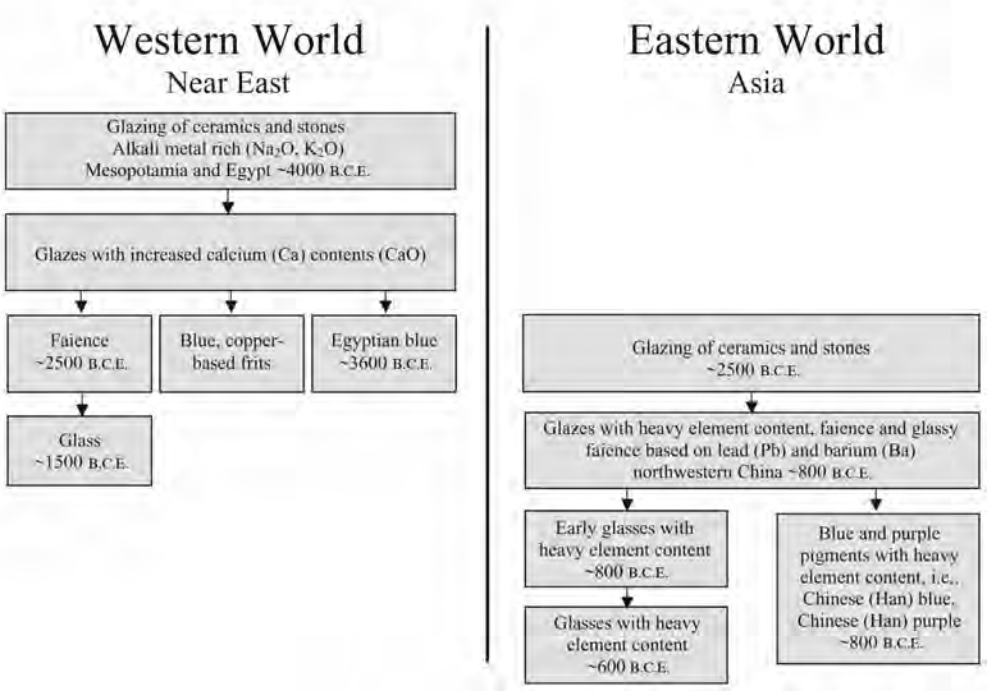

FIGURE 6 Flowchart showing possible pathways for the separate but parallel development of Egyptian blue and Chinese blue and purple in antiquity.

gesting that the Chinese syntheses were based on knowledge of the synthesis of the historically earlier Egyptian blue. Moreover, production of the Chinese pigments is more sophisticated because of the higher temperatures required and the need to carefully control component quantities and the physical conditions of the synthesis. These difficulties, along with the chemical similarities to Egyptian blue, suggest that the Chinese pigments were likely to have been improvements on the Egyptian predecessor rather than independent developments. The question remains as to how knowledge about Egyptian blue spread to China. A technology transfer might have occurred along the Silk Road, but this is a matter to be addressed by future archeometric studies.

Acknowledgments

We would like to thank Neville Agnew and David A. Scott of the Getty Conservation Institute for supporting Ma Qinglin as a visiting scientist during 2001. Thanks also to R. H. Brill of the Corning Museum of Glass for his referral to coauthor Ma Qinglin. We are indebted to the Ägyptisches Museum der Staatlichen Museen Preussischer Kulturbesitz zu Berlin, Germany, for providing a sample of the crown of Nefertiti to H.-G. W.

Notes

1 Lapis lazuli is a rock type. The term, however, is often used synonymously for its main mineral component, lazurite (empirical formula $Na_3CaAl_3Si_3O_{12}S$ or $(Na,Ca)_8(AlSiO_4)_6(S,SO_4;Cl)_{1-2}$), which is the source of the rock's distinctive blue color. The name ultramarine refers either to the blue pigment obtained from processed lapis lazuli rock or to the synthetically made variety.

2 The chemical structure of Egyptian blue possesses a highly robust, infinitely connected, puckered silicate sheet framework that binds to the alkaline earth and the copper ions (Pabst 1959).

3 Chinese purple has a unique structure with a copper–copper bond as its crucial structural moiety. Furthermore, although Chinese purple also has a layered structure, its layers are built up from planar isolated $[Si_4O_{12}]^{8-}$ rings held together by $[Cu_2]^{4+}$ units with the Ba^{2+} ions located between layers. The main feature is the Cu_2 unit, which has a Cu–Cu distance of 2.73 Å. It is held together by four bridging SiO_2 moieties from the eight-member silicate rings. Each copper ion is in a square pyramidal geometry.

4 Lazurite's somewhat variable calcium content is better shown by the notation $(Na,Ca)_8(AlSiO_4)_6(S,SO_4,Cl)_{1-2}$.

5 Sodalite is a defined aluminosilicate containing a framework built from six $AlSiO_4$ moieties.

References

Archaeological Institute of Henan Province. 1987. The tombs of Guo State in the village of Shang Cunling, Sanmenxia, Henan. *Hua Xia kao gu = Huaxia kaogu* 3: 104–13.

Archaeology Team of Baoji City. 1993. Excavation of the tomb no. 2 of the Spring and Autumn period at Yimencun in Baoji City, Shaanxi. *Wen wu* 10: 1–14.

Archaeology Team of Luoyang City. 1999. Excavation of some Warring States tombs in Luoyang. *Wen wu* 8: 4–13.

Ball, P. 2001. *Bright Earth: Art and the Invention of Color.* New York: Farrar, Straus & Giroux.

Bayer, G., and H. G. Wiedemann. 1976. Ägyptisch Blau, ein synthetisches Farbpigment des Altertums, Wissenschaftlich betrachtet. *Sandoz Bulletin: Sonderausgabe* 40: 20–39.

Berke, H. 2002. Chemistry in ancient times: The development of blue and purple pigments. *Angewandte Chemie—International Edition* 41 (14): 2483–87.

———. 2004. Blau und purpur: Die Erfindung von Farbpigmenten im Altertum. *Restauro* 110 (6): 401–5.

Berke, H., and H. G. Wiedemann. 2000. The chemistry and fabrication of the anthropogenic pigments Chinese blue and purple in ancient China. *East Asian Science, Technology, and Medicine* 17: 94–120.

Bouherour, S., H. Berke, and H. G. Wiedemann. 2001. Ancient man-made copper silicate pigments studied by Raman microscopy. *Chimia* 55 (11): 942–51.

Brill, R. H. 1993. Glass and glassmaking in ancient China, and some other things from other places. *Glass Art Society Journal: The Toledo Conference:* 56–69.

Brill, R. H., I. L. Barnes, and E. C. Joel. 1991. Lead isotope studies of early Chinese glasses. In *Scientific Research in Early Chinese Glass: Proceedings of the Archaemetry of Glass Sessions of the 1984 International Symposium on Glass, Beijing, September 7, 1984, with Supplementary Papers,* ed. R. H. Brill and J. H. Martin, 65–83. Corning, NY: Corning Museum of Glass.

Brill R. H., Shi Meiguang, E. C. Joel, and R. D. Vocke. 1991. Addendum to chapter 5. In *Scientific Research in Early Chinese Glass: Proceedings of the Archaemetry of Glass Sessions of the 1984 International Symposium on Glass, Beijing, September 7, 1984, with Supplementary Papers,* ed. R. H. Brill and J. H. Martin, 84–89. Corning, NY: Corning Museum of Glass.

Brill, R. H., S. S. C. Tong, and D. Dohrenwend. 1991. Chemical analyses of some early Chinese glasses. In *Scientific Research in Early Chinese Glass: Proceedings of the Archaemetry of Glass Sessions of the 1984 International Symposium on Glass, Beijing, September 7, 1984, with Supplementary Papers,* ed. R. H. Brill and J. H. Martin, 31–58. Corning, NY: Corning Museum of Glass.

Brill, R. H., S. S. C. Tong, and Zhang Fukang. 1989. The chemical composition of a faience bead from China. *Journal of Glass Studies* 31: 11–15.

Chase, W. T. 1971. Egyptian blue as a pigment and ceramic material. In *Science and Archaeology: Papers,* ed. R. H. Brill, 80–90. Cambridge, MA: MIT Press.

Chiari, G., R. Guistetto, and G. Ricchiardi. 2003. Crystal structure refinements of palygorskite and Maya blue from molecular modelling and powder synchrotron diffraction. *European Journal of Mineralogy* 15 (1): 21–33.

Clark, R. J. H. 1995. Raman microscopy: Application to the identification of pigments on medieval manuscripts. *Chemical Society Reviews* 24 (3): 187–96.

Clark, R. J. H., and D. G. Cobbold. 1978. Characterization of sulfur radical anions in solutions of alkali polysulfides in dimethylformamide and hexamethylphosphoramide and in the solid state in ultramarine blue, green, and red. *Inorganic Chemistry* 17 (11): 3169–74.

Colomban, P. 2003. Lapis lazuli as unexpected blue pigment in Iranian Lâjvardina ceramics. *Journal of Raman Spectroscopy* 34 (6): 420–23.

Dai Chunyang. 2000. Several problems concerning the royal graveyard of the Qin state at Dabuzi, Li-Xian, Gansu. *Wen wu* 5: 74–80.

Department of Archaeology of Beijing University and Institute of Archaeology of Shanxi Province. 1994. Second excavation of the cemetery of Jin State at Beizhao in Tianma-Qucun Site. *Wen wu* 1: 4–34.

Fenn, P. M., R. H. Brill, and M. G. Shi. 1991. Addendum to chapter 4. In *Scientific Research in Early Chinese Glass: Proceedings of the Archaemetry of Glass Sessions of the 1984 International Symposium on Glass, Beijing, September 7, 1984, with Supplementary Papers,* ed. R. H. Brill and J. H. Martin, 59–64. Corning, NY: Corning Museum of Glass.

FitzHugh, E. W., and L. A. Zycherman. 1983. An early man-made blue pigment from China: Barium copper silicate. *Studies in Conservation* 28 (1): 15–23.

———. 1992. A purple barium copper silicate pigment from early China. *Studies in Conservation* 37 (3): 145–54.

Janczak, J., and R. Kubiak. 1992. Refinement of the structure of barium copper silicate $BaCu[Si_4O_{10}]$ at 300 K. *Acta Crystallographica—Section C* 48: 1299–1301.

Ma Qinglin, A. Portmann, F. Wild, and H. Berke. 2006. Raman and SEM studies of man-made barium copper silicate pigments in ancient Chinese artifacts. *Studies in Conservation* 51 (2): 81–98.

Ma Qinglin, Su Bomin, Li Zuixiong, and Hu Zhide. 2001. Ancient Chinese pigments. In *Scientific Research and Conservation of Ancient Chinese Materials,* ed. S. J. Cao, 201–21. Beijing: Science Press.

Pabst, A. 1959. Structures of some tetragonal sheet silicates. *Acta Crystallographica* 12: 733–39.

Reinen, D., and G.-G. Lindner. 1999. The nature of the chalcogen colour centres in ultramarine-type solids. *Chemistry Society Reviews* 28 (2): 75–84.

Riederer, J. 1997. Egyptian blue. In *Artists' Pigments: A Handbook of Their History and Characteristics,* ed. E. W. FitzHugh, 3:23–45. Oxford: Oxford University Press; Washington, DC: National Gallery of Art.

Seel, F., G. Schäfer, H.-J. Güttler, and G. Simon. 1974. Das geheimnis des lapis lazuli. *Chemie in unserer Zeit* 8 (3): 65–71.

Su Bomin, Li Zuixiong, and Hu Zhide. 1999. Research on pigments of Kizil Grottoes. In *Conservation of Wall Paintings in Asia: Proceedings of the Ninth Seminar on the Conservation of Asian Cultural Heritage: November 16–19, 1999, Tokyo, Japan,* 59–67. Tokyo: National Research Institute for Cultural Properties.

Su Bomin, Li Zuixiong, Ma Zengang, Li Shi, and Ma Qinglin. 2000. Research on pigments of Kizil Grottoes. *Dunhuang Research* 63 (1): 65–75.

Thieme, C. 2001. Paint layers and pigments on the Terracotta Army: A comparison with other cultures of antiquity. In *The Polychromy of Antique Sculptures and the Terracotta Army of the First Chinese Emperor: Studies on Materials, Painting Techniques, and Conservation, International Conference in Xi'an, Shaanxi History Museum, March 22–28, 1999 = [Gu dai diao su cai hui Qiushihuang bing ma yong: Cai liao, hui hua ji shu he bao hu zhi yan jiu],* ed. Wu Yongqi, Zhang Tingbao, M. Petzet, E. Emmerling, and C. Blänsdorf, 52–58. Arbeitsheft (Bayerisches Landesamt für Denkmalpflege), vol. 111. Munich: Bayerisches Landesamt für Denkmalpflege.

Thieme, C., E. Emmerling, C. Herm, Yon Qi Wu, Zhou Tie, and Zhang Zhijun. 1995. Research on paint materials, paint techniques, and conservation experiments on the polychrome Terracotta Army of the first emperor Qin Shi Huang. In *The Ceramics Cultural Heritage: Proceedings of the International Symposium, The Ceramics Heritage, of the 8th CIMTEC—World Ceramics Congress and Forum on New Materials, Florence, Italy, June 28–July 2, 1994,* ed. P. Vincenzini, 591–601. Monographs in Materials and Society, no. 2. Faenza: Techna.

Tite, M., A. Shortland, and S. Paynter. 2002. The beginnings of vitreous materials in the Near East and Egypt. *Accounts of Chemical Research* 35 (8): 585–93.

Wiedemann, H. G., and G. Bayer. 1997. Formation and stability of Chinese barium copper silicate pigments. In *Conservation of Ancient Sites on the Silk Road: Proceedings of an International Conference on the Conservation of Grotto Sites,* ed. N. Agnew, 379–87. Los Angeles: Getty Conservation Institute.

Wiedemann, H. G., G. Bayer, and A. Reller. 1997. Egyptian blue and Chinese blue: Production technologies and applications of two historically important blue pigments. In *La couleur dans la peinture et l'émaillage de l'Égypte ancienne: Actes de la Table ronde, Ravello, 20–22 mars 1997,* ed. S. Colinart and M. Menu, 195–203. Scienze e materiali del patrimonio culturale, no. 4. Bari: Edipuglia.

Wiedemann, H. G., and H. Berke. 2001. Chemical and physical investigations of Egyptian blue and Chinese blue and purple. In *The Polychromy of Antique Sculptures and the Terracotta Army of the First Chinese Emperor: Studies on Materials, Painting Techniques, and Conservation, International Conference in Xi'an, Shaanxi History Museum, March 22–28, 1999 = [Gu dai diao su cai hui Qiushihuang bing ma yong: Cai liao, hui hua ji shu he bao hu zhi yan jiu],* ed. Wu Yongqi, Zhang Tingbao, M. Petzet, E. Emmerling, and C. Blänsdorf, 154–70. Arbeitsheft (Bayerisches Landesamt für Denkmalpflege), vol. 111. Munich: Bayerisches Landesamt für Denkmalpflege.

Zhou Tie. 2001. New developments in the conservation of the polychromy of the Terracotta Army. In *The Polychromy of Antique Sculptures and the Terracotta Army of the First Chinese Emperor: Studies on Materials, Painting Techniques, and Conservation, International Conference in Xi'an, Shaanxi History Museum, March 22–28, 1999 = [Gu dai diao su cai hui Qiushihuang bing ma yong: Cai liao, hui hua ji shu he bao hu zhi yan jiu],* ed. Wu Yongqi, Zhang Tingbao, M. Petzet, E. Emmerling, and C. Blänsdorf, 23–30. Arbeitsheft (Bayerisches Landesamt für Denkmalpflege), vol. 111. Munich: Bayerisches Landesamt für Denkmalpflege.

Zibo Museum. 1997. Excavation of the Warring States tomb at Shangwangcun, Linzi, Shandong. *Wen wu* 6: 14–26.

Ishkor Glazes of Uzbekistan

Pamela B. Vandiver, Amy Vandiver, Akbar Rakhimov, and Alisher Rakhimov

Abstract: *Reverse engineering of early craft technologies involves using the basics of materials science and engineering to a new end—their preservation and continuity. This paper presents a case study of the analysis and reconstruction of the traditional glazed pottery and tile technologies of Samarkand, Bukhara, Khiva, and other Silk Route cities of Uzbekistan that date to the twelfth century* C.E. *and possibly earlier. A comparison is made of these analyses to the analysis of wares of modern artisans who have kept alive traditional craft practices that they can document to the sixteenth century. Tiles made by the traditional* ishkor, *or plant ash, process are more durable and have a brilliant, translucent appearance similar to that of the architectural tiles on ancient monuments along the Silk Road and are once again being used in restoration. Further analysis has shown why the modern tiles typically used in restoration are not durable and do not have the correct appearance.*

From the thirteenth to the nineteenth century C.E., public architecture in Samarkand, Bukhara, Khiva, and other World Heritage Sites along the Silk Road in Uzbekistan was decorated with brilliant, glossy, translucent glazed tiles that display great variation in visual effect and underlying technology. The characteristic glaze, known as *ishkor* in Uzbek, is produced from the ash of desert plants. Conservation practice for these structures prior to this study was that modern tiles were manufactured in industrial factories in Uzbekistan with commercial materials first from Russia and later from Italy and Vietnam to replace ancient ones that had deteriorated or been lost. However, most of the modern tiles deteriorate faster than the old ones they replace, or they are fired to such a high temperature that they match neither the color nor the gloss of either the original tiles or older replacement tiles. To solve the problem of producing glazed tiles with a similar visual appearance, we studied traditional tile- and pottery-making workshops in Uzbekistan, many of which trace their master potter lineage to the seventeenth century. In this study, master potters were interviewed,[1] their working methods studied, and both raw materials and finished products sampled for analysis. Results of analyses of the traditionally made wares were compared with those of ancient tiles, and the traditionally made tiles were evaluated for durability.

Many of the modern but traditional Uzbek ceramic practices match the technologies used for the ancient tiles. However, these practices are no longer economically viable and should be considered as intangible cultural heritage. The International Council of Museums in October 2004 accepted a new UNESCO charter for the preservation of intangible cultural property, defined as performance-based arts and technologies (UNESCO and Korean National Committee 2003). Examples are cultural masterpieces of music, dance, puppetry, theater, festivals, and traditional craft knowledge and practice. This charter is similar to the Burra Charter of Australia ICOMOS (2000) and the Convention for World Cultural and Natural Heritage Protection (UNESCO 1972), which serve as the legal framework to preserve World Heritage Sites. Both charters have three major selection criteria for cultural property: cultural significance, authenticity, and integrity. Continuity is not one of these criteria. Thus craft knowledge, lost through disuse, death, or cultural calamity, can be reverse engineered, revived, and transmitted as intangible cultural heritage. Analysis and reconstruction of ancient technologies usually involves an iterative process

of contextual investigation, resource survey, analytical characterization, replication and use of standards, and, finally, reanalysis of the mechanisms of material transformations and their application to modern materials. The critical factor that is being recognized is the knowledge of the practitioner, or, as stated in the charter, the "outstanding value as a masterpiece of . . . human creativity" (UNESCO 1972: 30).

Many European and Asian countries have revived ancient and historic ceramic styles of cultural significance, and the products are sold as replicas, although they are not labeled as such. Ceramics are sold with an artist's signature only if value is enhanced, and in Asia this involves acceptance of Euro-American art standards. The Asian view, predominant in China for the past thousand years as well as in contemporary Uzbekistan, is that replicas are not fakes and forgeries but a complement to a past tradition that is being revived, continued, and collected as an heir to that tradition. The onus and challenge reside in the scholarship of the collector or collection agency to determine date or period of production. Only when a modern replica is described or sold as ancient is there intent to deceive, and only then does the object become a fake or forgery. The Asian view is that such replicas satisfy the market, keep a tradition and its attendant craft knowledge alive through practice, and remove at least some of the temptation to loot sites and ignore antiquities laws by carrying on illicit trade.

Uzbekistan is most fortunate to have more than twenty-five families practicing ceramics in traditional workshops, but each workshop master keeps its special practices secret. In 1930 more than one hundred pottery and tile workshops were documented (Rakhimov 1961). Today the traditional workshops produce only pottery, although tiles are produced in the traditional manner for use on private family tombs. UNESCO is helping to support a pottery school in Tashkent with the aim of transferring the old ceramic technology to future generations. That school was organized and is run by the last two authors of this study (Khakimov 1999). Our role as materials analysts is to reconstruct the missing steps and variability in the technology that the masters are unwilling to describe and to evaluate the durability of the ceramics and their suitability for monument conservation. This paper presents a case study of traditional glazed-tile technologies that date from the thirteenth to nineteenth centuries C.E. and that are still being practiced in Samarkand, Bukhara, Khiva, and other Silk Road cities of Uzbekistan, although they are no longer known and practiced in western China, Mongolia, or Turkmenistan.

Variation in Appearance of Traditional *Ishkor* Glazed Architectural Styles Used on Public Monuments

In addition to a distinguished tradition of pottery (Golombek, Mason, and Baily 1996), Uzbekistan is heir to an astounding and varied glazed-tile and glazed-brick architectural tradition (Michaud, Michaud, and Barry 1995). The characteristic glaze, or *ishkor,* is produced from the ash of desert plants. Most early monuments were made of earthen adobe walls, but starting in the twelfth and thirteenth centuries building walls were constructed of fired bricks made from local loess that fired at 1,100°C or below to yield a yellow color. The fired brick produces a much more durable monument even if only the surface is clad in fired tile (Amery and Curran 2001: cf. fired brick styles, 103–5, 109–12; and cover to preservation of unfired brick structures, 78, 129). Several special *ishkor* glazed architectural styles have developed.

Inset Ceramic Panel in Brick or Tile

The oldest Islamic style, dating to the twelfth and thirteenth centuries in Bukhara, is characterized by the stacking of bricks into deeply textured relief patterns; in some cases as many as twenty-five different stacking patterns occur in the same building. Some pattern blocks had bricks placed in mostly diagonal patterns, similar to woven reed patterns, with holes through the walls that allowed air to circulate inside the building for cooling. Inscriptions and relief friezes were glazed with a soft, almost opaque turquoise blue *ishkor* glaze that contrasts beautifully with the yellow brick; these glazed pieces were placed into only a few important places on the exteriors of buildings. This textured brick architectural style survives today in Khiva in the more highly fired (approx. 1200–1250°C) stacked patterns in reddish brick with dark brown trim bricks.

Single-Color Distributed Glazed Brick

The most common and widespread Uzbek monument style is rectilinear and dates from the thirteenth century; it continues to the present. It is characterized by uniform-sized yellow bricks stacked on edge in a variety of patterns and interspersed with same-sized bricks glazed on a single, exterior side with copper turquoise blue most commonly but also cobalt blue and, rarely, yellow and white. One example is the exterior of the Bibi Khanom mosque (1399 C.E.) in Samarkand (Michaud, Michaud, and Barry 1995: 82–83). This

architectural style and the one described above can be read and recognized at a considerable distance.

Mosaic Tile Panels and Surfaces

Uzbek architecture has a variety of other ways to employ *ishkor* glazes, primarily on tiles that are inset into walls or domes or applied to columns. Imported from the south, Afghanistan and Iran, are Persian-style mosaic-style tiles from the fourteenth and fifteenth centuries. The visual effect is much like curvilinear patterns in Persian carpets. Single-color glazed tiles are fired, and then, with a labor-intensive process akin to stone-working, different pattern pieces are cut and ground and closely fit together into a complex, multicolored, flat mosaic design. Many inset mosaic panels are found at the Shakhizinda burial complex, the Registan World Heritage Site, and the Bibi Khanom mosque, all in close proximity in Samarkand (see, e.g., Michaud, Michaud, and Barry 1995: 88, 89, 92, 93). In Turkey and Iran this mosaic style is practiced on a relatively small scale, with mosaic tile panels inset into niches, but in Uzbekistan this style is practiced on a monumental scale.

Deep Hand-Cut Incised Tiles

This style involves producing repeat curvilinear patterns in deep relief (Michaud, Michaud, and Barry 1995: 108–9, 113). A complex pattern is overlaid from a stamp or stencil; then a pattern is cut into the soft clay tile, followed by glazing. The pattern appears as in relief.

Molded Relief Tiles

An unfired, quite plastic clay body is pressed with or into an open-face mold that contains a design in deep relief (Michaud, Michaud, and Barry 1995: 114, 119). After the tile is removed from the mold, the relief is refined by hand tooling. This style is commonly found on single-colored tiles on the exterior of buildings, for example, at the Shakhizinda. The difference between this and the previous style is difficult to detect and requires examination of the tool marks in the indented pattern.

Applied Quartz-Slip Relief Tile

A quartz-based slip is applied to a flat tile to produce a gentle raised relief pattern that is only a few millimeters thick (Michaud, Michaud, and Barry 1995: 118–19). When the tile is painted and glazed with the background in a deep blue reserve, the light is reflected from the white, somewhat rounded and raised sculpted floral patterns. As one approaches a building with these tiles, it appears to shimmer in sunlight.

Interior Cobalt Blue, Gold-Foil Dome Tiles

Cobalt blue glazed tiles on the interiors of domes are decorated with gold-foil stars and other geometric shapes that are attached by applying and firing an opaque red, iron oxide–containing overglaze enamel onto the glazed tile where the foil is attached and beyond the edge of the foil, as seen, for example, at the Shakhizinda burial complex in Samarkand. While the enamel is still wet, the gold foil or gold leaf pieces are applied. The tile is then refired at a lower temperature than that used for the original glaze firing, such that the enamel partially melts to adhere the foil. Gazing upward into one of these domes is like viewing a dome of the night sky, a motif common to both Chinese and Egyptian tombs, but in the Islamic architecture of central Asia the reflection from the glassy and metallic surfaces produces an optical effect in which the stars flicker and the sky shimmers with light.

Each of these very different and wonderful visual effects is produced by a general *ishkor* glaze technology that is applied in a special way with certain difficult steps. The visual effect of these different glazed bricks and tiles changes depending on the light source—candles, oil lamps, or sunlight—and on the time of day and the extent of shadow and reflection.

Preserving Ancient Tiled Monuments

The use of commercial replacement tiles on ancient tiled monuments in Uzbekistan is creating preservation problems. These commercial tiles often have been fired at too low a temperature, resulting in porous tiles that are attacked by high groundwater levels, high humidity, and rain. Through capillary action, groundwater climbs through the walls of monuments to levels of 8 to 10 meters, leaving salts and discoloration, delaminating tiles, and partially eroding the walls, particularly at brick joints. Some industrial plants making commercial tiles also fire them quite high, to 1,200°C or more. Above this temperature the yellow-firing clay tends to turn reddish and darken, such that the color of the commercial tiles does not match that of the ancient tiles they are replacing. In addition, some firms state that they use glazes and colorants from Italy and Vietnam because of their low cost. The same industry that makes tile for interior floors and walls also makes replacement tiles for the exteriors and interiors of ancient monuments. The commercial glazed tiles that were being used at the Bibi Khanom mosque in Samarkand appeared quite opaque and lacked the brilliance and gloss of even the tiles that were used to replace originals during an early-twentieth-century restoration. The new tiles also dete-

Table 1 Chemical Composition of Glaze from Modern vs. Sixteenth-Century Tiles from Bibi Khanom Mosque, Samarkand, Uzbekistan

Modern (2001) Restoration Tiles: Tile body made of 80 wt% Khojigadish calcareous loess and 20% Angren clay															
Glaze	**Composition**														
	SiO_2	Al_2O_3	Fe_2O_3	CaO	MgO	K_2O	Na_2O	P_2O_5	PbO	TiO_2	CuO	CoO	MnO		
White, clear	43.31	3.59	1.02	2.03	1.04	1.27	8.34	0.24	32.02	0.12	0.79	0.08	0.04		
Blue, CuO	42.43	3.34	1.15	2.46	1.18	1.3	5.27	0.18	33.88	0.02	1.18	0.06	0.02		
Blue, CoO	38.01	1.9	0.57	1.38	0.38	0.75	2.33	0.04	47.85	0.43	0.03	0.58	0.04		
Blue, CuO	42.9	2.59	0.82	1.8	1.52	1.94	3.55	0.16	40.16	0.02	0.76	0.25	0.03		
Sixteenth-Century Tile: Tile body probably made of Khojigadish calcareous loess and quartz sand with 0.03 wt% Fe_2O_3 impurity*															
Glaze	**Composition**														
	SiO_2	Al_2O_3	Fe_2O_3	CaO	MgO	K_2O	Na_2O	P_2O_5	PbO	TiO_2	CuO	CoO	MnO	SO_3	Cl
Blue, CuO	49.78	4.23	0.91	2.18	1.09	2.08	7.05	0.15	24.99	0.1	1.29	0.05	0.01		
Blue, CoO	40.38	1.2	0.46	1.14	0.64	0.83	3.81	0.09	42.94	0.01	0.04	0.63	0.01		
Green, CuO	33.22	3.52	0.29	0.57	0.11	0.54	0.12	0.02	52.47	0.1	2.3	0.04	0.01		
Body	**Composition**														
Blue, CuO	62.89	24.46	3.37	2.45	0.8	3.02	1.25	0.27	0	0.94	0.17	0.14	0	0.22	0.02
Blue, CoO	62.08	22.5	4.12	1.26	1.25	3.4	0.78	0.28	0	0.95	0	0	0	0.44	0.14
Green, FeO	63.95	22.17	2.68	3.85	0.97	4.2	0.61	0	0.73	0.91	0	0	0	Present	Present

*These samples were collected by Mukhitdin Rakhimov, who believed they came from one workshop as they were placed in a mosaic panel alongside one another.

Analysis of polished, carbon-coated sample cross sections by electron probe microanalysis (EPMA, or microprobe analysis) using a wavelength-dispersive Cameca V, run at 15 V accelerating voltage, 10 seconds or 10,000 count, beam defocused to 10 microns and calibrated with geologic standards. Major elements are accurate to 3 to 5%; minor elements, to 10%. Each analysis is the average of 5 to 9 points.

riorated rapidly, displaying surface cracks that localize salts, especially at the end of drying, and that lead to delamination of the glaze from the body.

We analyzed glaze samples from modern tiles used during restoration of the Bibi Khanom mosque in 2001 and compared them with old tiles placed in the sixteenth century. The results showed that the chemical compositions of the old and new glazes do not differ significantly (table 1). However, the microstructures of the two glazes were very different (figs. 1, 2), and this explains the differences in visual appearance and durability. The color in the modern restoration tiles was concentrated in the upper 10 percent of the thickness of the glaze, leading to a loss of the desired depth and brilliance. This is the result of a manufacturing practice that reduces the amount of colorant used to make the glaze; this reduces costs but produces tiles with a flat, dull appearance.

In addition, quartz particles had been dusted onto the unfired, still-wet glaze surface of floor tiles at the Bibi Khanom mosque, a modern practice common for floor tiles to produce better wear resistance. As the glazed-tile floor wears during use, the quartz particles round a bit but remain in relief at or near their original level and protect the floor from further abrasion. However, these quartz particles have a different rate of contraction than does the glaze, and on cooling in the kiln, cracks form around them. These cracks are the weak link that serves to initiate corrosion, as the cracks will grow slowly with changes in temperature, relative humidity, and vibration. When moisture evaporates, salts will concentrate in these rough cracked areas. In summary, the modern ceramic technology produces tiles that are deleterious to monument preservation.

FIGURE 1 Tiles in yellow, white, a lapis lazuli or cobalt blue, and a turquoise or copper green from the Bibi Khanom mosque, sixteenth century. Tiles were glazed as large square tiles and then cut and ground to fit a flower-patterned freize, using a Persian mosaic style of tile decoration.

FIGURE 2 Modern tiles in a similar pattern and, to the left, the samples we analyzed in table 1.

Composition of Old and New Glazes

As table 1 shows, the traditional glazes have a wider range of composition than the glazes used on modern restoration tiles. The glazes were analyzed by electron probe microanalysis (EPMA), as described in table 1. However, both glazes are of a similar type, lead-alkali-silicates, but both are complex, each having several sources of alkali, alkaline earth, and other constituents. Having a range of these constituents is advantageous for melting the glaze during firing and for durability, but it is difficult to assess the sources of the raw materials. For instance, soda and potassa together are a stronger flux than either alone—known as the mixed-alkali effect, producing melting at a lower temperature than does the single alkali. For instance, the alkaline earths, MgO and CaO, that produce stability are in a ratio of about 1:2 and are similar to the ratio in a dolomite source rock. The process of understanding the technology involves thinking about the role of the different constituents, but in this case complex glaze compositions clearly were preferred; we cannot specify whether they were compounded from many raw materials or from a single complex material without additional information. The practice of modern pottery and tile workshops producing traditional pottery glazes involves the use of special plant ashes, and potters can document this practice for several hundred years as a conservative technological style or special, repeated way of making a culturally significant object. Akbar Rakhimov once characterized this special technology as the making of "natural vegetable glazes with organics."

Ishkor or Desert Plant Ash Glazes

To produce the varied visual effects seen in traditional glazed tiles made over a seven-hundred-year period involves a well-developed technology that could be practiced over a large geographic area with relatively little risk of failure. A readily available, single source of raw materials for the glaze was and still is available to potters in the form of plant ash, or *ishkor* in Uzbek, made from many desert plants. In the family Chenopodiaceae, special salt-concentrating *Salicornia* and *Salsola* desert plants, better known as tumbleweeds, saltwort, or Russian thistle, of which seventy-two are known in Uzbekistan (Komarov and Shishkin 1970), are harvested at the end of the summer, dried, and slowly burned in a reducing or smoky atmosphere at perhaps 500°C to 700°C to produce the ash. These plants include *Salsola soda, S. kali, S. foetida, Haloxylon recurvum, H. multiflorum,* and *Salicornia,* and we have found many of them from Khiva to Tashkent, as well as in the Ferghana Valley. Near Khiva, an especially revered grove of these plants was near tree height, about 20 feet tall, and could only be appreciated as a special vegetable by a hungry camel or a knowledgeable potter. The lumps and cakes of ash produced from these plants vary in appearance from black stonelike or slaglike with conchoidal fracture to a dense, gray ash with black carbonized plant debris and residual stems and plant bits.[2] To make an *ishkor* glaze out of the plant ash involves fritting and grinding the ash, sometimes repeatedly, and adding other constituents, such as quartz, colorants, and sometimes lead oxide as a flux and brightener and tin oxide as an opacifier and whitener. The use of plant ash in glass and glazes is widespread in the desert regions of a large part of central and southwestern Asia and the Mediterranean basin, and the formulations are quite consistent.[3] Ethnographic interviews with potters as well as textual evidence repeatedly suggest that to one part powdered quartz is added one to one and a half parts dried and ashed desert plants, that is, 50 to 60 wt% SiO_2. When Rye and Evans (1976) observed ashing, they noted that the best-quality alkali material formed a liquid below the burn-

ing plants, fused at a relatively low temperature, and could be used in the glaze or glass frit at a 1:1 ratio by weight with quartz. The author Abu'l-Qasim, writing in about 1200, also stated the latter was a high-quality material (Allan 1973); however, Rye and Evans found that Multan potters preferred the lower-quality ash that had to be mixed with quartz at a ratio of 1.5:1 by weight. Thus potters and others who use the ashed plant materials discern variability in composition that they relate to variation in properties that develop during the ashing step, not the variations in soil composition and various environmental factors that affect how the plant acts as a filter for constituents in the soil.

Figures 3–5 show the five plants that Uzbek potters most frequently use for their *ishkor* glazes, with the ash from each plant contributing different properties to the glaze. Based on microscopy of prepared cross sections, Harry Alden, botanist with the Smithsonian Institution, identified them as varieties of *Salsola kali* and *S. soda*. Scientists at the University of Arizona Herbarium stated that these particular Uzbek plants are not common in the American southwestern deserts, unlike many species that were spread with wheat seed by Russian colonists to the American and Canadian West. These plants are the following:

- *Gulaki:* Two red and yellow flowering varieties of *gulaki*, a local Uzbek name meaning "flowering," provide a low-melting-temperature ash that is used primarily for glazes on pottery vessels, especially serving bowls and plates that are sold in the marketplace to serve and prepare, but not store, food. These vessels have the highest fluxed glaze and are the least stable, and some potters said that they use this ash with the expectation that clients will replace the pottery yearly, an example of planned obsolescence, or that the pottery primarily serves a decorative function in modern homes and offices.
- *Qirqburun:* Two red and yellow flowering varieties of *qirqburun,* meaning "forty joints or knuckles," are lower in highly fluxing constituents, thus producing glazes that are more durable. They are used on tiles for family graves and on special vessels for display, for storage, and for food preparation. These are ceramics that are meant to last.
- *Balaq kuz: Balaq kuz,* meaning "fish-eyes" because of its large round seeds, is found primarily in the south near Termez and Boiysun, an area designated by UNESCO as an intangible cultural and natural

FIGURE 3 *Gulaki* plant in red and yellow flowering varieties and somewhat fused ash cake (upper right).

FIGURE 4 *Qirqburun* plant in red and yellow flowering varieties and poorly fused ash cake (upper right).

FIGURE 5 *Balaq kuz* plant and ash cake with an intermediate amount of glass (upper right).

site, but even there it is not as common as the other plants. This plant can also be found in the Ferghana Valley and near Tashkent, but its occurrence is not sufficiently abundant for use in *ishkor* glazes. The composition is intermediate between those of *gulaki* and *qirqburun*.

Uzbek potters are aware of the ecological problems created by overusing the plants, and many state that they are trying to maintain a delicate balance between using the plants in a way that will not cause their demise and keeping alive a traditional, but very labor-intensive, technology that produces glazes with a beautiful, brilliant appearance. Because of the yearly variability of these plants and the considerable effort required to make the plant ash, many young potters are changing to glaze compositions that are high in lead oxide or that are commercially available. Examples of this are given in note 1.

Analysis of Plants and Ash Used for *Ishkor* Glazes

In general, plants act as filters for elements that are present in the immediate soil environment, and desert plants in particular gather high concentrations of soluble salts and other minerals. Table 2 presents compositions of three common types of plant materials used in the production of *ishkor* glazes. The top group assesses variability in raw, unfired plant parts; the second, ash that is ready for use in a glaze. These analyses were conducted with a scanning electron microscope with simultaneous energy dispersive X-ray analysis (JEOL840-II with Thermo Electron System 6 EDS) using a 20 kV accelerating voltage, 150 to 180 seconds counting time. For concentrations above 10 percent, the numbers are accurate to about 5 percent; for concentrations below 10 percent, accuracy decreases to 10 percent. The analyses were standardized with the working standards of Corning glasses A through D. As shown in figures 3–5 and the upper part of table 1, the compositions of the various unfired or raw plant parts demonstrate lots of variability according to the function served. Analyses of the *gulaki* plants we ashed in August 2000 show a more potassia- and soda-rich ash composition, whereas the *qirqburun* contains more alumina, calcia, iron oxide, and phosphorus pentoxide, yielding a higher melting glass. These compositions are highly variable, but much of the sulfate and chloride in the raw plant parts has burned off. The plants were collected with the ceramic master, Gofferjahn Marajapov, in a 100-meter area near Gurumsaray in the northern Ferghana Valley and partially dried and burned at about 700°C in late August, though September is the preferred time as it is dryer and the plants contain less water. The Ferghana Valley is a high mountain valley in the east of Uzbekistan that is the source of the Syr Darya River and has served throughout history as an over-summer reserve for caravans wanting to avoid the hot, dry lower deserts and needing to find fodder for their animals.

Reconstructing the Secrets of the Process of *Ishkor* Glaze Production

Here the traditional process for producing and applying *ishkor* glazes is described in more detail. Figures 6–8 show most of the sequence of steps, or chain of operations.

Plant Collection and Ashing

We collected plants from a drainage swale near the town of Namangan in the Ferghana Valley with Gofferjahn Marajapov, a local pottery master. The surface of the soil was not covered with a layer of salt, nor was the soil salty tasting, having a pH of about 7.9, or only slightly alkaline. The plants are usually dried on the ground for about two weeks in the 40°C heat, then ashed in a slow, smoky fire to about 700°C; however, our plants were dried for only a day and then fired in near-windless conditions (fig. 6). The surface of the stack

FIGURE 6 Gofferjahn Marajapov and Akbar Rakhimov ashing a smaller than usual stack of *ishkor* plants in the Ferghana Valley, early September 2001. This firing was primarily a demonstration.

Table 2 Compositions of Plant Parts and Ash from Different Plants Used in *Ishkor* Glazes

	SiO_2	Al_2O_3	Fe_2O_3	CaO	MgO	K_2O	Na_2O	P_2O_5	SO_3	Cl	CuO	TiO_2	Total
Ishkor Plants Collected near Gurumsaray, Ferghana Valley													
Petal, *gulaki*, red flower	11.63	13.55	0.94	4.26	21.35	6.1	28.11	1.21	8.97	3.87	0	0	100
Seed, *gulaki*, red flower	15.36	5.12	8.09	11.48	8.79	12.23	15.4	2.22	17.85	3.09	0.6	0	100
Seed, *gulaki*, yellow flower	8.74	5.24	0	3.07	15.65	13.37	27.17	2.14	10.77	10.49	0	0	100
Stem exterior, *qirqburun*, red	34.28	16.17	5.19	8.01	16.35	2.2	10.4	0	5.15	2.26	0	0	100
Stem interior, *qirqburun*, red	2.06	0.43	0.46	7.49	1.94	26.51	19.18	4.11	15.38	20.89	1.56	0	100
Stem interior, *qirqburun*, yellow	4.58	0.98	0	5.39	9.08	2.24	50.43	1.45	19.87	5.15	0	0	100
Seed exterior, *qirqburun*, yellow	35.94	17.37	5.28	7.68	8.18	2.77	13.2	0	6.03	2.77	0.76	0	100
Seed interior, *qirqburun*, yellow	14.9	5.95	1.52	8.75	4.14	19.43	16.53	3.47	5.94	19.36	0	0	100
Petal, *balak kuz*, red flower	22.02	10.29	1.86	3.95	4.17	15.77	14.39	0.94	7.34	13.63	5.65	0	100
Seed interior, *balak kuz*	32.04	11.22	8.74	12.28	4.11	5.91	9.03	0	8.74	11.43	0.7	0	100
Seed exterior, *balak kuz*	31.72	13.11	4.11	4.19	6.33	4.9	15.29	4.63	7.82	6.36	1.55	0	100
Stem exterior, *balak kuz*	26.63	13.98	4.17	17.09	10.32	9.16	10.27	0.06	5.73	2.39	0.19	0	100
Stem interior, *balak kuz*	23.31	14.57	3.38	5.99	12.78	4.58	15.78	0	8.16	10.4	1.03	0	100
***Ishkor* Plant Ash Cake Made by Authors, Ferghana Valley**													
Gulaki ash cake	34.24	2.9	0.36	6.8	2.7	6.35	35.62	0.04	0	0	0	0	100
Qirqburun ash cake	26.74	8.79	0	27.04	1.79	1.08	26.54	3.67	0	0	0.59	0	100
Prepared Plant Ash Samples Collected from Potters in the Ferghana Valley													
Milled, mixed plant ash, Gofferjahn Marajapov, Gurumsaray, #1	58.45	6.34	1.38	9.06	4.76	7.34	12.13	0.32	0	0	0	0.21	100
Milled, mixed plant ash, Gofferjahn Marajapov #2	54.7	6.16	1.57	7.36	4.58	7.76	17.2	0.52	0	0	0	0.24	100
Mixed plant ash, Hakkim Satimov, Gurumsaray	53.31	6.27	1.67	7.59	4.68	6.36	18.7	0.51	0	0	0	0.91	100
Mixed plant ash, Masadullo Turapov, Rishton	55.6	6.52	1.84	8.41	4.57	7.56	14.57	0.5	0	0	0	0.27	100
Mixed plant ash, Ibrihim Kamillov, Rishton	60.03	6.59	0.75	2.45	0.25	4.06	26.02	0.06	0	0	0	0.02	100
Prepared *Ishkor* Plant Ash Variation, Ferghana Valley													
Ishkor mixed plant ash	63.5	7.62	1.81	5.56	2.91	4.77	13.13	0.37	0	0	0	0.35	100
n = 88 with standard deviations of	3.5	0.9	0.5	0.9	0.3	0.6	1.9	0.2				0.2	
Ishkor mixed plant ash	56.42	6.38	1.44	6.97	3.77	6.62	17.73	0.38	0	0	0	0.33	100
n = 57 with standard deviations of	4.6	0.8	0.4	1	0.4	0.8	2.4	0.2				0.2	

Number of analyses (n) was 1, unless otherwise noted. A JEOL 840-II SEM-EDS was used with operating parameters of 20 V, 15 mA. The largest possible single-phase-assemblage areas were analyzed for 2 minutes. Semiquantitative ZAF corrections were applied with totals normalized to 100. Corning Glass standards A to D were analyzed successfully as working standards both before and after those given above. Carbon and oxygen, though the major components of these samples, were not analyzed. Fresh fractured samples and powders were coated with a thin film of carbon using a vacuum evaporator.

FIGURE 7 Hand-operated quern for milling *ishkor* ash, with a bowl of ash for one milling operation on the top in the courtyard of the Marajapov family.

FIGURE 8 Gofferjahn Marajapov's circular, updraft kiln with a separate, lower firebox or chamber for fuel, being investigated by Amy Vandiver. Note the quartzite slab at the rear of the firebox.

was used to smother the fire within. If the flame threatened to burn through, more plants were added. Each type of plant was fired in a separate stack. The ash was milled dry in a hand quern over a period of one day and sieved to about 120 mesh (fig. 7). One workshop still retains a traditional donkey-driven mill, but it is used primarily for grinding clay, as the amount of *ishkor* glaze production is insufficient. Many workshops now compound an artificial ash composition made from commercial ceramic ingredients. The ash was then mixed at a ratio of 1.5 parts of ash with 1 part of quartz and, occasionally, small amounts of ground glass or lead compounds, then milled again. The final preparation of the glaze involves adding water to make a slurry with the consistency of cream.

Glaze Application and Firing

Wares to be glazed are usually made of a fine red clay for vessels, while the clay for tiles has a sandy, loessic consistency; representative analyses are presented in table 2. Before glazing, the object is coated with a white quartz-containing slip that has been ground and milled to a fine consistency; sometimes a quarter of a percent of an organic binder such as flour is added. After the slip has dried, an artisan paints a design on the ware using colored oxides that are often mixed with a small amount, perhaps a quarter of a percent, of flour binder and occasionally fine quartz. These additions are meant to prevent the colorants from running or blurring when the glaze is applied. The ware is allowed to air dry and is then glazed, dried again, and stacked in the upper chamber of a round cross-section, double chamber updraft kiln. Gofferjahn Marajapov's kiln is shown in figure 8; it is similar to those documented by Yoshida (1972) and Rye and Evans (1976) in Pakistan and Wulff (1966) in Iran. The kiln is fired over several days using field stubble, brush, and scrap wood in oxidizing conditions to a maximum temperature of between 800°C and 1,050°C, sometimes higher in some workshops. Tiles, plates, and small vessels are stacked on ceramic shelves supported by ceramic and occasionally iron rods that fit into holes in the kiln wall. The kiln structure and method of stacking have been excavated from archaeological

sites, the most complete of which are the kilns from Pajikent near Bukhara, and the earliest date of such kilns is late first millennium B.C.E.

Safeguarding Family Secrets

The process described above raises two anomalies that need to be addressed. First, no intermediate step consisting of a glassmaking or fritting process was described by any of the pottery masters. When the ashes of the various plants (see figs. 3–5) direct from field firing are exposed to increasingly high temperatures, the ash does not produce much glass until about 1,200°C and remains as a white to gray to black heterogeneous mass that in our replications does not produce a clear, transparent glaze when we follow the above process firing the ceramics to 1,050°C. In a sustained conversation with Ibrahim Kamillov, formerly senior ceramist in the Academy of Arts and Design of Uzbekistan, he stated that no refiring of the ash occurred, either in the firebox of the kiln or in a separate glass-fritting or melting kiln placed separately on his property, and this is his workshop's secret (fig. 9). This conversation was repeated in interviews with other pottery masters. When Kamillov was pressed further, he stated that the ash melted at 1,200°C, and he did so emphatically in the only English he used during our interpreter-mediated conversation, thus making it clear that no significant melting occurs during the ashing process. The anomaly, or even impossibility, consists in how a high-melting-temperature ash, when added to an even higher temperature material such as quartz, could produce a glaze, essentially a transparent glass, without any high temperature melting step. Piccolpasso, in his treatise on Renaissance Italian majolica production, tells of an intermediate fritting or partial melting step in the firebox of his kiln and even details the process with drawings (Piccolpasso, Lightbown, and Caiger-Smith 1980). The Multan potters of Pakistan employ it as well (Rye and Evans 1976).

FIGURE 9 Ibrahim Kamillov, the senior potter of Uzbekistan, in his home museum and showroom.

As indicated in the soda-lime-silica phase diagram (Levin, Robbins, and McCurdie 1964: 174–75), we see that the ash-quartz compositions lie below the liquidus region of 1,100°C to 1,200°C, at compositions between $2Na_2O$-CaO-$3SiO_2$ (34.3, 15.6, and 50 wt%, respectively, decomposition T = 1,141°C) and Na_2O-$2CaO$-$3SiO_2$ (17.5, 31.6, and 50.9 wt%, respectively, melting T = 1,284°C). Thus, based on our compositional and refiring studies, the ash does not melt to form a glass or glaze without high temperature. Increasing the silica content actually decreases the melting temperature toward 1,000°C. Thus an intermediate glass-melting step is required in the *ishkor* process.

Traditional family-run tile and pottery-making workshops closely guard the process they use to make *ishkor* glazes, which may explain this first anomaly. Wulff (1966) notes that competition among workshops has led each workshop to protect the future of its family's production, so straightforward information about techniques and materials was difficult to obtain for his famous treatise on Persian crafts. A large quartz or quartzite slab at the back of potter Gofferjahn Marajapov's kiln drew a noncommittal answer about fritting, although it was most likely a fritting platform rather than a target block to spread the heat, as was stated.

A second anomaly that emerged was how desert plants growing in soils with variable compositions and environments could themselves maintain a narrow range of composition, such that the fixed recipes for *ishkor* glaze with a variation of only 10 wt% SiO_2 would work every time without further testing. Often, a 1 to 15 wt% addition of lead oxide to Islamic glazes is interpreted as variability due to different workshops, for instance, with 1 to 3 percent being one workshop and 5 to 7 percent another. Workshops that produce lead glazes are thought to be different from those that produce soda-lime-silicate glazes. The unexpected practice

in Uzbek workshops, however, is to fire lead- and non-lead-containing glazes in the same kiln, though the firing of lead glazes is much more difficult because any reduction smelts a black lead residue on the surface of the glaze. Thus most Uzbek potters know both systems of glazing. Our hypothesis was that the lead compound is added to the mixed-alkali, alkaline-earth silicate ash glaze in various amounts as a flux, or melting aide, to correct for compositional variation in the ash, such that the glaze will melt and have the necessary aesthetic of brilliance and high gloss. The fritted ash is mixed with quartz and is tested to determine whether and how much lead oxide additive is necessary.

At first, this strategy of adding lead oxide is difficult to understand because we live in an industrial economy where the variations in geologic resources are eliminated through homogenization and special processing prior to use, but most Uzbek pottery workshops mine, process, and test the materials they use. Most contemporary potters in Europe and America expect to purchase uniform raw materials, and such uniformity is achieved primarily because of the large commercial and industrial scale on which these are processed and supplied to an entire market. Some modern potters even complain that the uniformity of raw materials precludes some special effects and the diversity of surface and texture that make handcrafted objects so appealing to modern sensibilities. Pye (1968) even suggests that we have lost the small-scale production processes that allow workshops to practice a "craftsmanship of risk" that makes ceramics aesthetically pleasing to view, handle, and use.

We hypothesized and found analytical evidence (table 3) to support that the *ishkor* process involves a yearly cycle with many intermediate steps for the preparation of glaze materials: gathering and ashing the plants at summer's end; melting, milling, and testing the ash and/or the glaze; and, finally, adjusting the composition with an addition of lead oxide or another flux. The other intermediate step in preparation that potters do not generally acknowledge involves a high-temperature melt, to at least 1,200°C, of the ash cakes, followed by milling to enable rapid melting of a homogeneous transparent glaze in the kiln at a lower temperature, about 1,000°C to 1,050°C. Caiger-Smith (1973) has noted that for centuries glaze making followed the practice of glass making. Years later, at the opening of the school for traditional pottery in Tashkent, where the analytical data for the reconstructed process was presented, representatives of the twenty-five major family pottery workshops corroborated this hypothesized practice. One group even stated that three melts produced optimum brilliance and clarity and later gave us samples from each of the melts.

FIGURE 10 Four bowls by Ibrahim Kamillov, each showing a variation on the *ishkor* technique. Note the difference in gloss as shown in the specular reflectivity. The right side shows two bowls in traditional *ishkor* technique: the upper one with no lead oxide addition and the lower one with low lead. The left side shows two innovative bowls: the upper one with high barium oxide and the lower one with very high lead oxide content.

Table 3 provides evidence of innovation and special practices in the *ishkor* glazing process in some traditional workshops. For instance, Ibrahim Kamillov's glazed wares (fig. 10) exhibit a wide range of gloss, reflectance, and translucency that he achieves by using materials, such as barium oxide and probably borax, that are fluxes, but their use is outside the lead and *ishkor* traditions. Rye and Evans (1976) documented the use of borax in glazes among pottery workshops in Pakistan, and the low compositional totals, for example, 94 percent, imply ingredients that we cannot detect by our methods of analysis. Kamillov's glazes also have lower iron content, evidence that he used especially pure materials, such as quartz, to promote translucency.

These data support the conjecture that ancient glazed ceramics attributed to different workshops alternatively may represent variability within one workshop. Similar variations in quality, appearance, and technology occurred in the

Table 3 Glaze Compositions of Traditional Potters and Calculated *Ishkor* Plant Ash Compositions from the Glazes

	SiO_2	Al_2O_3	Fe_2O_3	CaO	MgO	K_2O	Na_2O	P_2O_5	PbO	TiO_2	CuO	CoO	MnO
Gofferjahn Marajapov #1 (one bowl)													
White, translucent	71.49	3.53	0.88	5.36	2.63	4.34	8.47	0.24	1.01	0.16	0.06	0.02	0.07
Light blue, copper	71.79	4.58	0.86	4.73	2.34	4.64	8.39	0.23	0.92	0.14	0.23	0.01	0.04
Purple, manganese	64.43	4.28	1.85	7.6	4.34	5.35	6.83	0.16	1.32	0.15	0.89	0.01	4.44
Gofferjahn Marajapov #2 (one bowl)													
White, translucent	65	4.45	1.24	5.44	3.43	4.43	14.43	0.4	0.61	0.18	0.25	0.02	0.11
Blue, copper	66.25	4.4	1.17	5	3.06	5.3	11.58	0.33	0.1	0.18	2.53	0	0.36
Purple, manganese	67.85	3.47	0.74	4.28	2.69	5.8	8.21	0.31	0	0.12	0.95	0.12	3.12
Hakkim Satimov (one bowl)													
White, translucent	65.54	4.26	1.09	5.28	3.36	4.4	11.8	0.33	0.55	0.18	0.8	0	0.42
Blue, copper	64.61	4.16	1.15	4.91	2.93	4.13	13.32	0.4	0	0.16	2.93	0	0.8
Masadallo Turapov (one plate)													
Clear	67.83	4.25	1.15	5.95	3.45	4.65	9.6	0.33	0	0.2	0.43	0.01	0.12
Purple, manganese	63.28	4.31	1.16	5.42	3.09	4.97	10.02	0.4	0.19	0.18	2.68	0.07	2.76
Blue, copper, turquoise	67.12	4.22	1.01	4.07	2.43	5.26	9.25	0.29	0.32	0.17	3	0	1.32
Ibrahim Kamillov #1 (one bowl)*													
Clear, transparent	69.95	3.5	0.27	1.85	0.18	2.61	16.04	0.04	1.22	0.09	0.28	0	0.01
Blue, cobalt	69.07	4.26	0.39	1.62	0.12	2.62	16.77	0.04	1.02	0.11	0.43	0.43	0.01
Ibrahim Kamillov #2 (one plate)*													
Blue, cobalt, transparent	66.92	4.26	0.39	1.39	0.16	2.43	16.24	0.35	0.85	0.1	4.05	0.4	0.02
Blue, copper, turquoise†	68.04	3.87	0.05	1.36	0.15	2.44	16.3	0.04	0.61	0.1	4.43	0.04	0.02
***Ishkor* Plant Ash Compositions Calculated from the Above Glaze Compositions††**													
Marajapov pot #1	58.45	6.34	1.38	9.06	4.76	7.34	12.13	0.32		0.21			
Marajapov pot #2	54.7	6.15	1.57	7.36	4.58	7.76	17.2	0.52		0.24			
Satimov	53.31	6.27	1.67	7.59	4.68	6.36	18.7	0.51		0.91			
Turapov	55.6	6.52	1.84	8.41	4.57	7.56	14.57	0.5		0.27			
Kamillov	60.03	6.59	0.75	2.45	0.25	4.06	26.02	0.06		0.02			
Average of the 57 analyses	56.42	6.38	1.44	6.97	3.77	6.62	17.73	0.38		0.33			

The above analyses were conducted by microprobe analysis (EPMA) using a wavelength-dispersive Cameca V at 15 V accelerating voltage, 10 seconds or 10,000 count, beam defocused to 10 microns. Major elements are accurate to 5%; minor elements, to 10%. Each analysis is the average of 5 to 9 points taken on a carbon-coated polished cross section.

*These glazes contain 3.7–5.36% BaO, barium oxide, an average of 4.39%. The glazes were renormalized in the table to eliminate this additive, which represents a variant technology. Note the unusually pure ingredients indicated by the low iron oxide concentration and the low MgO, which indicates a limestone source rather than dolomite.

†This is the only glaze to have a constantly low probe total of 93%, perhaps due to the addition of borax, B_2O_3.

††A simple calculation of removing 55% of the silica, lead, and colorants should approximate the ash composition. Al_2O_3 and TiO_2 were assumed to have entered the glaze with the ash rather than the quartz, and this assumption is clearly an error but has only a relatively minor effect. Analyses of quartz sands show low alumina but some TiO_2.

central Asian ceramic workshops of the past. It is hoped that these analytical data and reconstructed practices from modern family workshops and inappropriate restorations will aid in the understanding of ancient ceramic craft and in the future conservation, preservation, and appreciation of Silk Road architectural monuments.

Summary

The analysis and reconstruction of the processes of making things are useful to the understanding of art masterpieces and archaeological artifacts and to the elucidation of human behavior, as well as some of the underlying science and technology. Such studies of material culture, when the results are used to sustain a traditional craft, also serve to preserve and project that craft and craft knowledge into the future. They serve to promote a sense of cultural identity and to develop an appreciation of cultural diversity.

Our work aimed to reconstruct Uzbek traditional tile and pottery manufacture and examine it scientifically outside the context of the family pottery workshops. For conservation science, this study helps to provide a baseline for comparison of new and old practices, and it resolves questions of process. For conservation, this study helps to provide appropriate-quality tiles for restoration, as well as objects of the appropriate technology to test new conservation treatments, methods, and materials. Our work has also helped to support establishment of a UNESCO-funded school for traditional pottery and tile production in Tashkent that is run by two of the coauthors, the Rakhimovs, and that provides durable tiles and traditional pottery of the correct appearance, durability, and colors. The school's aim is to protect and promulgate an intangible cultural property, craft knowledge, and craft practice that is at least 500 and perhaps more than 1,000 years old. By encouraging the recognition of excellent practitioners who offer an outstanding alternative to the purchase of illicit antiquities and by helping them to produce wares that are even closer in structure, composition, and appearance to the originals, we are taking some of the pressure off the looting of archaeological sites. One result, we hope, will be the continued development of wares with a strong tie to traditional technologies that will become the antiques of the future.

Acknowledgments

The authors gratefully acknowledge the discussions, guidance, and help of many friends during the research that led to this paper, among them, Kenneth Domanik, Lunar and Planetary Laboratory, University of Arizona; Michael Barry Lane, formerly head of UNESCO-Tashkent; and the many potters and their families who generously informed this study and whose legendary reputation for hospitality is well deserved. We also wish to thank Richard Englehart and Harry Alden for help, discussions, and comments. The Institute of Geology and Geophysics of Uzbekistan kindly allowed access to their data. The authors wish to thank Neville Agnew and the staff at the Getty Conservation Institute and the Dunhuang Academy for organizing a wonderful conference and field study and for their expertise and perseverance in the production of this volume.

Notes

1 Below, listed according to their location in Uzbekistan and the wares they produce, are the master potters who use the *ishkor* glazing process and who were interviewed by the authors (UNESCO 2000: 103–28; Rakhimov 1961, 1968). Table 2 presents analyses of glazes from these workshops.

Ferghana Valley: This high, fertile valley where people and animals traditionally have oversummered on their travels along the Silk Road is where widespread practice of *ishkor* glazing occurs. The potters interviewed and workshops visited are as follows:

Ibrahim Kamillov (b. 1926), Rishtan (this also has a commercial ceramic factory descended from a large state factory); *ishkor* glaze and experimental glaze compositions on white-slipped red earthenware, but two sons, including Ismail (b. 1961), produce only lead-glazed, white-slipped red earthenware that is beautifully decorated beneath the glaze;

Sharafidden Yusupov (b. 1945), Rishtan; *ishkor* glaze on white-slipped red earthenware, but son, Firdaus (b. 1974), is mainly using lead glazes;

Masadullo Turopov (b. 1952), Gurumsaray, Namangan province; *ishkor* glaze on white-slipped, underpainted, red earthenware;

Khakim Satimov (b. 1900, now deceased), Gurumsaray; *ishkor* glaze on white-slipped, underpainted, red earthenware;

Gofferjahn Marajapov (b. ca. 1939), Gurumsaray; *ishkor* glaze on underglaze painted in copper and manganese oxides over white quartz-rich slip on red earthenware body.

Tashkent area: This political and economic hub combines artistic and industrial ceramic production with a ceramic school and museums. Ash is not locally available, so the *ishkor* process, although practiced and taught, is adapted to city

practice. The potters are two of the authors of this paper and various factory researchers and managers:

Akbar (b. 1949) and Alisher (b. 1975) Rakhimov, Tashkent; coauthors and two generations of potters who use various techniques and are quite experimental in their approach, including use of *ishkor* glaze, lead glazes, and postfire paint. They run a UNESCO-backed school that teaches traditional *ishkor* technology. The senior potter of this family, Muchitdin (b. 1903, d. 1985), researched and wrote two treatises on the decorative ceramics and architectural ceramics of Uzbekistan (Rakhimov 1961, 1968). These serve as the basis for the study of Uzbek ceramics and are being translated into English. Tashkent also has factories and workshops for commercial ceramic production and for production of tiles to be used in architectural restoration.

Samarkand and Bukhara region: In this area of high tourism, potters are turning away from the labor-intensive traditional *ishkor* technology and replacing it with lead glazes and figurine manufacture. A conservation workshop and training center was found here but has since ceased operation. The potters interviewed are:

Alisher (b. 1955) and Abdullo (b. 1965) Nazrullaev, Gijduvan, Bukhara province; redware body, coated with slip and painted with oxides of Cu, Fe, Mn, Cr, and Co; a final lead glaze is applied, but their training and their father's practice was with the *ishkor* glazes;

Numon (b. 1964) and his son Inom (b. 1988) Ablakulov, Urgut, Samarkand region; redware body, partial white quartz slip, incised ornament, clear lead glaze with oxides of Cu and Fe. Through family records, they can trace ancestry of their Urgut ceramists' dynasty through nine generations to potter Abdullo (b. 1648, d. 1735).

Abduakhad Muzaffarov (b. 1955, d. 1990), Shakhrisabz, Kashkadarya province; red earthenware with partial white slip with Cu, Fe, Co, Mn oxides, and Sb complexes underpainted and coated with a lead-containing glaze;

Jabor Rakhimov, Uba, Bukhara province; Islom Muhtarov, Samarkand; and also workshops in Denau, Sukhandarya province; red earthenware body, hand-formed into birds, animals, whistles, whimsical figurines, decorated mostly with postfire paints.

Khiva, Khorezm province: A traditional religious center in the west, Khiva is home to silk, textile, and rug industries and a UNESCO-backed natural dye and rug school; it is also known for a brilliant, shiny variant of *ishkor* glaze, underpainted with detailed geometric scroll patterns, practiced mainly at Madir village. The potters interviewed are Raimberdy (b. 1909) and Odilbek Matchanov (b. 1971), who use a mixture of lead oxide, commercial glass frit, and *ishkor* glaze that they fuse and grind several times and apply on a white-slipped red body.

2 The ash lumps and cakes are used to make soap, glass, and glazes. They are ground and used directly to clean silk thread unspun from cocoons prior to drying and dyeing. They are used as a mordant for some dyes and sometimes as food for camels. Sometimes to make a better washing powder for clothes, calcium oxide is added as a whitener, in which case the more friable ash cake (*nura* in Arabic) is used instead of the harder and glassier form (*chinan* or *shinam* in Arabic).

3 The use of ashed plants by glassmakers in Herat, Afghanistan, has been filmed and reported by Robert Brill (Brill and Rising 1999). Wulff (1996) documented their use for Iranian blue glazes on white bodies; they have been documented in the ethnographic studies of glazes in Pakistan by Rye and Evans (1976: 182–83). Matson (2000) has collected similar materials and pottery from workshops in an even wider area of Southwest Asia and the Mediterranean. Kenoyer has collected ash from Pakistan, particularly the area around Harappa.

Rye and Evans reviewed studies by botanists who, in the early twentieth century, collected plant and ash specimens, such as *Salsola soda, S. kali, S. fortida, Halozylon recurvum, H. multiflorum,* and *Salicornia,* mostly in the family Chenopodiaceae.

In characterizing glazes from Kashan and Iznik, Vandiver found a wide range of chemical variability in the glazes and considered it an anomaly bearing further investigation (Kingery and Vandiver 1986). At Nippur, Iraq, in 1989, Vandiver gathered salty-tasting plants from a low-lying drainage ditch, dried them for a few days, and ashed them with the help of the cook, who used some of them as soap. From them, a reasonably formable, light grayish glass was made. In 1995 Mark Kenoyer gave me plant ash, called *sajji* in Urdu, from Harappa, Pakistan, that produced a similar analysis and glass. Matchanov in Khiva has since shown us results of his tests that show that optimum transparency and clarity are produced by melting the glass three times with a grinding step between melts. This is a process, called drygading, that traditional glass factories in America and Britain commonly used to make high-quality glass in the eighteenth and nineteenth centuries.

References

Allan, J. W. 1973. Abu'l-Qasim's Treatise on Ceramics. *Iran* 11: 111–20.

Amery, C., and B. Curran. 2001. *Vanishing Histories: 100 Endangered Sites from the World Monuments Watch.* New York: Harry N. Abrams in association with World Monuments Fund.

Australia ICOMOS. 2000. *The Burra Charter: Australia ICOMOS Charter for Places of Cultural Significance (1999): With Associated Guidelines and Code on the Ethics of Co-Existence.* www.icomos.org/australia/burra.html.

Brill, R. H., and B. A. Rising. 1999. *Chemical Analyses of Early Glasses.* 2 vols. Corning, NY: Corning Museum of Glass.

Caiger-Smith, A. 1973. *Tin-Glaze Pottery in Europe and the Islamic World: The Tradition of 1000 Years in Maiolica, Faience, and Delftware.* London: Faber and Faber.

Golombek, L., R. B. Mason, and G. A. Bailey. 1996. *Tamerlane's Tableware: A New Approach to the Chinoiserie Ceramics of Fifteenth- and Sixteenth-Century Iran.* Islamic Art and Architecture, vol. 6. Costa Mesa, CA: Mazda Publishers in association with Royal Ontario Museum.

Grazhdankina, N. S., M. K. Rakhimov, and I. E. Pletnev. 1968. *Arkhitekturnaia keramika Uzbekistana: Ocherk istoricheskogo razvitiia I opyt restavratsii.* Tashkent: Fan.

Khakimov, A. 1999. *Dynasty of Rakhimovs = Rakhimovlar Sulolasi.* Tashkent: n.p.

Kingery, W. D., and P. B. Vandiver. 1986. *Ceramic Masterpieces: Art, Structure, and Technology.* New York: Free Press; London: Collier Macmillan.

Komarov, V. L., and B. K. Shishkin, eds. 1970. *Flora of the U.S.S.R.,* vol. 6, *Centrospermae.* Jerusalem: Israel Program for Scientific Translations.

Levin, E. M., C. R. Robbins, and H. F. McCurdie. 1964. *Phase Diagrams for Ceramists.* Vol. 1. Columbus, OH: American Ceramic Society.

Michaud, R., S. Michaud, and M. Barry. 1995. *Faïences d'zzur.* Paris: Imprimerie nationale.

Piccolpasso, C., R. W. Lightbown, and A. Caiger-Smith. 1980. *The Three Books of the Potter's Art = I tre libri dell'arte del vasaio: A facsimile of the manuscript in the Victoria and Albert Museum, London.* London: Scolar Press.

Pye, D. 1968. *The Nature and Art of Workmanship.* Cambridge: Cambridge University Press.

Rakhimov, M. K. 1961. *Khudozhestvennaia keramika Uzbekistana.* Tashkent: Izd-vo Akademii nauk Uzbekskoi SSR.

Rye, O. S., and C. Evans. 1976. *Traditional Pottery Techniques of Pakistan: Field and Laboratory Studies.* Smithsonian Contributions to Anthropology, no. 21. Washington, DC: Smithsonian Institution Press.

UNESCO. 1972. *Convention Concerning the Protection of the World Cultural and Natural Heritage.* Paris: UNESCO. http//:whc .unesco.org/en/conventiontext/.

UNESCO and Korean National Committee for UNESCO. 2003. *Guidelines for the Establishment of Living Human Treasure Systems.* Paris: UNESCO. www.unexco.org/culture/ich/doc/ src/00031-EN.pdf.

UNESCO Tashkent Office, National Commission of the Republic of Uzbekistan for UNESCO. 2000. *Proceedings of the International Symposium on Revitalization of Traditional Ceramic Techniques in Central Asia: "Blue of Samarkand," Samarkand, Uzbekistan, 6–9 June 2000.* Tashkent: UNESCO Tashkent Office [and] National Commission of the Republic of Uzbekistan for UNESCO.

Vandiver, P. B. 2005. Craft knowledge as an intangible cultural property: A case study of Samarkand tiles and traditional potters in Uzbekistan. In *Materials Issues in Art and Archaeology VII: Symposium Held November 30–December 3, 2004, Boston, Massachusetts, U.S.A.,* ed. P. B. Vandiver, J. L. Mass, and A. Murray, Materials Research Society Symposium Proceedings, vol. 852. Warrendale, PA: Materials Research Society.

Wulff, H. E. 1966. *The Traditional Crafts of Persia: Their Development, Technology, and Influence on Eastern and Western Civilizations.* Cambridge, MA: MIT Press.

Yoshida, M. 1972. *In Search of Persian Pottery.* lst ed. New York: Weatherhill.